

Portland State University

PDXScholar

Dissertations and Theses

Dissertations and Theses

1-1-2011

Microbial Ecology of Active Marine Hydrothermal Vent Deposits: The Influence of Geologic Setting on Microbial Communities

Gilberto Eugene Flores
Portland State University

Follow this and additional works at: https://pdxscholar.library.pdx.edu/open_access_etds

Let us know how access to this document benefits you.

Recommended Citation

Flores, Gilberto Eugene, "Microbial Ecology of Active Marine Hydrothermal Vent Deposits: The Influence of Geologic Setting on Microbial Communities" (2011). *Dissertations and Theses*. Paper 250.
<https://doi.org/10.15760/etd.250>

This Dissertation is brought to you for free and open access. It has been accepted for inclusion in Dissertations and Theses by an authorized administrator of PDXScholar. Please contact us if we can make this document more accessible: pdxscholar@pdx.edu.

Microbial Ecology of Active Marine Hydrothermal Vent Deposits: The Influence of
Geologic Setting on Microbial Communities

by

Gilberto Eugene Flores

A dissertation submitted in partial fulfillment of the
requirements for the degree of

Doctor of Philosophy
in
Biology

Dissertation Committee:
Anna-Louise Reysenbach, Chair
Michael Bartlett
Radu Popa
Parmely H. Pritchard
Mircea Podar
Dirk Iwata-Reuyl

Portland State University
© 2011

Abstract

The discovery of deep-sea hydrothermal vents in 1977 revealed an ecosystem supported by chemosynthesis with a rich diversity of invertebrates, Archaea and Bacteria. While the invertebrate vent communities are largely composed of endemic species and exist in different biogeographical provinces, the possible factors influencing the distribution patterns of free-living Archaea and Bacteria are still being explored. In particular, how differences in the geologic setting of vent fields influence microbial communities and populations associated with active vent deposits remains largely unknown. The overall goal of the studies presented in this dissertation was to examine the links between the geologic setting of hydrothermal vent fields and microorganisms associated with actively venting mineral deposits at two levels of biological organization. At the community level, bar-coded pyrosequencing of a segment of the archaeal and bacterial 16S rRNA gene was employed to characterize and compare the microbial communities associated with numerous deposits from several geochemically different vent fields. Results from these studies suggest that factors influencing end-member fluid chemistry, such as host-rock composition and degassing of magmatic volatiles, help to structure the microbial communities at the vent field scale. At the population level, targeted cultivation-dependent and -independent studies were conducted in order to expand our understanding of thermoacidophily in diverse hydrothermal environments. Results of these studies expanded the phylogenetic and physiological diversity of thermoacidophiles in deep-sea vent environments and

provided clues to factors that are influencing the biogeography of an important thermoacidophilic archaeal lineage. Overall, these studies have increased our understanding of the interplay between geologic processes and microorganisms in deep-sea hydrothermal environments.

Dedication

I dedicate this dissertation to my lovely wife, Sarah, and to my parents, Gilbert and Deborah, for their everlasting belief in me.

Acknowledgments

First, I would like to thank my advisor, Anna-Louise Reysenbach, for teaching me how to be an academic scientist and providing me with numerous opportunities to broaden both my scientific and personal explorations. I would also like to thank my committee members, Michael Bartlett, Dirk Iwata-Reuyl, Mircea Podar, Radu Popa and Parmely (Hap) Pritchard, for their guidance throughout this process. Thanks to all my collaborators, especially Mircea Podar, Margaret (Meg) Tivey and Jeff Seewlad. Also, thanks to all crew members of the R/V *Atlantis*, R/V *Thomas G. Thompson*, R/V *Roger Revelle*, HOV *Alvin* and ROV *Jason 2*. I would also like to acknowledge and thank all past and present members of the Reysenbach laboratory, especially Yitai Liu, Jennifer Meneghin, Isabel Ferrera and Josh Steinberg, for help in the laboratory, insightful conversations and friendship. Without you I would not be here today. Finally, thanks to all my family and friends, especially my best friend and wife Sarah who risked her safety over the last several months while I earned little money and had my head in the deep-sea. Funding for this research was provided by the National Science Foundation through an IGERT fellowship and by grants OCE-0728391 and OCE-0937404 to Anna-Louise Reysenbach.

Table of Contents

Abstract	i
Dedication	iii
Acknowledgments	iv
List of Tables	ix
List of Figures	xii
Chapter 1: Introduction	1
Preface	1
Geologic Setting	2
Hydrothermal fluid generation	3
Hydrothermal mineral deposits	7
Energy sources	8
Microbial Habitats and Diversity	10
Active vent deposits	11
Inactive vent deposits	14
Biotic and abiotic surfaces	15
Endosymbionts	16
Hydrothermal plumes	17
Scope of Dissertation	18
Chapter 2: Microbial Community Structure of Hydrothermal Deposits from Geochemically Different Vent Fields Along the Mid-Atlantic Ridge	20

Abstract	20
Introduction.....	21
Results and Discussion	27
Alpha- and beta-diversity.....	27
Taxonomy	31
Archaea	34
Bacteria	45
Conclusions.....	48
Materials and Methods.....	50
Sample collection and DNA extraction.	50
Hydrothermal fluid chemistry.....	51
454 Pyrosequencing.....	52
Sequence analysis	54
SIMPER analysis	57
Quantitative PCR	57
Nucleotide sequence accession numbers	58
Contributions.....	58
Chapter 3: Microbial Community Structure of Six Hydrothermal Vent Fields From the Lau Back-Arc Basin.....	59
Abstract.....	59
Introduction.....	60
Methods.....	65

Sample collection.....	65
Site descriptions.....	65
DNA extraction, pyrosequencing and sequence analysis	69
Results.....	70
Bacterial community composition	70
Interfield bacterial community comparisons	77
Archaeal community composition	78
Interfield archaeal community comparisons	82
Discussion	83
Bacterial communities	83
Archaeal communities	86
Conclusion	89
Contributions.....	90
Chapter 4: <i>Hippea jasoniae</i> sp. nov. and <i>Hippea alviniae</i> sp. nov., Thermoacidophilic <i>Deltaproteobacteria</i> Isolated From Deep-Sea Hydrothermal Vent Deposits.....	91
Summary	91
Emended description of the genus <i>Hippea</i>	105
Description of <i>Hippea jasoniae</i> sp. nov.....	106
Description of <i>Hippea alviniae</i> sp. nov.	107
Contributions.....	108
Chapter 5: Biogeography of the Thermoacidophilic Deep-Sea Hydrothermal Vent Euryarchaeota 2 (DHVE2).....	109

Abstract	109
Introduction.....	110
Materials and Methods.....	114
Sample collection.....	114
Quantitative polymerase chain reaction (qPCR).....	115
Local similarity analysis	115
Enrichment culturing and phylogenetic analysis	116
Results and Discussion	117
Occurrence and relative abundance of the DHVE2	117
Co-occurrence patterns of the DHVE2	130
Genetic diversity of cultivable DHVE2	134
Conclusion	136
Contributions.....	137
Chapter 6: Conclusion.....	138
References.....	142
Appendix A: <i>Sulfurihydrogenibium kristjanssonii</i> sp. nov., a hydrogen and sulfur-oxidizing thermophile isolated from a terrestrial Icelandic hot spring	173
Summary	173
Appendix B: Electron microscopy encounters with unusual thermophiles helps direct genomic analysis of <i>Aciduliprofundum boonei</i>	175
Abstract.....	175
Appendix C: Summary of MAR 16S rRNA gene clones	176

List of Tables

Table 1.1. Representative chemical compositions of hydrothermal fluids from different geologic settings.....	4
Table 1.2. Examples of thermodynamically favorable redox reactions utilized by microorganisms from marine hydrothermal environments.....	9
Table 2.1. Range of physico-chemical characteristics of end-member hydrothermal fluids from different vent fields along the Mid-Atlantic Ridge.....	22
Table 2.2. Hydrothermal vent deposits used to characterize the microbial communities from the Rainbow (Rb) and Lucky Strike (LS) vent fields.....	26
Table 2.3. Comparison of OTU richness and Chao1 diversity estimates generated from two different clustering methods for archaeal and bacterial communities of hydrothermal vent deposits collected along the Mid-Atlantic Ridge.....	30
Table 2.4. SIMPER analysis was used to identify archaeal genera responsible for the dissimilarity observed in the communities of Rainbow and Lucky Strike vent deposits.....	38
Table 2.5. End-member fluid chemistry of samples used for microbial community characterizations.....	44
Table 2.6. SIMPER analysis was used to identify bacterial genera responsible for the dissimilarity observed in the communities of Rainbow and Lucky Strike vent deposits.....	47

Table 3.1. Range of physico-chemical characteristics of end-member hydrothermal fluids from different vent fields along the Eastern Lau Spreading Center.....	64
Table 3.2. Hydrothermal deposits collected from the Eastern Lau Spreading Center used for microbial community characterization.....	67
Table 3.3. Results of AmpliconNoise analysis of four archaeal pyrosequencing libraries from vent deposits of the Eastern Lau Spreading Center.....	71
Table 3.4. Results of pairwise comparisons of bacterial communities from different vent fields along the Eastern Lau Spreading Center using the ANOSIM test in Primer v6.....	78
Table 3.5. Results of pairwise comparisons of archaeal communities from different vent fields along the Eastern Lau Spreading Center using the ANOSIM test in Primer v6.....	82
Table 4.1. Location of hydrothermal vent fields where novel thermoacidophilic bacteria were isolated.....	95
Table 4.2. Several of the new isolates and other Deltaproteobacteria have intervening sequences (IVSs) in their 16S rRNA genes.....	99
Table 4.3. Comparison of physiological traits of four new isolates with <i>Hippea maritima</i> MH2 ^T	102
Table 5.1. Summary of 16S rRNA gene sequences previously detected in marine hydrothermal environments.....	111

Table 5.2. Results of qPCR assays to determine the occurrence and relative abundance of the DHVE2 in hydrothermal vent deposits from several different vent fields.....	119
Table 5.3. Results of qPCR assays to determine the occurrence and relative abundance of the DHVE2 in hydrothermal vent deposits from the East Pacific Rise (EPR).....	121
Table 5.4. Results of qPCR assays to determine the occurrence and relative abundance of the DHVE2 in hydrothermal vent deposits from the Guaymas Basin.....	122
Table 5.5. Results of qPCR assays to determine the occurrence and relative abundance of the DHVE2 in hydrothermal vent deposits from the Mid-Atlantic Ridge...	124
Table 5.6. Results of qPCR assays to determine the occurrence and relative abundance of the DHVE2 in hydrothermal vent deposits from the Eastern Lau Spreading Center.....	126
Table 5.7. Results of local similarity analysis illustrating the co-occurrence of the DHVE2 with other archaeal OTUs.....	131
Table 5.8. Hydrothermal vent deposits from which new DHVE2 isolates were obtained.....	135

List of Figures

Figure 1.1. Global distribution of known (red) hydrothermal venting along mid-ocean ridges, back-arc basins, rifted arcs, and at submerged island-arc volcanoes.....	3
Figure 1.2. Hydrothermal circulation along mid-ocean ridges depicting compositional changes of seawater and microbial habitats supported by hydrothermal fluids...	6
Figure 2.1. Photographs of hydrothermal vent samples collected from the Rainbow and Lucky Strike vent fields.....	25
Figure 2.2. Rarefaction analysis illustrates the greater diversity observed in the bacterial communities of twelve hydrothermal deposit samples collected from the Rainbow and Lucky Strike vent fields.....	29
Figure 2.3. 16S rRNA gene surveys reveal partitioning of the archaeal and bacterial communities between the ultramafic-hosted Rainbow (red) and basalt-hosted Lucky Strike (blue) vent fields along the Mid-Atlantic Ridge.....	32
Figure 2.4. 16S rRNA gene surveys reveal partitioning of the archaeal and bacterial communities between the ultramafic hosted Rainbow (red) and basalt-hosted Lucky Strike (blue) vent fields along the Mid-Atlantic Ridge. Communities clustered using MDS of the unweighted (A and D) and weighted (B and E) UniFrac distances for archaeal (A, B) and bacterial (D, E) communities.....	33
Figure 2.5. Comparison of taxonomic variation in the archaeal and bacterial communities of Rainbow and Lucky Strike hydrothermal vent deposits.....	36

Figure 2.6. Quantitative polymerase chain reaction assays targeting the gene diagnostic for methanogenesis (<i>mcrA</i>) confirms the absence of methanogens at Lucky Strike.....	37
Figure 2.7. Concentrations across a uniformly porous ($\phi=0.5$) 3-cm thick chimney wall resulting from transport between seawater (at position = -3 cm) and A, 220°C Sintra vent fluid (Lucky Strike), B, 305°C Marker 6 vent fluid (Lucky Strike), C, 350°C Flores5 vent fluid (Rainbow) at position = 0 cm by diffusion and advection of vent fluid outward at a rate of 2×10^{-7} m s ⁻¹ (u).....	40
Figure 2.8. Concentrations across a uniformly porous ($\phi=0.5$) 3-cm thick chimney wall resulting from transport between seawater (at position = -3 cm) A, 220 °C Sintra vent fluid (Lucky Strike), B, 305 °C Marker 6 vent fluid (Lucky Strike), C, 350 °C Flores5 vent fluid (Rainbow) at position = 0 cm by diffusion only.....	41
Figure 2.9. Photograph of the hydrothermal vent chimney used for samples Rb-2 and Rb-3.....	44
Figure 2.10. Comparison of taxonomic variation in the bacterial communities of Rainbow and Lucky Strike hydrothermal vent deposits.....	46
Figure 3.1. Location of hydrothermal vent fields along the Eastern Lau Spreading Center in the western Pacific Ocean.....	63
Figure 3.2. Location of deposits collected from each hydrothermal vent field along the Eastern Lau Spreading Center.....	68

Figure 3.3. OTU richness (dark grey bars) and Chao1 diversity estimates (light grey bars) of bacterial diversity for each vent deposits characterized from the Eastern Lau Spreading Center.....	73
Figure 3.4. Rarefaction curves for bacterial communities of hydrothermal vent deposits from different vent fields along the Eastern Lau Spreading Center.....	74
Figure 3.5. OTU richness (dark grey bars) and Chao1 diversity estimates (light grey bars) of archaeal diversity for each vent deposits characterized from the Eastern Lau Spreading Center.....	75
Figure 3.6. Relative abundance of epsilonproteobacterial genera (a) and other bacterial taxa (b) observed in hydrothermal vent deposits collected from the Eastern Lau Spreading Center.....	76
Figure 3.7. Non-metric multidimensional scaling plots (MDS) based on Bray-Curtis similarities of the bacterial (a) and archaeal (b) communities of hydrothermal vent deposits from the Eastern Lau Spreading Center.....	77
Figure 3.8. Rarefaction curves for archaeal communities of hydrothermal vent deposits from different vent fields along the Eastern Lau Spreading Center.....	79
Figure 3.9. Relative abundance of archaeal families (a) observed in individual deposits and average abundance of discriminating archaeal families (b) observed in deposits within individual vent fields along the Eastern Lau Spreading Center.....	81
Figure 4.1. Predicted secondary structure of intervening sequences in the 16S rRNA of several of the new isolates and close relatives.....	98

Figure 4.2. Maximum-likelihood tree based on 16S rRNA gene sequence comparisons of thirteen novel thermoacidophilic <i>Desulfurellaceae</i> and other families of the <i>Deltaproteobacteria</i>	101
Figure 4.3. Thin section electron micrographs of strains Mar08-272rT (a), Mar08-368r (b), KM1T (c) and EP5rT (d).....	106
Figure 5.1. Photographs of a horizontal flange deposit (A) and vertical chimneys (B) from the Eastern Lau Spreading Center.....	120
Figure 5.2. Results of local similarity analysis showing OTUs that are negatively (red lines) and positively (green lines) correlated with the DHVE2 (yellow circles).....	132
Figure 5.3. Neighbor-joining tree based on 16S rRNA gene sequence comparisons of 15 novel DHVE2 isolates and other archaeal families.....	137

Chapter 1: Introduction

Flores, G. E. and Reysenbach, A.-L. (2011) Hydrothermal environments, marine. *In Encyclopedia of Earth Science Series: Encyclopedia of Geobiology*, J. Reitner, and V. Thiel (ed.), Springer, Dordrecht, The Netherlands, p. 456-466.

Preface

The discovery of deep-sea hydrothermal vents and the lush biological communities associated with these environments in the late 1970's ushered in a new era for marine biologists. Prior to this discovery, life in the deep-sea was thought to be dependent on the settling of detrital material from the productive overlaying surface waters. While this is true for much of the ocean basins, the level of production observed at these newly discovered vent sites was too great to be supported by these mechanisms alone. It soon became evident that life in these environments was supported by chemosynthetic primary production in which microorganisms harnessed the abundant geochemical energy available in the hydrothermal fluids. This challenged one of the basic ecological premises that all ecosystems on Earth were dependent on light energy and driven by photosynthetic primary production.

Since those initial revelations, research efforts have focused on assessing the microbial diversity and attempting to understand the intimate associations between microbial productivity, geology and geochemistry in marine hydrothermal

environments. The following is a general discussion of the trends that are beginning to emerge from these efforts. Included in the discussion are overviews of the geologic setting of marine hydrothermal systems, the generation of hydrothermal fluids from different geologic settings and the types of mineral structures formed.

Geologic Setting

Most seafloor hydrothermal vent systems are associated with extensional tectonic activity and heated by magmatic heat as it is convected into the crust (Seyfried and Mottl, 1995). The most well studied areas of hydrothermal circulation are along divergent plate boundaries where basaltic seafloor is made and mid-ocean ridges (MOR) arise (Figure 1.1). Hydrothermal circulation along MORs results from the active heating of seawater that percolates through newly formed crust. Hydrothermal venting is also commonly found along convergent plate margins where an oceanic plate is subducted beneath a continental plate forming island arcs and back-arc basins. Vents along back-arc basins are actively heated in the same way as those along MOR, although the fluids tend to be more heterogeneous due to the variability in magma composition and additional inputs from the subducting plate. A third location where seafloor hydrothermal systems can be found is at intra-plate volcanic hot spots. Volcanic hot spot systems are not directly associated with tectonic plate margins, but are actively heated as plumes of molten magma push up through the mantle and crust (Seyfried and Mottl, 1995).

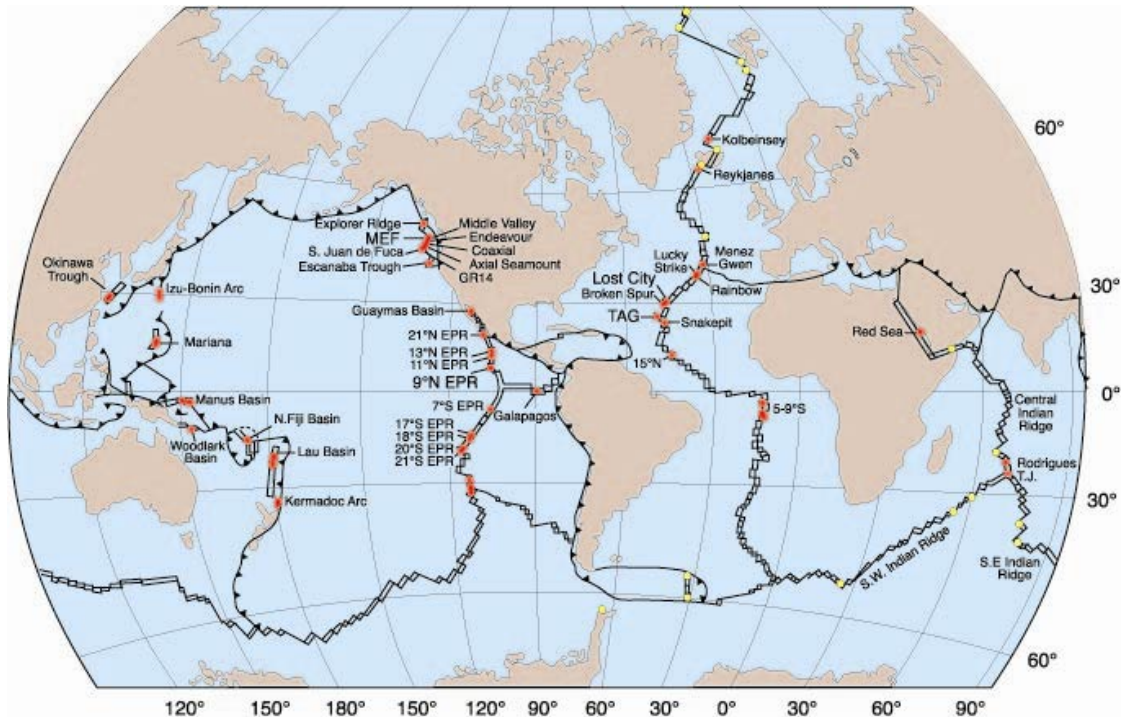


Figure 1.1. Global distribution of known (red) hydrothermal venting along mid-ocean ridges, back-arc basins, rifted arcs, and at submerged island-arc volcanoes. Yellow circles indicate areas where mid-water column chemical anomalies have been detected suggesting hydrothermal activity. EPR = East Pacific Rise, TAG = Trans Atlantic Geotraverse, MEF = Main Endeavour Field, and GR-14 = Sea Cliff hydrothermal field on the northern Gorda Ridge. Figure modified after (Tivey, 2007).

Hydrothermal fluid generation

Seawater heated in contact with subsurface rocks significantly alters the chemical composition of the end member fluids. The degree of alteration is influenced by several factors including the initial composition of the seawater, the type and structure of the host rock, the presence of sediment overlaying the host rock and the type, depth, and size of the heat source (Tivey, 2007). Understanding these interactions and how they affect the composition of hydrothermal fluids is important as the fluids set

the physiological parameters and provide the metabolic menu for colonizing microbes. For comparison, representative compositions of hydrothermal fluids from different geologic settings are presented in Table 1.1.

Table 1.1. Representative chemical compositions of hydrothermal fluids from different geologic settings.

	Bottom seawater	Mid-ocean ridge	Back-arc basin	Sediment hosted	Ultramafic- hosted vent field (Rainbow)
T (°C)	2	≤ 405	278-334	100-315	365
pH (25°C)	8	2.8-4.5	< 1-5.0	5.1-5.9	2.8
SO ₄ , mmol/kg	28	0	0	0	0
Mg, mmol/kg	53	0	0	0	0
Cl, mmol/kg	545	30.5-1245	255-790	412-668	750
Na, mmol/kg	464	10.6-983	210-590	315-560	553
Ca, mmol/kg	10.2	4.02-109	6.5-89	160-257	67
K, mmol/kg	10.1	1.17-58.7	10.5-79	13.5-49.2	20
H ₂ S, mmol/kg	-	0-19.5	1.3-13.1	1.10-5.98	1
H ₂ , mmol/kg	-	0.0005-38	0.035-0.5	-	13
CO ₂ , mmol/kg	2.36	3.56-39.9	14.4-200	-	-
CH ₄ , mmol/kg	-	0.007-2.58	0.005-0.6	-	0.13-2.2
NH ₃ , mmol/kg	-	< 0.65	-	5.6-15.6	-
Fe, μmol/kg	-	7-18700	13-2500	0-180	24000
Mn, μmol/kg	-	59-3300	12-7100	10-236	2250
Cu, μmol/kg	-	0-150	0.003-34	< 0.02-1.1	140
Zn, μmol/kg	-	0-780	7.6-3000	0.1-40	160
Pb, μmol/kg	-	0.183-0.1630	0.036-3.9	< 0.02-0.652	0.148

Modified after Tivey (2007).

Water-rock reactions begin as cold seawater infiltrates shallow crustal-rocks in the recharge zones (Figure 1.2). Initial low temperature reactions ($\leq 60^{\circ}\text{C}$) result in the removal of alkali metals from seawater and the oxidation of basaltic minerals (e.g., olivine and plagioclase) with the concomitant leaching of silica (Si), sulfur (S), and sometimes magnesium (Mg) from the minerals (Alt, 1995). Magnesium is eventually completely removed from the fluids as Mg-rich clays precipitate at temperatures above 150°C . Anhydrite (CaSO_4) precipitation and seawater sulfate (SO_4^{2-}) reduction also occurs in the recharge zone at temperatures above 150°C resulting in the complete removal of SO_4^{2-} from the fluids. As the fluid continues through the crust, reactions with iron-bearing minerals like olivine and pyroxene result in highly reducing fluids with elevated concentrations of hydrogen gas (H_2) (Tivey, 2007). Upon reaching the reaction zone where fluids are heated upwards of 400°C , the fluid obtains its chemical signature by leaching S and metals (copper-Cu, iron-Fe, manganese-Mn, zinc-Zn) from the surrounding rocks (Alt, 1995). Phase separation may also occur in the reaction zone if temperature and pressure are greater than 407°C and 298 bars, respectively (Von Damm, 1995). Phase separation can have a significant impact on the composition of end member fluids as volatiles like hydrogen-sulfide (H_2S) tend to partition in the vapor phase while metals like Fe become enriched in the liquid (brine) phase. Gasses such as helium (He), methane (CH_4) and carbon-dioxide (CO_2) may also be added to the hydrothermal fluids as volatiles from the underlying magma (Alt, 1995). In total, these reactions result in end member fluids that are acidic (pH 2.8 – 4.5), highly reduced, rich in H_2S and metals, and up to 400°C . The fluid is also extremely buoyant relative to

seawater and is forced back to the seafloor through the discharge zone and may emerge as diffuse or focused flow depending on the degree of subsurface mixing during the ascent (Figure 1.2).

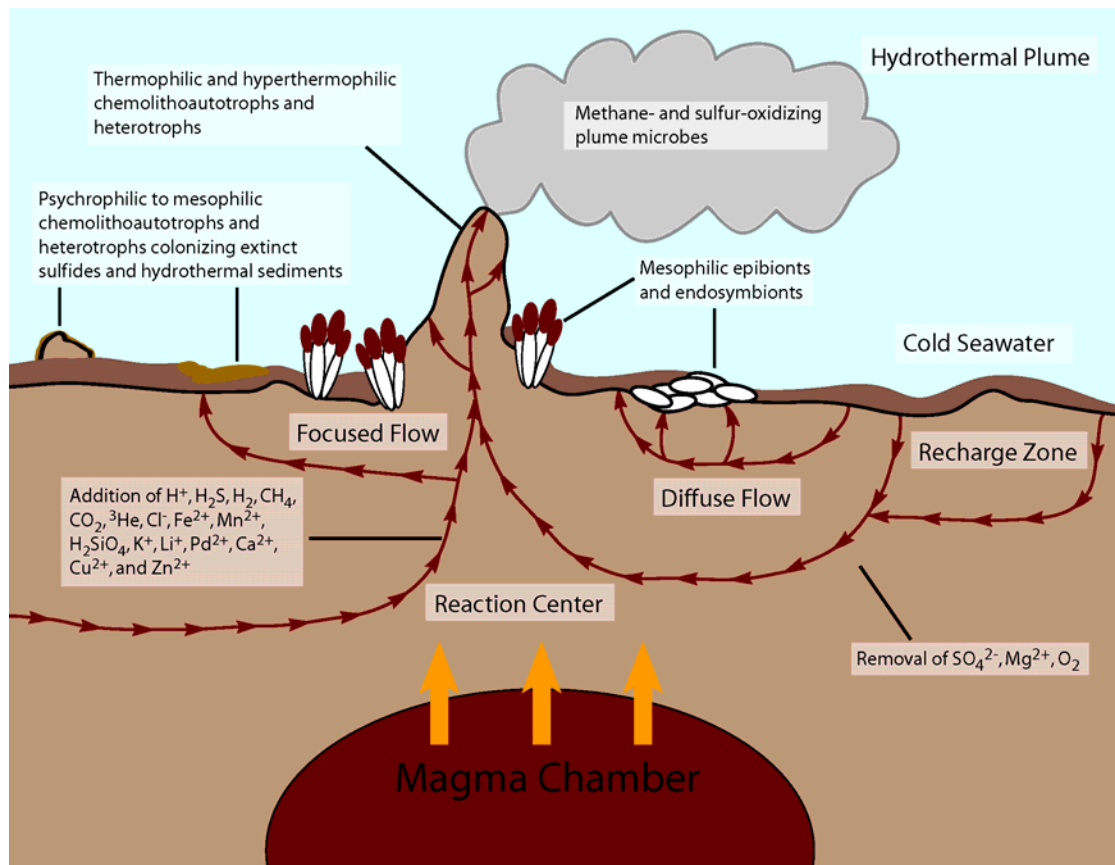


Figure 1.2. Hydrothermal circulation along mid-ocean ridges depicting compositional changes of seawater and microbial habitats supported by hydrothermal fluids. Small arrows indicate fluid flow while large arrows indicate heat transfer from magmatic source. Image is not drawn to scale.

While the transformations described above generally apply to all marine hydrothermal environments, other factors, such as differences in host rock composition and sediment cover, can contribute to the geochemistry of end member fluids. The

impact that different host rocks have on fluid chemistry is best illustrated by the ultramafic-hosted (peridotite) Rainbow vent field along the Mid-Atlantic Ridge (Douville *et al.*, 2002). Fluids from Rainbow vent field are lower in pH, have much higher Fe concentrations, are enriched in H₂ and CH₄, and are depleted in H₂S relative to fluids from most MOR systems (McCollom, 2007). Sediments overlying the host rock, as is seen in the Guaymas Basin, can also affect the composition of end-member fluids. In general, sediment hosted systems generate fluids that are higher in pH (5.1 – 5.9) and lower in metal contents than those from unsedimented systems. Chemical differences largely depend on the amount and type of organic matter present in the sediments (Tivey, 2007).

Hydrothermal mineral deposits

When acidic hydrothermal fluids rich in reduced chemical species interact with cold, oxygenated seawater, minerals rapidly precipitate out of solution forming large mineral deposits (Juniper and Tebo, 1995). Mineral phases found in these deposits include sulfides, sulfates, oxides, hydroxides, silicates and carbonates. Deposit formation can occur in the subsurface as the fluids ascend through oceanic crust and mix with infiltrating seawater or directly on the seafloor as high temperature fluids erupt into bottom seawater. Subsurface precipitation of minerals generates stockwork deposits in the shallow crust and results in low-temperature venting on the seafloor. Low-temperature fluids are generally low in metal-sulfides and as result, precipitate oxides upon reaching the seafloor. In contrast, fluids that have not been diluted and

cooled in the subsurface rapidly precipitate metal sulfides like pyrite (FeS_2), chalcopyrite (CuFeS_2) and sphalerite (ZnS) upon mixing with seawater. Precipitation of metal sulfides results in the appearance of “black smoke” and ultimately forms massive sulfide deposits (> 60% sulfide minerals). Several types of sulfide features are found in vent fields with the most spectacular being the black smoker chimney. Other sulfide structures generated at marine hydrothermal vents include diffuse flow beehives, horizontal shelf-like flanges and complex flow sulfide mounds (Van Dover, 2000). In all cases, active deposits provide extreme physical and geochemical gradients that sustain diverse microbial populations.

Energy sources

Seafloor hydrothermal ecosystems are supported primarily by chemosynthetic primary production fueled by the chemical disequilibrium between the oxygenated seawater and the reduced hydrothermal fluids. Microorganisms capture this energy by way of reduction/oxidation (redox) reactions in which seawater typically provides the oxidant (O_2 , SO_4^{2-} , NO_3^- , CO_2) and the hydrothermal fluids provide the reductant (H_2 , H_2S , HS^- , S^0 , $\text{S}_2\text{O}_2^{3-}$, Fe^{2+}). Redox reactions generate energy that is used to fix CO_2 into cellular material that then provides organic carbon for various heterotrophic microbes and animals that make up the remainder of the community. Examples of thermodynamically favorable reactions found in marine hydrothermal environments are presented in Table 1.2.

Table 1.2. Examples of thermodynamically favorable redox pairs utilized by microorganisms from marine hydrothermal environments.

Conditions	Electron donor	Electron acceptor	Free energy ΔG^a (kJ/mol)	Metabolic Process
Aerobic	H ₂	O ₂	-237	hydrogen oxidation
	HS ⁻	O ₂	-797	sulfide oxidation
	S ⁰	O ₂	-585	sulfur oxidation
	S ₂ O ₂ ³⁻	O ₂	-952	thiosulfate oxidation
	Fe ²⁺	O ₂	-44.3	iron oxidation
	NH ⁴⁺	O ₂	-275	nitrification
	CH ₄ + other C-1 compounds	O ₂	~810	methane oxidation
	Organics	O ₂	~477	heterotrophic metabolism
Anaerobic	H ₂	NO ₃ ⁻	-239	denitrification
	H ₂	S ⁰	-98.3	sulfur reduction
	H ₂	SO ₄ ²⁻	-38.1	sulfate reduction
	H ₂	CO ₂	-34.7	methanogenesis
	Organics	SO ₄ ²⁻	~40.6	heterotrophic sulfate reduction
	Organics	S ⁰	~25.1	heterotrophic sulfur reduction
	Organics	Organics	~38.5	fermentation ^b

Compiled and adapted from Jannasch (1995), and Karl (1995b).

^aValues calculated using standard conditions (pH 7, 25°C, 1 atm)

^bexample reaction calculated from acetate + ethanol → butyrate + water.

Reactions are expressed in terms of the change in free energy (ΔG) where the more negative the value the more energy an organism will gain by catalyzing the reaction. Calculated values suggest that aerobic oxidation of reduced sulfur compounds (HS⁻, S⁰, S₂O₂³⁻) are the most energetically favorable and potentially the most significant reactions in terms of biomass production in marine hydrothermal environments. Thermodynamic calculations, however, can be misleading as they do not consider the bioavailability of certain reactants and potential kinetic inhibition under different environmental conditions (Takai *et al.*, 2006a). Several past studies have attempted to model the overall energetics in a variety of marine hydrothermal systems considering such factors (McCollom and Shock, 1997; McCollom, 2000; McCollom,

2007). An interesting conclusion from a theoretical study is that four times as much energy per kg of hydrothermal fluid is available to H₂-oxidizers in ultramafic hosted systems than to sulfur-oxidizers because of the increase concentrations of H₂ (McCollom, 2007). This suggests that H₂-oxidizers may be more important than sulfur-oxidizers in ultramafic hosted systems. A recent report lends support to this hypothesis as the diversity of H₂-oxidizing bacteria was found to increase as the concentration of H₂ gas increased in vents sampled from the ultramafic hosted Logatchev vent field along the MAR (Perner *et al.*, 2007). These studies speak to the tight coupling of geochemistry and microbial primary production in marine hydrothermal environments.

Microbial Habitats and Diversity

Seafloor hydrothermal systems provide several habitats over a wide range of physical environments that sustain distinct microbial communities. Such environments include active and inactive vent deposits, biotic and abiotic surfaces receiving hydrothermal fluid inputs, inside vent animals (endosymbionts) and hydrothermal vent plumes (Figure 1.2) (Karl, 1995a; Van Dover, 2000; Takai *et al.*, 2006a). Many of these environments are exposed to varying inputs of hydrothermal fluids resulting in fluctuating temperatures and chemistry. Below is a brief discussion of each of these habitats and their associated microbial biodiversity. These biodiversity assessments are based on growing and characterizing isolates under laboratory conditions (cultivation-dependent) and through molecular phylogenetic approaches that are cultivation-independent. This latter approach is based on extracting genomic DNA from

environmental samples, and then amplifying a section of a diagnostic phylogenetic marker for Bacteria and Archaea, the small subunit rRNA gene (16S rRNA), using the polymerase chain reaction (PCR).

Active vent deposits

Using cultivation-dependent and cultivation-independent techniques, a rich diversity of Bacteria and Archaea has been found associated with active vent deposits (Jannasch, 1995; Karl, 1995b; Takai *et al.*, 2006a). Free-living microorganisms supported by active deposits include mesophilic, thermophilic and hyperthermophilic chemolithoautotrophs, heterotrophs and mixotrophs. Organisms can be anaerobes, facultative anaerobes, microaerophiles and obligate aerobes. In general, Bacteria are the most numerically abundant microorganisms associated with vent deposits (Jannasch, 1995; Karl, 1995b; Takai *et al.*, 2006a). Their abundance can range anywhere from 35 – 99% of the microbial population depending on the method used to measure abundance (e.g., FISH, qPCR, MPN), the type of vent structure (e.g., chimney, flange, diffuse flow beehive), and where within a deposit one examines (e.g., outer, inner) (Harmsen *et al.*, 1997; Takai and Horikoshi, 1999; Takai *et al.*, 2001; Hoek *et al.*, 2003; Schrenk *et al.*, 2003; Nakagawa *et al.*, 2006).

Within the Bacteria, members of the *Epsilonproteobacteria* consistently dominate microbial communities in deep-sea hydrothermal environments (Reysenbach *et al.*, 2000; Hoek *et al.*, 2003; Nakagawa *et al.*, 2005c; Campbell *et al.*, 2006). These free-living deep-sea *Epsilonproteobacteria* are mesophilic to moderately thermophilic.

Recently, several representatives have been obtained in pure culture that are chemolithoautotrophs capable of oxidizing H_2 and sulfur compounds while using O_2 , NO_3^- or sulfur compounds as terminal electron acceptors (Campbell *et al.*, 2006). Like in cave environments, the *Epsilonproteobacteria* play an essential role in sulfur and carbon cycling at deep-sea vents.

Other commonly identified but less abundant bacterial members of the free-living microbial communities include the thermophilic *Aquificales* and *Thermotogales*, as well as other classes of *Proteobacteria* (Miroshnichenko and Bonch-Osmolovskaya, 2006). The *Aquificales* are globally distributed at marine hydrothermal environments but are restricted to active deposits and hydrothermal fluids due to their thermophilic lifestyle. They are generally chemolithoautotrophs and chemoorganotrophs capable of oxidizing H_2 , S^0 and $S_2O_3^{2-}$ either aerobically or anaerobically with NO_3^- or sulfur compounds as electron acceptors. The *Thermotogales*, on the other hand, are strictly anaerobic, thermophilic heterotrophic fermenters (Boone *et al.*, 2001).

As stated above, Archaea are less abundant in active vent deposits, yet they play a key biogeochemical role especially at the higher temperatures. Some of the most exhaustive studies on microbial diversity at deep-sea vents have focused solely on the Archaea revealing a high phylogenetic and metabolic diversity within this domain (Takai and Horikoshi, 1999; Takai *et al.*, 2001; Nercessian *et al.*, 2003; McCliment *et al.*, 2006). Most of the Archaea found here are thermophilic to hyperthermophilic and are thus restricted to areas most influenced by hydrothermal fluids. Within the Archaea, the two main phyla, the *Crenarchaeota* and *Euryarchaeota*, are well represented at

deep-sea vents, while the enigmatic *Korarchaeota* and *Nanoarchaeota* are occasionally detected (Takai *et al.*, 2006a).

Crenarchaeota commonly detected in deep-sea vent deposits include cultivated members of the *Desulfurococcales* (e.g., *Pyrodictium* and *Pyrolobus*) and several uncultivated groups like the deep-sea hydrothermal vent crenarchaeotal group (DHVC1), and the marine group I (Takai and Horikoshi, 1999; Takai *et al.*, 2006a). *Pyrodictium* is an example of a hyperthermophilic mixotrophic organism with the ability to use either H₂ or complex organics to reduce elemental sulfur (Reysenbach *et al.*, 2002). *Pyrolobus* is also a hyperthermophile but, unlike *Pyrodictium*, *Pyrolobus* is an obligate chemolithoautotroph that can only use H₂ to reduce nitrate (NO₃⁻), thiosulfate (S₂O₃²⁻) or O₂.

Euryarchaeota commonly found at marine hydrothermal systems include the hyperthermophilic methanogens (*Methanocaldococcus* spp.), the hyperthermophilic SO₄²⁻ reducing *Archaeoglobales*, and a variety of thermophilic fermentative *Thermococcus* species (Takai and Horikoshi, 1999; Takai *et al.*, 2006a). While these are readily grown in the laboratory, their relative abundance in the environment has been shown to vary from site to site (Reysenbach *et al.*, 2000; Takai *et al.*, 2001; Hoek *et al.*, 2003; Nercessian *et al.*, 2003; McCliment *et al.*, 2006). Several lineages often detected at vent sites around the globe have been classified as the deep-sea hydrothermal vent euryarchaeota (DHVE) groups (Takai and Horikoshi, 1999; Reysenbach *et al.*, 2000; Takai *et al.*, 2001; Hoek *et al.*, 2003; Nercessian *et al.*, 2003). Several subdivisions exist within this group but at least one lineage, the DHVE2,

appears to be endemic to deep-sea vents. Little was known about this lineage until Moussard *et al.* (2006b) showed optimal activity and thermostability of a DNA polymerase belonging to this lineage which suggested a thermophilic lifestyle. Thermophily was confirmed when the first isolate was obtained in pure culture (Reysenbach *et al.*, 2006). The organism, *Aciduliprofundum boonei*, is a heterotrophic thermoacidophile capable of fermenting peptides and reducing Fe and S. Isolation of this organism was significant because it is the first obligate acidophile isolated from a deep-sea vent and the first member of the DHVE2 lineage to be grown in the laboratory. Prior to this discovery, the absence of acidophiles from a deep-sea vent had always puzzled microbiologists as hydrothermal fluids are acidic and geochemists had predicted the presence of acidic microhabitats within sulfide chimneys (Von Damm, 1995; Tivey, 2004).

Inactive vent deposits

Hydrothermal fluid flow through individual deposits is temporary as subsurface flow paths constantly change and structures collapse. Inactive deposits are subjected to low temperature oxidative weathering in which the reduced sulfur moiety is converted to soluble SO_4^{2-} and the metals, mostly Fe, are converted to insoluble oxy-hydroxide crusts (Juniper and Tebo, 1995). Oxidation occurs abiotically as oxygenated seawater penetrates the rock but can also be mediated by S- and Fe-oxidizing bacteria (Edwards, 2004; Edwards *et al.*, 2005). While microbial mediated sulfide weathering in terrestrial systems has been studied for decades, this area of research is in its infancy in the deep-

sea (Edwards *et al.*, 2003a; Edwards *et al.*, 2003b; Rogers *et al.*, 2003; Edwards, 2004; Suzuki *et al.*, 2004). Culturing studies have resulted in the isolation of several psychrophilic, neutrophilic Fe-oxidizing bacteria belonging to the *Alphaproteobacteria* and *Gammaproteobacteria* from sulfide rocks collected along the Juan de Fuca Ridge (Edwards *et al.*, 2003b). A follow up study with one of the *Gammaproteobacteria* isolates showed that the organism promoted the dissolution of native sulfide minerals under anaerobic conditions (Edwards, 2004). Although the mechanism of dissolution remains unclear, these studies illustrate that Fe-oxidizing bacteria are associated with extinct sulfide minerals on the seafloor and can actively promote the dissolution of these minerals at least in the laboratory.

Biotic and abiotic surfaces

Microbes are opportunistic organisms and will colonize any surface where growth substrates are provided. In areas influenced by hydrothermal fluids, this includes the sulfide deposits as described above and surfaces of invertebrate animals (reviewed in Van Dover, 2000). Some of these relationships are commensal as the host does not appear to gain an advantage by being colonized while others are symbiotic (episymbiosis) with both the host and microbes benefiting. An episymbiotic relationship is found on the polychaete worm *Alvinella pompejana* (Van Dover, 2000). *Alvinella pompejana* lives in tubes on the sides of black smoker chimneys where water temperatures can exceed 70°C (reviewed in Desbruyeres *et al.*, 1998). It has a fully functional digestive system and appears to feed upon microbial mats inside of its tube as

well on sulfide surfaces. The worm also houses diverse microbial communities on its dorsal surfaces including microaerophilic H₂S-oxidizing members of the *Epsilonproteobacteria*. Although the exact nature of this relationship is unknown, it is thought that the bacteria may detoxify H₂S or provide nutritional supplement to the worm.

In addition to surfaces of vent animals, microbes often colonize rocks and sediments surrounding hydrothermal vents. These environments are primarily sustained by hydrothermal fluids flowing diffusely through the underlying porous sediments. The best studied and possibly most diverse microbial mat system found in marine hydrothermal environments is in the sediment-hosted Guaymas Basin. Microbes found here include thermophilic/mesophilic methanogens and methanotrophs (Dhillon *et al.*, 2005), SO₄²⁻ reducing Bacteria (Kallmeyer and Boetius, 2004), H₂S-oxidizing *Gammaproteobacteria* (Nelson *et al.*, 1989) and even spore forming Mn-oxidizers (Dick *et al.*, 2006). Much of this diversity is fueled by the presence of overlying sediments which provides different combinations of organic/inorganic substrates typically not found in non-sediment hosted systems.

Endosymbionts

Several invertebrate animals form obligate symbiotic relationships in which the bacteria are hosted inside the animal cells. The best studied example is in the giant tube worm *Riftia pachyptila* (reviewed in Minic and Herve, 2004). As adults, *Riftia* completely lack a mouth, digestive system and anus and are sustained by

chemoautotrophic H₂S-oxidizing *Gammaproteobacteria* (Cavanaugh *et al.*, 1981; Felbeck, 1981; Jones, 1981; Minic and Herve, 2004). In this relationship, *Riftia* provides the bacteria with inorganic carbon, O₂, H₂S and NO₃⁻ and, in turn is provided with organic carbon. Other invertebrate organisms like the giant clam *Calypptogena magnifica* and the mytilid mussels *Bathymodiolus* spp. also house H₂S-oxidizing endosymbionts in their gill tissues (Van Dover, 2000). The symbiotic relationship between mussels and bacteria, however, is not obligate as they retain some of their filter feeding capabilities. In addition, certain species of *Bathymodiolus* have methanotrophic (CH₄-oxidizing) endosymbionts and even dual symbionts with both sulfur- and CH₄-oxidizing bacteria.

Hydrothermal plumes

Upon reaching neutral buoyancy, hydrothermal vent plumes carrying elevated concentrations of S, metals (Fe and Mn), H₂, and CH₄ extend hundreds of meters laterally into the water column. Not surprising, elevated biomass has been detected in plumes suggesting that these environments are areas of high productivity (reviewed in (Winn *et al.*, 1995). Methane-oxidation has been measured in plume waters collected along the Juan de Fuca Ridge further supporting microbial activity in vent plumes (De Angelis *et al.*, 1993). More recently, Sunamura and colleagues, (2004) used cultivation-independent techniques to assess the diversity of microbes in plumes over the Suiyo Seamount. Members of the *Gammaproteobacteria* and *Epsilonproteobacteria* were dominant in the plume waters and are likely using reduced

sulfur compounds because of their close phylogenetic relationship with known sulfur-oxidizers (Sunamura *et al.*, 2004).

The first aerobic anoxygenic photosynthetic bacteria from the deep-sea were isolated from plumes (Yurkov and Beatty, 1998). These organisms belong to the *Alphaproteobacteria* and appear to supplement heterotrophic growth with photosynthesis under laboratory conditions. Their presence in deep-sea hydrothermal environments seems puzzling because of the lack of sunlight, but high-temperature fluids ($\approx 350^{\circ}\text{C}$) have been detected to emit photons capable of supporting facultative photosynthetic bacteria (Van Dover *et al.*, 1996). Their role and significance in the environment, however, remains unknown.

Scope of Dissertation

Despite over thirty years of study, the abiotic controls on microbial diversity in marine hydrothermal environments remain largely unknown. In particular, how differences in the geologic settings of vent fields influence archaeal and bacterial communities of active hydrothermal vent deposits at the vent field scale is poorly understood. Differences in the geologic settings of vent fields can alter end-member fluid chemistry and are expected to influence microbial diversity as the fluids provide metabolic energy sources and set the physiological boundaries for colonizing microbes. Geologic factors that alter end-member fluid chemistry include differences in host-rock composition and inputs from a subducting plate along back-arc basins. For Chapter 2, I characterized the archaeal and bacterial communities of several deposits from the

basalt-hosted Lucky Strike and ultramafic-hosted Rainbow vent fields along the Mid-Atlantic Ridge (MAR) using bar-coded pyrosequencing to determine if differences in host-rock composition influenced microbial diversity of active vent deposits. This same approach was extended in Chapter 3 to six vent fields along the Eastern Lau Spreading Center (ELSC) to compare the microbial communities from geochemically distinct systems located in a back-arc basin.

While advances in sequencing technologies have revolutionized microbial ecology, cultivation-based studies remain necessary in order to make ecological inferences about microorganisms in the environment. In deep-sea hydrothermal environments, numerous archaeal and bacterial lineages are represented by none or only a few cultivated organisms. Also, for many of the organisms in culture, we know very little about global distribution patterns and what factors may be influencing these patterns. With the recent isolation of the first obligate thermoacidophile from one of the previously uncultivated archaeal lineages (Reysenbach *et al.*, 2006), it seems likely that some of the other uncultivated lineages may also be acidophilic. The overall objective for this section of my dissertation was to investigate thermoacidophily in geologically diverse hydrothermal environments by isolating novel thermoacidophiles (Chapter 4) and by conducting an in-depth survey of the distribution of the thermoacidophilic DHVE2 (Chapter 5).

Chapter 2: Microbial Community Structure of Hydrothermal Deposits from Geochemically Different Vent Fields Along the Mid-Atlantic Ridge.

Flores, GE, Campbell, JH, Kirshtein, JD, Meneghin, J, Podar, M, Steinberg, JI,
Seewald, JS, Tivey, MK, Voytek, MA, Yang, ZK and Reysenbach, A-L (2011).
Environmental Microbiology, **13**: no. doi: 10.1111/j.1462-2920.2011.02463.x.

Abstract

To evaluate the effects of local fluid geochemistry on microbial communities associated with active hydrothermal vent deposits, we examined the archaeal and bacterial communities of twelve samples collected from two very different vent fields; the basalt-hosted Lucky Strike (37°17'N, 32°16.3'W, depth 1600 to 1750 m) and the ultramafic-hosted Rainbow (36°13'N, 33°54.1'W, depth 2270 to 2330 m) vent fields along the Mid-Atlantic Ridge (MAR). Using multiplexed bar-coded pyrosequencing of the variable region 4 (V4) of the 16S rRNA genes, we show statistically significant differences between the archaeal and bacterial communities associated with the different vent fields. Quantitative polymerase chain reaction (qPCR) assays of the functional gene diagnostic for methanogenesis (*mcrA*), as well as geochemical modeling of sulfide deposits, support the pyrosequencing observations. Collectively, these results show that the less reduced, hydrogen-poor fluids of Lucky Strike limit the colonization of such strict anaerobes as methanogens, and allow for hyperthermophilic

microaerophiles, like *Aeropyrum*. In contrast, the H₂-rich reducing vent fluids of the ultramafic-influenced Rainbow vent field drive the prevalence of methanogens and other hydrogen-oxidizing thermophiles at this site. These results demonstrate that biogeographical patterns of hydrothermal vent microorganisms are shaped in part by large scale geological and geochemical processes.

Introduction

Deep-sea hydrothermal environments support highly productive biological communities comparable in total biomass production to the most prolific marine ecosystems (Sarrazin and Juniper, 1999). As the high temperature hydrothermal fluid mixes with cold oxygenated seawater, minerals precipitate to form vent mineral deposits (Tivey, 2007). These porous deposits are quickly colonized by a diversity of Archaea and Bacteria that harness the abundant geochemical energy available in the hydrothermal fluids (Page *et al.*, 2008). One of the major processes controlling the chemical composition of hydrothermal fluids is the interaction of subsurface circulating seawater with surrounding igneous rocks (Von Damm, 1995). The majority of magmatically heated vent systems thus far studied are hosted by basaltic rocks and give rise to fluids rich in H₂S (Von Damm, 1995). However, along slow- and ultra-slow spreading ridges like the Mid-Atlantic Ridge (MAR), some hydrothermal systems include reactions with ultramafic rocks (peridotite), which have significant impacts on fluid chemistry. For example, due to serpentinization reactions, hydrothermal fluids can

have elevated concentrations of H₂, Fe and CH₄, and lower levels of H₂S relative to basalt-hosted systems (Charlou *et al.*, 2002) (Table 2.1).

Table 2.1. Range of physico-chemical characteristics of end-member hydrothermal fluids from different vent fields along the Mid-Atlantic Ridge. Fluids from 13°N along the East Pacific Rise and seawater are added for comparison.

	Basalt-hosted			Ultramafic-hosted			Seawater
	13°N (EPR)	TAG	Lucky Strike	Rainbow	Logatchev	Lost City	
Temp. (°C)	317-380	290-321	163-324	191-370	347-353	40-75	4
pH (25°C)	ND	3.1	3.6-3.9	3.0-3.4	3.3-3.9	9.0-9.8	8.1
H ₂ (mM)	0.14	0.15-0.37	0.025- 0.071	12.3-16.9	12-19	0.25- 0.43	0.0004
H ₂ S (mM)	2.9-8.2	6.7	2.4-3.4	1.8-3.3	0.5-2.5	0.064	0
CH ₄ (mM)	0.051	0.124- 0.147	0.77-1.1	1.9-2.3	2.1-3.5	0.13- 0.28	0.0003
CO ₂ (mM)	11.8-18.4	2.9-3.4	35-133	21-25	10.1	ND	2.3
Fe (μM)	1450- 10,800	1640	31-863*	8100- 24100 ⁺	2410-2500	ND	0.0045
Reference	(Von Damm, 1995)	(Charlou <i>et al.</i> , 2002)	This work	This work	(Charlou <i>et al.</i> , 2002; Schmidt <i>et al.</i> , 2007)	(Kelley <i>et al.</i> , 2001)	(Schmidt <i>et al.</i> , 2007)

*Iron values reported are from Charlou *et al.*, (2002).

+Iron values reported are from Seyfried *et al.*, (2011).

Abbreviations: TAG = Trans-Atlantic Geotraverse, EPR = East Pacific Rise, ND = not determined.

While numerous molecular- and cultivation-based studies have been conducted to document the diversity of microorganisms associated with hydrothermal vent deposits, relatively few studies have explored the possible abiotic controls on microbial biogeography in these systems. Theoretically, the types and amounts of energy sources available in the hydrothermal fluids have been predicted to play a major role in determining the distribution patterns of deep-sea vent microorganisms (Shock *et al.*, 1995; Shock and Holland, 2004; Tivey, 2004; Takai *et al.*, 2006b; McCollom, 2007;

Takai and Nakamura, 2010). Of the studies that have attempted to link hydrothermal fluid chemistry with microbial community composition, most have focused on single vent fields and have been hampered by inadequate sample number and/or sequencing depth (Takai *et al.*, 2004b; Nakagawa *et al.*, 2005d; Sogin *et al.*, 2006; Huber *et al.*, 2007; Perner *et al.*, 2007; Takai *et al.*, 2008; Nunoura and Takai, 2009; Opatkiewicz *et al.*, 2009; Takai and Nakamura, 2010). Recently, Huber *et al.* (2010) overcame these limitations by employing next generation sequencing techniques to characterize the bacterial communities of diffuse fluid samples at 5 seamounts along the Mariana Arc. While the study revealed non-random distribution patterns of the dominant *Epsilonproteobacteria*, no correlations could be made between hydrothermal fluid chemistry and the observed patterns. Several factors, including the inability to detect fine-scale patterns with short 16S ribosomal RNA (rRNA) gene fragments from the hypervariable region 6 (V6), were suggested as possible reasons as to why community structure could not be correlated with fluid chemistry. As such, the impact of hydrothermal fluid chemistry on microbial community composition and/or structure remains largely unknown.

As the potential for direct coupling of geochemistry and biology is greatest at the interface where the hydrothermal fluids mix with seawater to produce mineral deposits, we hypothesized that the microbial communities associated with active vent deposits would be different in vent fields of contrasting chemistry. To address this question, we characterized the archaeal and bacterial communities of twelve deposits from two magmatically-heated hydrothermal systems; the ultramafic-hosted Rainbow

(36°13'N, 33° 54.1'W, depth 2270 to 2330 m) and the basalt-hosted Lucky Strike (37°17'N, 32° 16.3'W, depth 1600 to 1750 m) vent fields along the MAR (Figure 2.1, Table 2.2). Due to the relatively close proximity of the two vent fields (approx. 180 km apart), the likelihood that any observed differences are due to a distance-decay relationship is minimized, and therefore provide model sites for assessing the impact geological processes controlling fluid chemistry has on microbial biogeography. Both vent fields have been fairly well characterized with respect to fluid chemistry (Langmuir *et al.*, 1997; Von Damm *et al.*, 1998; Charlou *et al.*, 2002; Douville *et al.*, 2002), geologic setting (Langmuir *et al.*, 1997; Charlou *et al.*, 2002; Douville *et al.*, 2002; Humphris *et al.*, 2002; Singh *et al.*, 2006), deposit mineralogy (Rouxel *et al.*, 2004b, a; Marques *et al.*, 2006) and macrobiological communities (Desbruyeres *et al.*, 2000; Desbruyeres *et al.*, 2001).

The Rainbow vent field is located within ultramafic rocks on the western flank of a non-volcanic ridge at the intersection between the non-transform system faults and the ridge faults (Douville *et al.*, 2002). The vent field is tectonically controlled and is composed of at least ten active chimneys that emit acidic, high-temperature fluids (365°C) with relatively consistent end-member compositions indicative of a single source for the entire field (Charlou *et al.*, 2002). Hydrothermal fluids from Rainbow are influenced by serpentinization reactions and are characterized by high gas, particularly H₂, CH₄ and CO, and metal concentrations but relatively low H₂S concentrations (Table 2.1) (Charlou *et al.*, 2002; Douville *et al.*, 2002). Minerals

present in these chimneys include pyrrhotite and isocubanite, indicating relatively reducing environments (Rouxel *et al.*, 2004a).

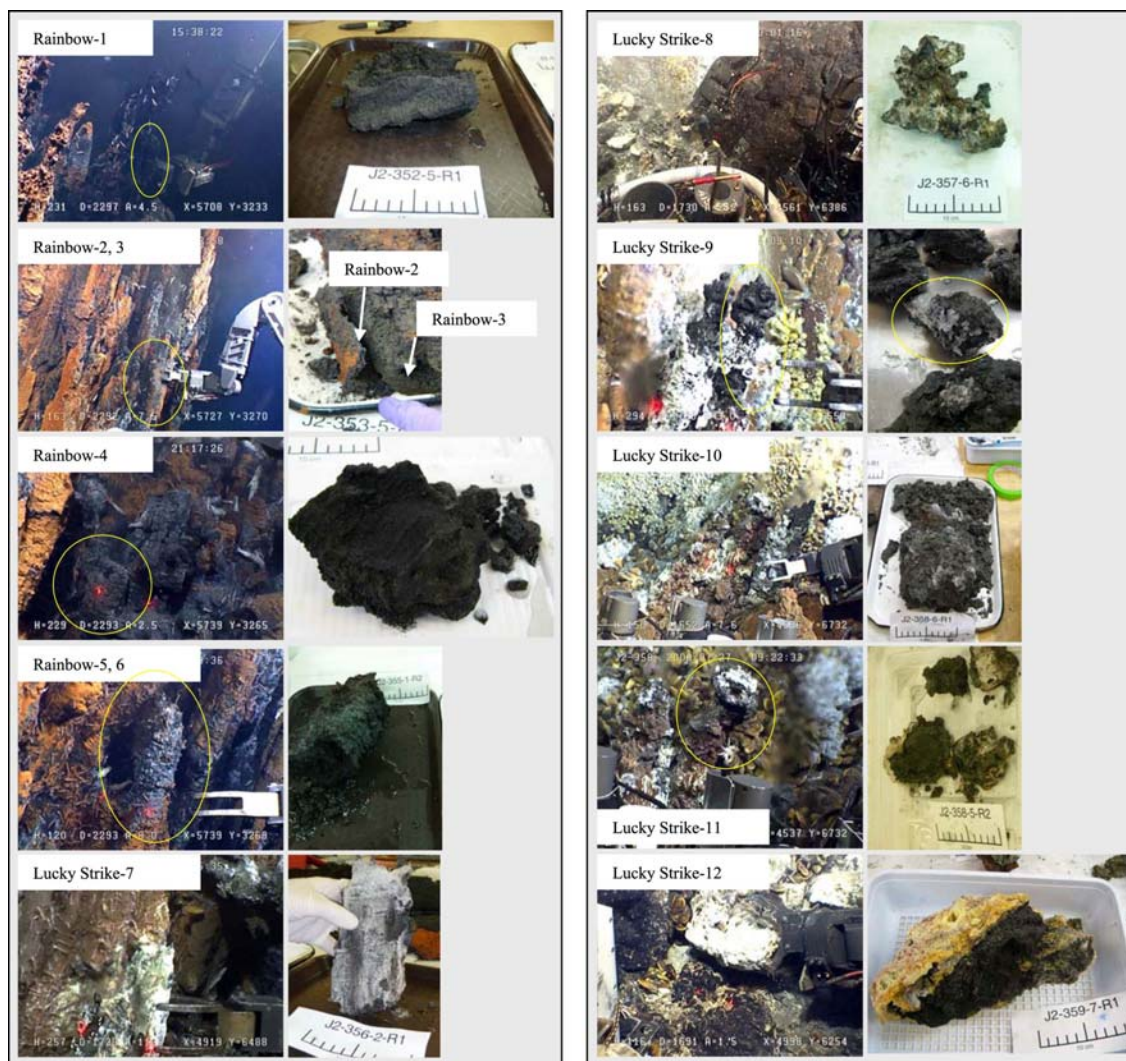


Figure 2.1. Photographs of hydrothermal vent samples collected from the Rainbow and Lucky Strike vent fields. Yellow circles indicate which chimney/section was used for sampling.

Table 2.2. Hydrothermal vent deposits used to characterize the microbial communities from the Rainbow (Rb) and Lucky Strike (LS) vent fields.

Sample name	Latitude / Longitude	Depth (m)	Deposit type	# of Archaeal pyrotags ¹	# of Bacterial pyrotags ²
Rb-1	36° 13.7487'N / 33° 54.1915'W	2297	Chimney	11037	9211
Rb-2 ⁺	36° 13.7688'N / 33° 54.1796'W	2292	Chimney	5210	4476
Rb-3	36° 13.7688'N / 33° 54.1796'W	2292	Chimney	1280	8080
Rb-4	36° 13.7661'N / 33° 54.1664'W	2293	Chimney	4370	9622
Rb-5 ⁺	36° 13.7672'N / 33° 54.1714'W	2293	Chimney	618	10539
Rb-6 ⁺	36° 13.7672'N / 33° 54.1714'W	2293	Chimney	6037	8024
LS-7 ⁺	37° 17.5075'N / 32° 16.6743'W	1732	Chimney	5565	8931
LS-8	37° 17.4528'N / 32° 16.9161'W	1730	Flange	1123	7368
LS-9	37° 17.6395'N / 32° 16.9329'W	1652	Chimney	1865	7365
LS-10	37° 17.5410'N / 32° 16.8795'W	1729	Chimney	1540	5424
LS-11	37° 17.6487'N / 32° 16.9046'W	1660	Chimney	5128	8646
LS-12	37° 17.3787'N / 32° 16.6212'W	1690	Flange	1422	3921

⁺denotes samples for which partial 16S rRNA gene clone libraries were generated.

¹Average read length = 247 nucleotides

²Average read length = 207 nucleotides

The Lucky Strike vent field is located at the summit of the Lucky Strike seamount along the MAR near a young, solidified lava lake and is one of the largest vent fields along the MAR (Langmuir *et al.*, 1997; Humphris *et al.*, 2002).

Hydrothermal activity here has been episodic but ongoing for hundreds to thousands of years (Humphris *et al.*, 2002). The fluids from Lucky Strike originate from reactions

with relatively oxic, and previously altered basalt, and are somewhat unique for a basalt-hosted system with respect to the relatively high pH and low Fe, manganese (Mn), lithium (Li) and zinc (Zn) concentrations (Table 2.1) (Von Damm *et al.*, 1998). Minerals present in chimneys and flanges include pyrite, marcasite, chalcopyrite and sphalerite, indicative of relatively more oxidizing conditions than at the Rainbow vent field (Langmuir *et al.*, 1997; Rouxel *et al.*, 2004b). There is also evidence that fluids from Lucky Strike may have two sources as fluids from the northern segment are systematically different than those from the south. Unlike fluids from Rainbow, the predominant gas in Lucky Strike fluids is CO₂ with H₂ two- to three-orders of magnitude less in concentration (Von Damm *et al.*, 1998; Charlou *et al.*, 2002). Such dramatic differences in H₂ concentrations are likely to be a strong force in structuring hydrothermal vent microbial communities as has been previously predicted (Shock *et al.*, 1995; Shock and Holland, 2004; Takai *et al.*, 2006b; McCollom, 2007; Takai and Nakamura, 2010) since many chemosynthetic primary producers utilize H₂ as an energy source.

Results and Discussion

Alpha- and beta-diversity

Because of the limitations of using the V6 region of the 16S rRNA gene in multiplexed bar-coded pyrosequencing (Claesson *et al.*, 2009; Huber *et al.*, 2010; Schloss, 2010), we targeted the V4 region to characterize the archaeal and bacterial

communities associated with hydrothermal deposits. Using this approach, we generated 45,195 and 91,607 high-quality archaeal (average 3,766 sequences/sample, 247-249 nt length) and bacterial (average 7,634 sequences/sample, 207-208 nt length) sequences, respectively (Table 2.2). Pyrosequencing amplicons were aligned and clustered using the Ribosomal Database Projects (RDP) pyrosequencing and the SLP/PW-AL pipelines at operational taxonomic unit (OTU) definitions of 95% and 97% sequence similarity, respectively (Cole *et al.*, 2009; Huse *et al.*, 2010). Alpha-diversity assessments (OTU richness, Chao1 index and rarefaction analysis) revealed comparable results with both alignment/clustering approaches providing confidence that overestimates of diversity were minimized (Figure 2.2, Table 2.3). Overall, bacterial diversity was greater than archaeal diversity in all samples. Furthermore, several of the archaeal rarefaction curves are near-asymptotic, indicating that we have nearly completely sampled the archaeal V4 diversity of these samples (Figure 2.2A).

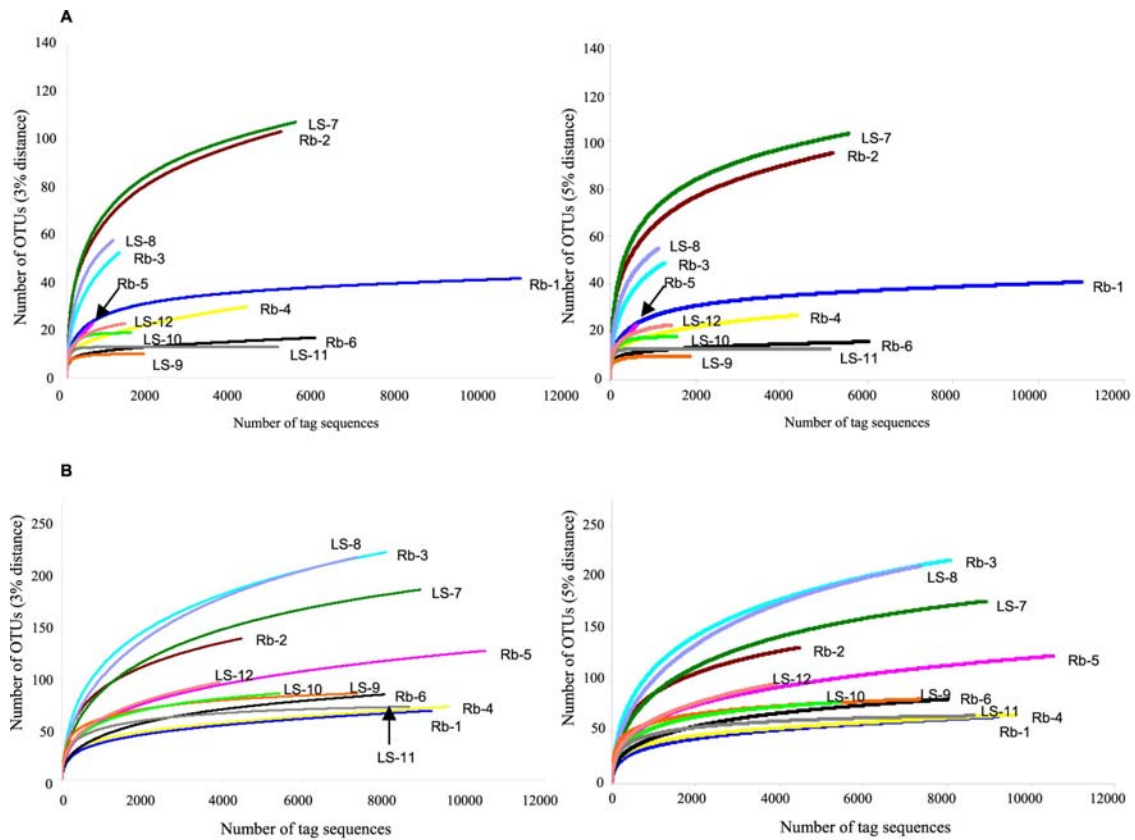


Figure 2.2. Rarefaction analysis illustrates the greater diversity observed in the bacterial communities of twelve hydrothermal deposit samples collected from the Rainbow and Lucky Strike vent fields. **A**, Archaeal rarefaction curves at two sequence similarity levels (97% and 95%) using two different alignment/clustering methods. Note the near-asymptotic appearance of several curves suggesting nearly complete sampling of the V4 sequences. **B**, Bacterial rarefaction curves. Rb = Rainbow, LS = Lucky Strike.

Table 2.3. Comparison of OTU richness and Chao1 diversity estimates generated from two different clustering methods for archaeal and bacterial communities of hydrothermal vent deposits collected along the Mid-Atlantic Ridge.

	Archaea				Bacteria			
	97% OTU definition ⁺		95% OTU definition [#]		97% OTU definition ⁺		95% OTU definition [#]	
Sample	OTUs	Chao1*	OTUs	Chao1*	OTUs	Chao1*	OTUs	Chao1*
Rb-1	42	44-96	41	43-95	68	77-150	65	73-146
Rb-2	104	115-185	95	106-191	139	151-204	132	141-185
Rb-3	53	58-106	49	51-81	224	251-324	217	240-305
Rb-4	30	33-74	27	28-45	72	95-281	67	80-206
Rb-5	23	27-136	23	45-220	127	146-226	124	142-224
Rb-6	17	19-70	16	16-42	84	97-187	82	92-170
LS-7	108	119-197	103	111-174	187	204-261	177	192-245
LS-8	58	63-114	55	60-115	219	247-316	211	232-290
LS-9	10	-	10	-	85	87-117	82	84-114
LS-10	19	-	18	-	85	90-134	79	82-115
LS-11	13	-	13	-	72	72-87	66	66-80
LS-12	23	23-35	23	23-31	96	108-167	97	107-160

Dashes indicate samples for which the Chao1 estimator could not be calculated for due to the lack of singleton/doubleton OTUs. Rb = Rainbow, LS = Lucky Strike

⁺Clusters generated using the SLP/PW-AL pipeline Huse *et al.*, (2010).

[#]Clusters generated using the RDP furthest-neighbor clustering method.

*Ranges of Chao1 indices include 95% confidence intervals.

Differences in overall community composition between vent fields (beta-diversity) were assessed using both OTU-based metrics (Bray-Curtis, Sørensen) and the phylogeny-based metric, UniFrac (Lozupone *et al.*, 2006; Hamady *et al.*, 2010).

UniFrac distances were calculated to account for abundances of individual taxa (weighted) or based solely on presence/absence (unweighted). Non-metric multidimensional scaling (MDS) plots built using all metrics revealed that the communities from the two vent fields were distinct (Figure 2.3A and B, Figure 2.4A – F). Statistically significant patterns, as determined by ANOSIM (Primer v6), were

observed in 7 of the 8 analyses with the sole exception being the bacterial weighted UniFrac distances (Figure 2.4E). It is likely that the dominance of closely related *Epsilonproteobacteria* in the bacterial data mask the significant differences observed using the unweighted UniFrac distances, although the bacterial communities were significantly different in both weighted (Bray-Curtis) and unweighted (Sørensen) OTU-based analyses. Moreover, we found that the archaeal and bacterial community composition varied significantly less within vent fields than between vent fields and hence, community composition was more similar within than between vent fields (Figure 2.3C, Figure 2.4G, H and I). This suggests that the geochemical differences between the two vent fields are a stronger force in structuring microbial communities than any within vent field force. Together, these results clearly show that the microbial communities are different between the Rainbow and Lucky Strike vent fields.

Taxonomy

While beta-diversity metrics provide insights into overall community differences, assigning taxonomic identities to sequences allows for determining how these communities differ taxonomically and possibly functionally. To achieve this, we used the RDP-classifier (Wang *et al.*, 2007) set at a bootstrap value of 50% (Claesson *et al.*, 2009) to classify representative sequences of each OTU defined using the RDP-95% clusters. Manual classifications using ARB (Ludwig *et al.*, 2004) and BLAST were also done for many unclassified OTUs as known lineages (e.g., *Aciduliprofundales*) were not classified by the RDP-classifier.

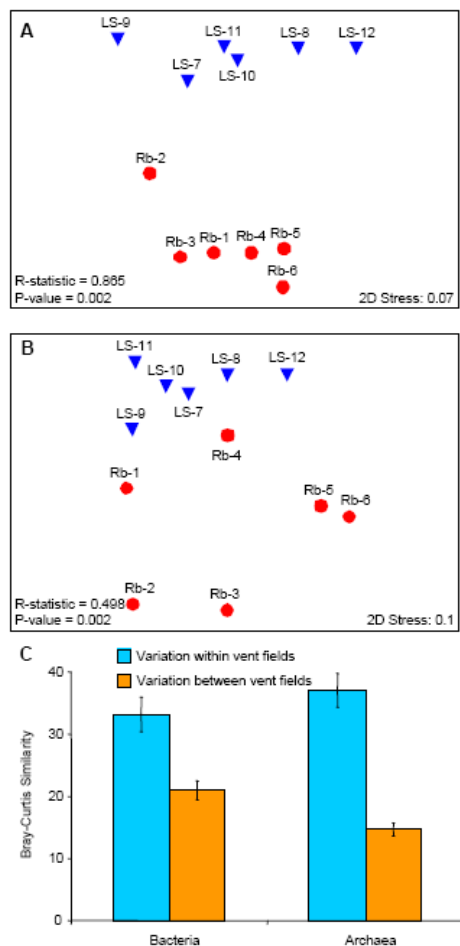


Figure 2.3. 16S rRNA gene surveys reveal partitioning of the archaeal and bacterial communities between the ultramafic-hosted Rainbow (red) and basalt-hosted Lucky Strike (blue) vent fields along the Mid-Atlantic Ridge. Communities clustered using NMDS of the Bray-Curtis similarities for archaeal (**A**) and bacterial (**B**) communities. Each point represents an individual vent sample. Results of ANOSIM analysis showing that the observed patterns are significant are presented in the bottom left corner of each plot. **C**, Average Bray-Curtis similarity within and between vent fields. Average distances were significantly different for both archaeal and bacterial communities as determined by one-tailed *t*-tests ($P < 0.001$). Error bars indicate the standard error of the mean (SEM).

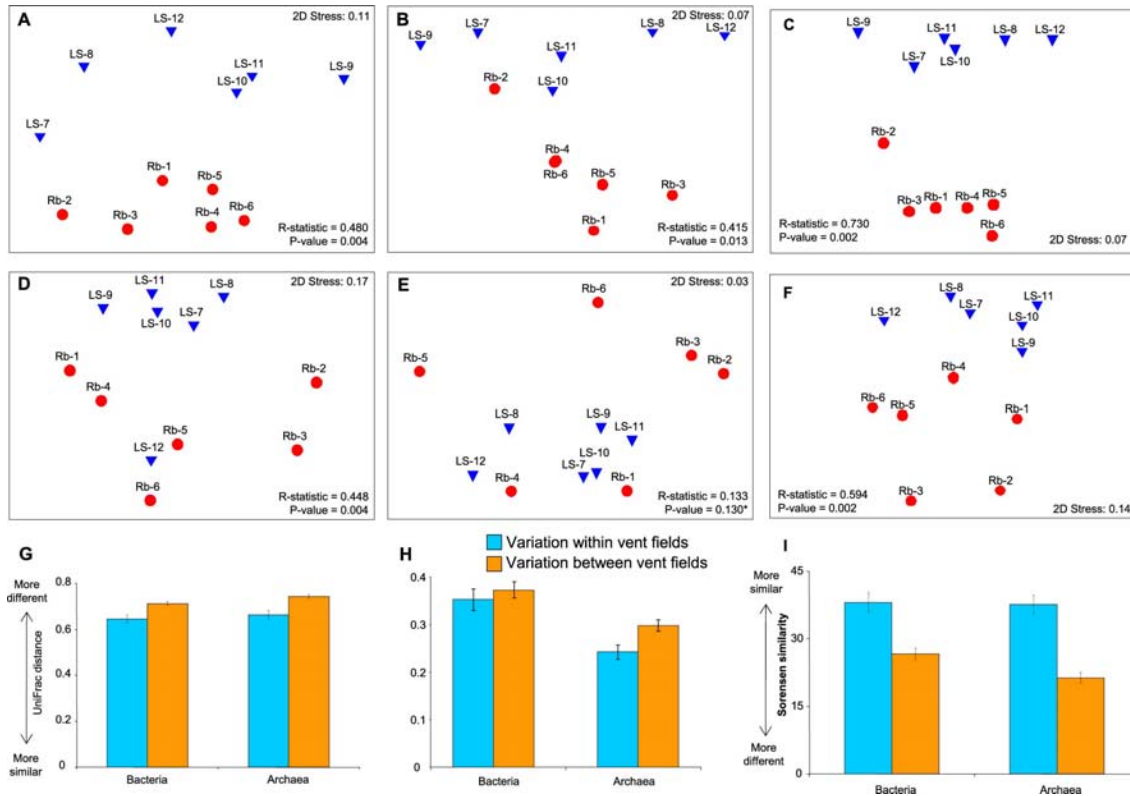


Figure 2.4. 16S rRNA gene surveys reveal partitioning of the archaeal and bacterial communities between the ultramafic hosted Rainbow (red) and basalt-hosted Lucky Strike (blue) vent fields along the Mid-Atlantic Ridge. Communities clustered using MDS of the unweighted (**A** and **D**) and weighted (**B** and **E**) UniFrac distances for archaeal (**A**, **B**) and bacterial (**D**, **E**) communities. Sorensen similarity values for archaeal (**C**) and bacterial (**F**) communities also clustered by vent site. Each point represents an individual vent sample. Results of ANOSIM analysis showing that the observed patterns are significant are presented in the bottom right or left corner of each plot. (**G**) Average unweighted and weighted (**H**) UniFrac distance within and between vent fields. Average distances were significantly different for archaeal weighted ($P < 0.01$) and unweighted ($P < 0.001$), and bacterial unweighted ($P < 0.001$) communities as determined by one-tailed t -tests. Sorensen similarities were also significantly different (**I**) for both bacteria ($P < 0.001$) and archaea ($P < 0.001$). Error bars indicate the standard error of the mean (SEM).

Archaea

Overall, the archaeal lineages observed at both vent fields were typical for this environment and likely represent the core archaeal microbiome. Archaeal families shared between all vent samples include the thermophilic *Desulfurococcaceae*, *Thermococcaceae* and *Thermofilaceae* (Figure 2.5A). Other thermophilic lineages shared by most samples include the mixotrophic *Archaeoglobaceae*, the acidophilic fermentative *Aciduliprofundales* (DHVE2), and the *Nanoarchaea* (Takai and Horikoshi, 1999; Boone *et al.*, 2001; Huber *et al.*, 2002a; Reysenbach *et al.*, 2006; Reysenbach and Flores, 2008). Several novel lineages with no known isolates in culture were also observed. For example, three OTUs (“Unclassified *Euryarchaeota* A”) were found in all but three samples. Sequences of these OTUs are related to clones found in other deep-sea vent environments (>94% similarity) (Moussard *et al.*, 2006a). Homologous sequences were also identified in the 16S rRNA gene clone libraries generated for this study (data not shown).

The most striking difference between the two vent fields was the absence of known methanogens (*Methanococcaceae* and *Methanocaldococcaceae*) at Lucky Strike (Figure 2.5A). This is notable because methanogens are common inhabitants of most vent fields (Takai *et al.*, 2006a), although a few single chimney surveys with limited sequencing depth have also failed to detect methanogens at other vent fields (Takai *et al.*, 2001; Hoek *et al.*, 2003; Kormas *et al.*, 2006; Zhou *et al.*, 2009). Nevertheless, this is the first report with this level of sampling and sequencing depth (12 samples, 45,195 sequences) that shows their absence at the vent field scale. The lack of detectable

methanogens was confirmed by quantitative polymerase chain reaction (qPCR) assays of a functional gene diagnostic for methanogenesis (*mcrA*) in 18 vent deposits from Lucky Strike (Figure 2.6). Furthermore, methanogens were not detected in 16S rRNA gene clone libraries constructed from the most diverse of the Lucky Strike samples (data not shown). The absence of methanogens at Lucky Strike in conjunction with their abundance at Rainbow is in agreement with theoretical calculations of free-energy yield for thermophilic hydrogenotrophic methanogenesis based on H₂ concentrations as previously reported (McCollom, 2007; Takai and Nakamura, 2010). Other notable differences in the archaeal communities between vent fields were observed within the *Desulfurococcaceae* at the genus level. For example, the obligate anaerobe *Staphylothermus*, was prevalent in Rainbow deposits while the microaerophilic *Aeropyrum* was prevalent in Lucky Strike deposits (Figure 2.5B).

SIMPER analysis (Primer v6) (Clarke and Gorley, 2006) was used to determine which archaeal genera were most responsible for the differences observed between sites (Table 2.4). The top four of these indicator, or "discriminating" OTUs were two methanogens (*Methanocaldococcus* and *Methanothermococcus*) as well as *Staphylothermus* and *Aeropyrum*, which clearly points to these genera driving the differences observed between the two sites.

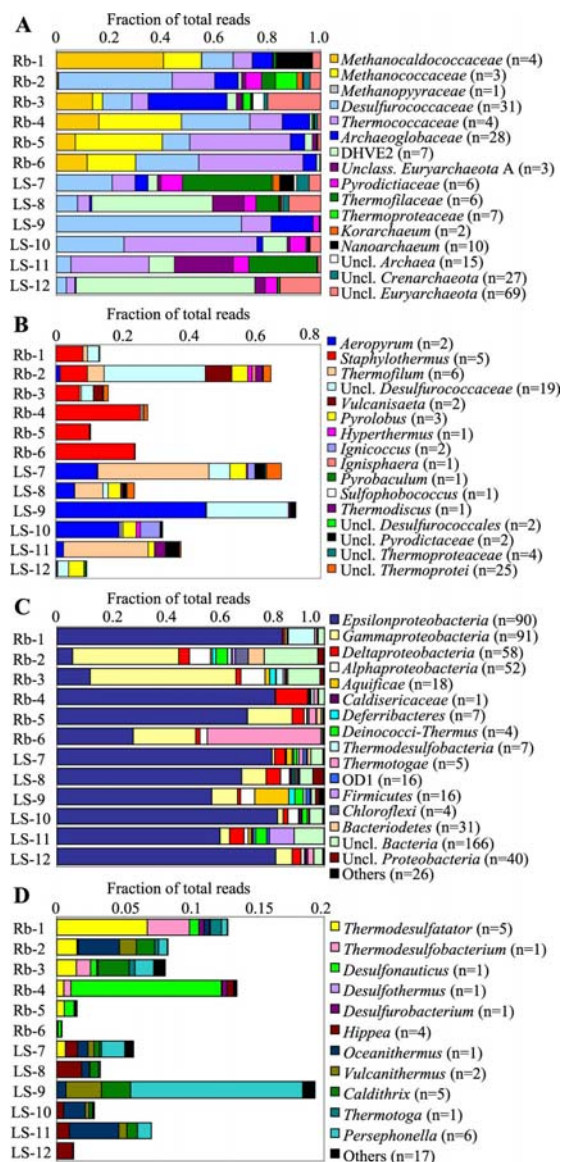


Figure 2.5. Comparison of taxonomic variation in the archaeal and bacterial communities of Rainbow and Lucky Strike hydrothermal vent deposits. **A**, Relative abundances of archaeal families observed in each vent deposit. Note the absence of methanogens in all Lucky Strike samples. **B**, Relative abundances of crenarchaeal genera observed in each vent deposit. **C**, Relative abundances of bacterial orders observed in each vent deposit. **D**, Relative abundances of less abundant thermophilic genera observed in each vent deposit. Note that the abundant, unclassified *Thermotogae* lineages shown in figure C have been omitted in D to allow for visualization of low abundance genera. Numbers in parentheses following taxonomic classifications indicate the number of OTUs classified to that particular group. Rb = Rainbow, LS = Lucky Strike.

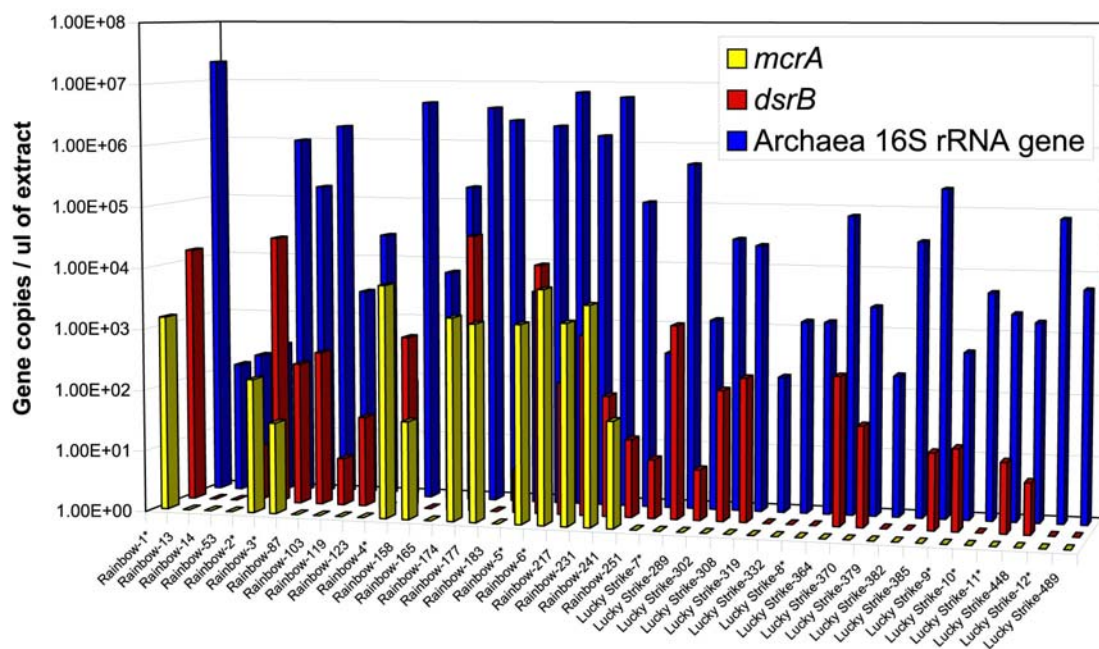


Figure 2.6. Quantitative polymerase chain reaction assays targeting the gene diagnostic for methanogenesis (*mcrA*) confirms the absence of methanogens at Lucky Strike. The archaeal 16S rRNA and the dissimilatory sulfide reductase (*dsrB*) genes were also targeted in order to verify the presence of amplifiable DNA in each sample. All gene copy numbers were normalized/g of chimney material extracted. Amplified *mcrA* and *dsrB* products were verified by cloning and sequencing of the gene (not shown). Asterisks denote samples surveyed by 454-pyrosequencing.

Table 2.4. SIMPER analysis was used to identify archaeal genera responsible for the dissimilarity observed in the communities of Rainbow and Lucky Strike vent deposits.

Genus classification	ID #	Rainbow Ave. Abun*	Lucky Strike Ave. Abun*	Dissimilarity contribution (%)	Cumulative dissimilarity (%)
<i>Methanocaldococcus</i>	10	3.54	0	6.70	6.70
<i>Staphylothermus</i>	2	3.59	0.11	6.53	13.24
<i>Methanothermococcus</i>	1	3.33	0	6.40	19.63
<i>Aeropyrum</i>	1679	0.11	3.09	5.56	25.20
DHVE2_Cultured	22	0.91	2.88	4.44	29.64
<i>Thermococcus</i>	819	1.96	3.42	4.30	33.94
<i>Thermococcus</i>	3	2.26	0.81	4.29	38.23
<i>Archaeoglobus</i>	76	2.44	0.14	4.13	42.35
DHVE2_Group_1	396	0.02	2.2	3.98	46.34
<i>Thermofilum</i>	796	0.69	2.55	3.59	49.93
<i>Pyrolobus</i>	1181	0.17	1.71	2.89	52.82
Unclass. <i>Euryarchaeota_A</i>	1474	0.45	1.63	2.78	55.61
<i>Thermococcus</i>	15	1.76	0.61	2.76	58.37
<i>Methanococcus</i>	9	1.35	0	2.59	60.96
Unclass. <i>Desulfurococcaceae</i>	972	1.08	1.13	2.52	63.48
DHVE2_Cultured	3077	0	1.26	2.22	65.70
Unclass. <i>Pyrodictaceae</i>	1726	0	1.12	2.01	67.71
<i>Archaeoglobus</i>	0	1.13	0.48	1.85	69.55
<i>Aeropyrum</i>	1681	0.18	1.02	1.75	71.30
Unclass. <i>Archaeoglobaceae</i>	1684	0	0.9	1.72	73.02

*Calculated by standardizing abundances by percentage of each sample library, taking the square root and then averaging by vent field.

Models based on the geochemical characteristics of end-member fluids and their mixing styles in porous, permeable vent deposits (i.e., diffusion and advection across deposits walls bound on one side by vent fluid and the other by seawater) predict wide oxidizing zones in exterior portions of Lucky Strike deposits and an absence of any oxidizing zone in exterior portions of Rainbow deposits (Figure 2.7A – C, Figure 2.8A

– C). The calculations were carried out as described in Tivey (2004), considering diffusion and advection of aqueous species across a porous (porosity 0.5) chimney wall bound on one side by cold seawater, and on the other by the appropriate vent fluid. Compositions of vent fluids from the Sintra and Marker 6 vents at Lucky Strike (Charlou *et al.*, 2000), and from the Flores5 vent at Rainbow (Charlou *et al.*, 2002), were used in calculations. Concentrations of relevant aqueous species as a function of position within the chimney wall are shown in Figure 2.7.

The very large differences in redox conditions for mid to exterior layers (those at less than $\sim 120^{\circ}\text{C}$) are a result of the extremes in aqueous H_2 concentrations in the different end-member fluids (16 mM at Rainbow versus 3.3 μM (Sintra) and 77 μM (Marker 6) at Lucky Strike). Even with advection of vent fluid outward through the chimney wall, conditions of pore fluids within a chimney at the Sintra vent, Lucky Strike, would be relatively oxidizing at all temperatures up to 177°C (Figure 2.7A). Other vents at Lucky Strike have higher concentrations of aqueous H_2 in end-member fluids, but still, conditions within a chimney at the Marker 6 vent, would be relatively oxidizing at temperatures up to 60°C (Figure 2.7B). These “relatively oxidizing zones” are zones where the free energy of the reactions for oxidation of sulfide and for methanotrophy are less than zero and thus favorable, while the free energy for the reactions for reduction of sulfate and for methanogenesis are greater than zero, and thus not favorable. Metabolic energies that would be produced from the favorable reactions at Lucky Strike (e.g., sulfide-oxidation and methanotrophy) are comparable to those calculated for chimneys from other vent fields considering diffusion and advection

across chimney walls (Tivey, 2004), and mixing of seawater and vent fluid (McCollom and Shock, 1997; Takai and Nakamura, 2010). Metabolic energy from methanogenesis in a Lucky Strike chimney at Marker 6 vent, in zones of the chimney that are at temperatures greater than 60°C, would be less than half of that from sulfate-reduction.

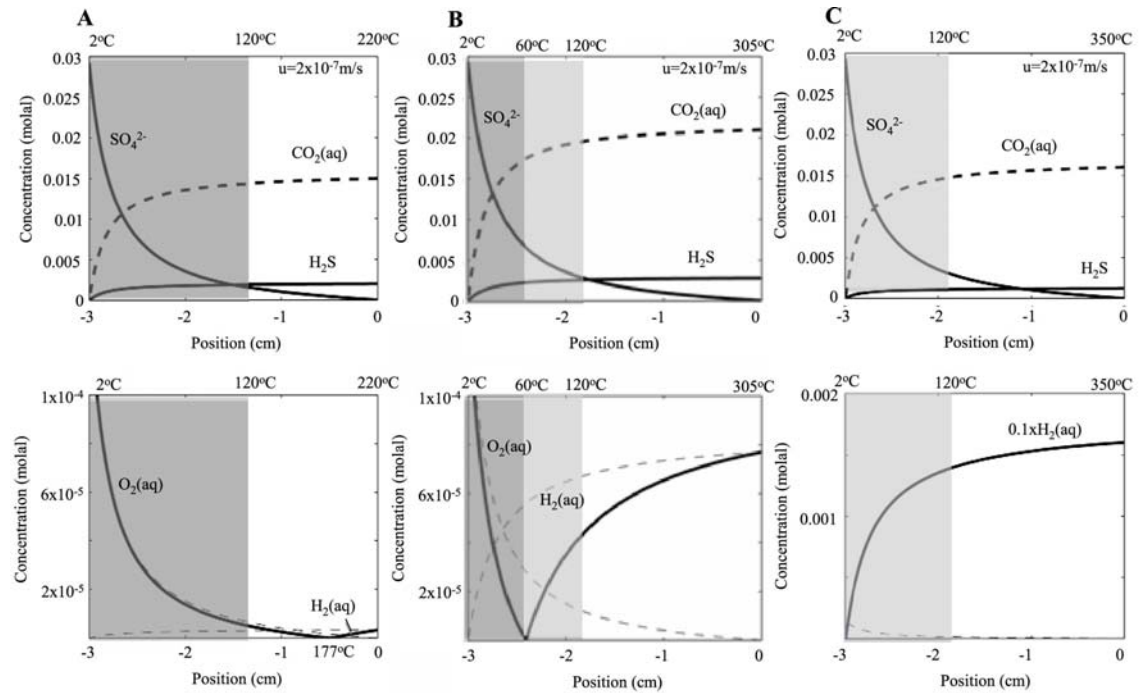


Figure 2.7. Concentrations across a uniformly porous ($\phi=0.5$) 3-cm thick chimney wall resulting from transport between seawater (at position = -3 cm) and **A**, 220°C Sintra vent fluid (Lucky Strike), **B**, 305°C Marker 6 vent fluid (Lucky Strike), **C**, 350°C Flores5 vent fluid (Rainbow) at position = 0 cm by diffusion and advection of vent fluid outward at a rate of $2 \times 10^{-7} \text{ m s}^{-1}$ (u). Shading indicates where conditions at temperatures $\leq 120^\circ\text{C}$ are relatively oxidizing (dark grey) or highly reduced (light grey). Calculations were done as described by Tivey (2004). End-member concentrations (For Flores5, $\text{H}_2 = 16 \text{ mM}$, $\text{H}_2\text{S} = 1.2 \text{ mM}$; $\text{CO}_2 = 16 \text{ mM}$; for Sintra $\text{H}_2 = 3.3 \text{ uM}$, $\text{H}_2\text{S} = 2 \text{ mM}$; $\text{CO}_2 = 15.1 \text{ mM}$; for Marker 6 $\text{H}_2 = 77 \text{ uM}$, $\text{H}_2\text{S} = 2.8 \text{ mM}$; $\text{CO}_2 = 20.7 \text{ mM}$; from Charlou *et al.* (2000; 2002). Note the absence of relatively oxidizing conditions within the Rainbow (Flores5) chimney versus the prediction of oxidizing conditions up to temperatures of 177°C and 60°C for Lucky Strike chimneys, depending on the concentration of aqueous H_2 in the end-member vent fluid and the advection rate. (Dashed lines in lower half of figure are for O_2 and H_2 concentrations if oxidation of H_2 is inhibited as suggested by Shock and Holland (2004)).

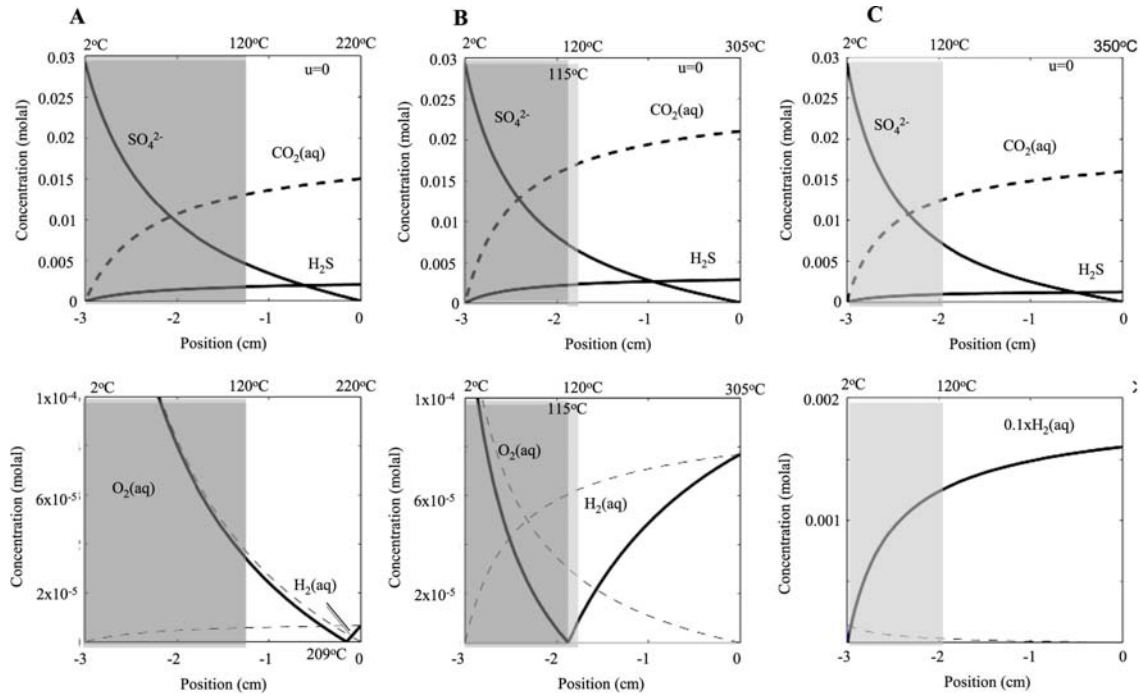


Figure 2.8. Concentrations across a uniformly porous ($\phi=0.5$) 3-cm thick chimney wall resulting from transport between seawater (at position = -3 cm) A, 220°C Sintra vent fluid (Lucky Strike), B, 305°C Marker 6 vent fluid (Lucky Strike), C, 350°C Flores5 vent fluid (Rainbow) at position = 0 cm by diffusion only. (see Figure 2.7 caption for more details of calculations). Note the lack of oxidizing zone for the Rainbow chimney even with no outward advection of vent fluid.

In contrast to at Lucky Strike, the very high concentrations of aqueous H_2 in Rainbow fluids result in reducing pore fluids within all portions of Rainbow chimneys, even exterior layers surrounded by oxic seawater (Figure 2.7C). Methanogenesis and sulfate-reduction are energetically favorable reactions that would produce metabolic energies comparable to those calculated for reducing zones in other chimneys (Tivey, 2004) and reduced mixing zones (McCollom and Shock, 1997; Takai and Nakamura, 2010). On the other hand, sulfide-oxidation and methanotrophy would not be expected

to be favorable reactions anywhere within Rainbow chimneys, though could occur if equilibrium between H_2 and O_2 was kinetically inhibited, as proposed by Shock and Holland (2004) and demonstrated as possible, particularly at lower temperatures, by Foustoukos *et al.* (2011). The dashed lines in the bottom panels of Figures 2.7 and 2.8 show predicted amounts of H_2 and O_2 if equilibration between the two species is completely inhibited (i.e., maximum amounts of O_2 or H_2 that might be present in zones that would be predicted to be relatively oxidizing or reducing assuming equilibrium between the two species). For example at the Flores5 vent at Rainbow, a very small amount of metabolic energy (an order of magnitude less than in Lucky Strike outer layers), would be available in outermost layers (e.g., at 7°C) from methanotrophy if there was complete inhibition of equilibrium between H_2 and O_2 , and the amount of metabolic energy from sulfate-reduction would be comparable to that in Lucky Strike exterior layers. At the low temperature of 7°C , inhibition might be expected (Foustoukos *et al.*, 2011). In Lucky Strike chimneys, if equilibration is completely inhibited, methanogenesis would be thermodynamically favorable in chimneys formed from Marker 6 fluids at temperatures less than 60°C , and from Sintra fluids at temperatures less than 177°C , but amounts of metabolic energy would be considerably less than from sulfide-oxidation (two-thirds less for Sintra fluids, half for Marker 6 fluids). In addition, at these higher temperatures, the rate of equilibration between H_2 and O_2 would be higher than at lower temperatures (Foustoukos *et al.*, 2011).

The differences in predicted redox conditions in the exteriors of the deposits help to explain the abundance of *Aeropyrum* at Lucky Strike and *Staphylothermus* and

methanogens at Rainbow. Additionally, the unusually low concentrations of H₂ in exteriors of Lucky Strike deposits (Figure 2.7A – C, Figure 2.8A – C) most likely cannot support methanogenesis, particularly given competition with other thermophilic hydrogen-oxidizers such as members of the *Archaeoglobaceae* and *Desulfurococcaceae*. Certain members of these families would also have an advantage over methanogens by being able to use alternative electron-donors when H₂ was unavailable (Boone *et al.*, 2001). Interestingly, the archaeal diversity of Rb-2 shows some similarity with those of Lucky Strike deposits (Figure 2.5A). This sample is from a highly-porous few-millimeter-thick distinct outer layer of a chimney (Figure 2.9). The Rb-3 sample was taken from the less porous, harder interior layer adjacent to Rb-2. The fluid sampled from this vent had slightly lower measured H₂ as compared to other Rainbow fluids (~12 mmol/kg versus ~16 mmol/kg, Table 2.5). More efficient mixing of seawater may have occurred within the very porous (and likely more permeable) outer layer (Rb-2), which would result in even lower H₂, while the interior layer (Rb-3) would remain reducing and support methanogens. These findings suggest that in addition to local hydrothermal fluid chemistry influencing microbial diversity, within-field variability in archaeal diversity can be influenced by fluid mixing styles and deposit porosity and permeability.



Figure 2.9. Photograph of the hydrothermal vent chimney used for samples Rb-2 and Rb-3. Note how the porous, outer layer (Rb-2) cleanly peels away from the rest of the chimney sample.

Table 2.5. End-member fluid chemistry of samples used for microbial community characterizations.

Sample name	Max. fluid temp (°C) [#]	pH (25°C)	H ₂ (mmol/L)	ΣH ₂ S (mmol/L)	CH ₄ (mmol/L)	ΣCO ₂ (mmol/Kg)
Rb-1	370	3.3	16	2.4	2.0	23
Rb-2	350	3.4	12	3.3	1.9	21
Rb-3	350	3.4	12.3	3.3	1.9	21
Rb-4	-	-	-	-	-	-
Rb-5	-	-	-	-	-	-
Rb-6	-	-	-	-	-	-
LS-7	324	3.9	0.071	3.1	1.1	35
LS-8	-	-	-	-	-	-
LS-9	236	3.7	0.025	2.4	0.84	101
LS-10	217	-	-	-	-	-
LS-11	184	-	-	-	-	-
LS-12	-	-	-	-	-	-

[#]maximum fluid temperatures recorded after sample collection when possible.

Bacteria

Of the 91,607 bacterial V4 amplicons sequenced from the 12 hydrothermal vent samples, approximately 61% (56,091) were classified as *Epsilonproteobacteria* (Figure 2.5C). *Epsilonproteobacteria* are known to play significant roles in carbon and sulfur cycling and have consistently been shown to be the most numerically abundant bacteria in these environments (Longnecker and Reysenbach, 2001; Nakagawa *et al.*, 2005c; Campbell *et al.*, 2006; Opatkiewicz *et al.*, 2009; Huber *et al.*, 2010). On a sample by sample basis, *Epsilonproteobacteria* were the most abundant sequences observed in three of the Rainbow and all of the Lucky Strike samples (Figure 2.5C). Within the *Epsilonproteobacteria*, the moderately thermophilic *Caminibacter* and *Nautilia*, and the mesophilic *Nitratifractor* and *Sulfurovum* were detected in all samples although abundances differed likely reflecting the different temperature regimes across individual deposits (Figure 2.10A). The diversity within the *Sulfurovum*, *Caminibacter* and *Nitratifractor* was surprisingly high with several OTUs identified by SIMPER as being found exclusively at one vent field (Table 2.6). This suggests that differences in the epsilonproteobacterial communities between Rainbow and Lucky Strike are at a finer scale (e.g., species or ecotype level) than what can be resolved with 16S rRNA gene sequences alone. These differences, however, may be significant as different OTUs within the same genus could be filling different ecological niches. For example, two hydrogen-oxidizing *Caminibacter* species previously isolated from Rainbow show differences in their oxygen tolerance as *C. mediatlanticus* is a strict anaerobe while *C. profundus* grows optimally with 0.5% oxygen (Miroshnichenko *et al.*, 2004;

Voordeckers *et al.*, 2005). Therefore, although all OTUs classified as *Caminibacter* are treated equally, OTU level differences may be in response to similar geochemical properties that shape the archaeal communities. Yet, the isolated nature of these environments may also foster allopatric speciation within each vent field. Nonetheless, these results suggest that biogeographical provincialism occurs for free-living microbes as it does with vent invertebrates in deep-sea hydrothermal environments (Ramirez-Llodra *et al.*, 2007).

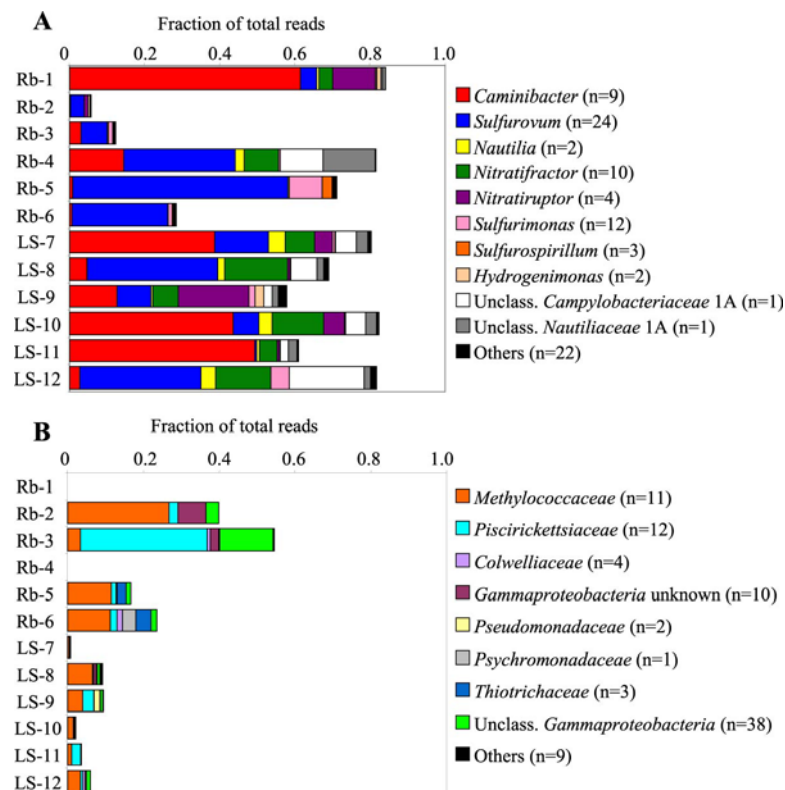


Figure 2.10. Comparison of taxonomic variation in the bacterial communities of Rainbow and Lucky Strike hydrothermal vent deposits. **A**, Relative abundances of epsilonproteobacterial genera observed in each vent deposit. **B**, Relative abundances of gammaproteobacterial families observed in each vent deposit. Numbers in parentheses following taxonomic classifications indicate the number of OTUs classified to that particular group. Rb = Rainbow, LS = Lucky Strike.

Table 2.6. SIMPER analysis was used to identify bacterial genera responsible for the dissimilarity observed in the communities of Rainbow and Lucky Strike vent deposits.

Genus classification	ID #	Rainbow Average Abundance*	Lucky Strike Average Abundance*	Dissimilarity contribution (%)	Cumulative dissimilarity (%)
<i>Caminibacter</i>	1293	1	0	2.06	2.06
<i>Nitratifractor</i>	7	0	1	2.06	4.12
<i>Thermodesulfatator</i>	929	1	0	2.06	6.17
<i>Thermodesulfobacterium</i>	1907	1	0	2.06	8.23
<i>Nautilia</i>	1094	1	0	2.06	10.29
Unclassified <i>Bacteria</i>	21	0	1	2.06	12.35
<i>Thermodesulfatator</i>	1263	1	0	2.06	14.4
<i>Desulfonauticus</i>	863	0.83	0	1.72	16.12
<i>Nautilia</i>	5	0.17	1	1.71	17.83
<i>Hipaea</i>	122	0.17	1	1.71	19.53
<i>Sulfurovum</i>	30	0	0.83	1.68	21.21
<i>Caldithrix</i>	62	0	0.83	1.68	22.89
Unclassified <i>Bacteria</i>	20	0	0.83	1.68	24.57
<i>Desulfobulbus</i>	1672	0.83	0.17	1.5	26.07
<i>Caldisericum</i>	6	0.17	0.83	1.48	27.54
<i>Caminibacter</i>	10	0.17	0.83	1.47	29.01
<i>Colwellia</i>	914	0.67	0	1.33	30.35
OD1	152	0.33	1	1.33	31.68
<i>Sulfurovum</i>	242	0	0.67	1.33	33.01
<i>Sulfurovum</i>	14	0.33	0.83	1.27	34.28

*Abundances reflect the presence or absence of particular OTUs in each sample from the two vent fields with 1 indicating the presence of that OTU in all samples from that vent field and 0 representing a complete absence.

Of the samples not dominated by *Epsilonproteobacteria*, two were dominated by *Gammaproteobacteria* (Rb-2, -3) and one by unclassified sequences related to the *Thermotogae* (Rb-6) (Figure 2.5C). Taxa of the *Gammaproteobacteria* observed in most samples include the mesophilic sulfide-oxidizing *Thiomicrospira* and several genera within the methylotrophic *Methylococcaceae* (Figure 2.10B). Although two of the Rainbow deposits (Rb-1, -4) had very few sequences classified as *Gammaproteobacteria*, there was an overall greater diversity of *Methylococcaceae* at Rainbow, perhaps reflecting the higher concentrations of abiotic (and biotic) methane generated in ultramafic environments and identifying another metabolism preferentially

enriched for in ultramafic environments. Because the sequences in Rb-6 are only distantly related to the *Thermotogales*, they are likely a novel deep-sea group whose primary metabolism is unknown.

Differences in the less abundant bacterial thermophilic members corroborated many of the archaeal community observations (Figure 2.5D). For example, the hydrogen-oxidizing sulfate-reducing *Thermodesulfatator* and *Thermodesulfobacterium* were detected in all Rainbow samples but were only detected in one of the Lucky Strike deposits. Within the *Deltaproteobacteria*, the genus *Desulfonauticus*, a moderately thermophilic hydrogen-oxidizing sulfate-reducer, was observed in five of six Rainbow samples and not in any of the Lucky Strike deposits further suggesting enriched diversity of thermophilic hydrogen-oxidizers at Rainbow. SIMPER also identified these OTUs as being some of the most significant drivers of bacterial community differences (Table 2.6).

Conclusions

As some studies have pointed to the possible role of subsurface geochemical processes such as phase-separation as drivers for microbial diversity at vents, the small sample sizes have compromised the reported conclusions (Nakagawa *et al.*, 2005d; Nunoura and Takai, 2009). Our data from the microbial communities colonizing hydrothermal deposits show at multiple taxonomic levels that there is a direct coupling of geological, geochemical and microbiological processes at deep-sea hydrothermal vents. At the ultramafically-hosted site, Rainbow, the high concentrations of aqueous

H₂ in the vent fluids resulting from serpentinization reactions allows for methanogens to flourish. Conversely, Lucky Strike vent fluids have very low aqueous H₂ concentrations and are oxidizing relative to most mid-ocean ridge vent fluids (Charlou *et al.*, 2000; Charlou *et al.*, 2002). In addition, some of the vent fluids at Lucky Strike exhibit evidence of conductive cooling in the subsurface (attributed to the presence of impermeable cap rocks that trap fluids, Rouxel *et al.*, 2004b) and for seawater entrainment into the subsurface (Humphris *et al.*, 2002), which would result in venting of even more oxidizing fluids at the seafloor. Therefore, in the actively venting deposits at Lucky Strike, the conditions are not suitable for the growth of thermophilic methanogens, but are for growth of microaerophilic hyperthermophiles.

Here we have only considered the pore fluids as the source of reduced or oxidized species providing energy for the microbial communities. The mineral surfaces may also play a role, but that was not investigated in this study. What is known both from past studies of deposits samples at Lucky Strike and Rainbow vent fields, and from analysis of samples collected in this study, is that the mineral assemblages present in Rainbow versus Lucky Strike vent deposits indicate significantly more reducing conditions in Rainbow deposits, with pyrrhotite (Fe_{1-x}S) and cubanite (CuFe₂S₃) more prevalent at Rainbow and marcasite and pyrite (FeS₂) and chalcopyrite (CuFeS₂) more prevalent at Lucky Strike (Langmuir *et al.*, 1997; Rouxel *et al.*, 2004a, b). The redox state of these minerals (more versus less reducing) may further affect microenvironments within the chimneys, further influencing microbial communities.

Lucky Strike and Rainbow vent fields represent the opposite ends of the geochemical spectrum along the Mid-Atlantic Ridge hydrothermal vent fields, particularly with respect to H₂ concentrations. Extending this sampling and deep sequencing approach to other vent fields in different geologic settings and including more fine scale mineralogical and textural analyses, is needed to identify the full suite of geologic and geochemical properties that influence microbial community structure and will provide boundaries for future modeling efforts.

Materials and Methods

Sample collection and DNA extraction.

Vent deposit samples were collected during July/August 2008 from the Rainbow and Lucky Strike vent fields using the robotic manipulators of the remotely operated vehicle (ROV) *Jason II*. Upon collection, samples were placed in sealed, custom made bioboxes to minimize contamination from surrounding seawater. After surfacing, samples were removed from bioboxes and sampled using published methods (Götz *et al.*, 2002; Reysenbach *et al.*, 2006). For samples Rainbow-1, -2, -4, -5 and Lucky Strike-7, -8, -9, -12 approximately 1-4 mm of the outer biofilm-encrusted surface was removed and homogenized using sterile mortar and pestles. For samples Lucky Strike-10 and -11, outer biofilm crusts were homogenized with inner sections as they could not be easily separated from the rock. For samples Rainbow-3 and -6, interior sections of the deposits were homogenized after removal of the outer crust. Homogenized samples

were stored in cryovials at -80°C for subsequent DNA extraction. Nucleic acids for pyrosequencing, clone libraries and qPCR were extracted from homogenized samples ($\approx 1.6 - 3.2$ grams) using the Ultra Clean Soil DNA Isolation Kit (MoBio Laboratories) according to the modified protocol of Reysenbach *et al.* (2006).

Hydrothermal fluid chemistry

Hydrothermal fluids were collected using isobaric gas-tight fluid samplers (Seewald *et al.*, 2002) deployed from the ROV *Jason II* and processed immediately following recovery on the ship. Vent fluid temperature was monitored continuously during fluid sampling using a thermocouple attached to the end of the sampler inlet snorkel. The reported temperatures (Tables 2.1 and 2.5) represent maximum values recorded for each vent. Shipboard analysis of dissolved H_2 and CH_4 concentrations was accomplished using gas chromatography following headspace extraction. Samples aliquots were archived in gas-tight serum vials for shore-based determination of total dissolved CO_2 (ΣCO_2) by gas chromatography following acidification and headspace extraction. Total dissolved H_2S ($\Sigma\text{H}_2\text{S}$) and pH (25°C) were determined at sea by electrochemical titration using a sulfide specific electrode and a Thermo-RossTM glass electrode, respectively.

454 Pyrosequencing

For amplifying the hypervariable V4 region of the SSU rRNA gene of Archaea, we used as forward primer oligonucleotides that contained a modified U519F primer sequence (Suzuki and Giovannoni, 1996) fused to 6-nucleotide key tags (Cole *et al.*, 2009) and to the 454 FLX sequencing primer A

(5'GCCTCCCTCGCGCCATCAGxxxxxx**CAGYMGCCRCGGKAAHACC**, where the x region represents the key tag and the SSU rRNA primer is bold). To allow

multiplex sequencing, ten such primers were synthesized (Integrated DNA

Technologies; HPLC purified), each with a different key tag. The reverse

oligonucleotide primer represented a fusion of the 454 FLX sequencing primer B and a modified Arch806R primer (Takai and Horikoshi, 2000a)

(5'GCCTTGCCAGCCCGCTCAGGG**ACTACNSGGTMTCTAAT**, where the 16S rRNA region is bold). PCR reactions (50- μ l volume) contained 300nM of each of

forward and reverse primers, 20-50 ng template DNA and were performed using

Platinum Taq High Fidelity polymerase (Invitrogen, Carlsbad, CA) using the thermal

profile 95°C for 2 min followed by 27 cycles of denaturation at 95°C for 15 sec, primer

annealing at 53°C and extension at 68°C for 45 sec, with final extension of 68°C for 3

min. For a few samples the amount of template DNA was limiting and additional 3-5

PCR cycles were necessary in order to obtain a sufficient product. Negative control

reactions without template were always performed.

The bacterial hypervariable V4 region of the SSU rRNA gene was amplified using a similar approach, using as forward primer key-tagged oligonucleotides

5'GCCTCCCTCGCGCCATCAGxxxxxx**AYTGGGYDTAAAGNG**3') and a mix of reverse primers (5'GCCTTGCCAGCCCGCTCAG:**TACCRGGGTHTCTAATCC**, **:TACCAGAGTATCTAATTC**, **:CTACDSRGGTMTCTAATC** and **:TACNVGGGTATCTAATCC**3' in a 6:1:2:12 ratio, respectively), designed to cover most of the Bacteria domain (Cole *et al.*, 2009). The amplification protocol was the same as for Archaea except that the annealing temperature was 55°C.

The amplicon products were purified using AMPure paramagnetic beads (Agencourt Bioscience Corporation, Beverly, MA) followed by analysis of their concentration and size using DNA 1000 chips on an Agilent 2100 Bioanalyzer (Agilent Technologies, Inc., Waldbronn, Germany). Amplicon libraries were prepared for unidirectional sequencing using the emPCR Kit II (Roche) followed by sequencing on a 454 Life Sciences Genome Sequencer FLX (Roche Diagnostics, Indianapolis, IN). Based on the use of identifying key tags, twenty individual samples were pooled and sequenced on each of the two sides of the picotiter plate.

Raw sequence data was initially processed through the RDP's (Ribosomal Database Project) Pyrosequencing Pipeline (<http://pyro.cme.msu.edu/>) (Cole *et al.*, 2009). Sequences were excluded from analysis if they had a mean quality score < 20, were < 200 or > 275 bp in length (Archaea) (> 250 for Bacteria), contained ambiguous nucleotides (N's), or had any mismatches in the forward and reverse primers. The sequences were assigned to individual samples by their key tag and the 16S rRNA primers were removed prior to analysis. Trimmed sequences were then subjected to an initial pre-classification step using the RDP-classifier (Wang *et al.*, 2007) in which

unclassified sequences (not Archaea or Bacteria) or sequences classified to the incorrect domain (e.g., Bacteria in the archaeal data set) were removed. The resulting datasets contained 207-208 nt of the bacterial and 247-249 nt of the archaeal V4 region, respectively.

Sequence analysis

Trimmed sequenced files were aligned with the secondary-structure aware Infernal aligner (Nawrocki *et al.*, 2009) and clustered using the complete-linkage clustering method (furthest-neighbor) available through the RDP's pyrosequencing pipeline (Cole *et al.*, 2009). Sequences were also aligned and clustered using the SLP/PW-AL pipeline (Huse *et al.*, 2010). Individual cluster files from both methods were used to generate rarefaction curves (Colwell and Coddington, 1994) and Chao1 richness estimator (Chao and Bunge, 2002) at different OTU similarity levels (97% and 95%). Custom perl scripts were used on combined cluster files to develop abundance matrices for both archaeal and bacterial clusters. A second script was used to select representative sequences of each cluster and these sequences were run through the RDP classifier (Wang *et al.*, 2007) set at a 50% bootstrap cutoff as recommended by Claesson *et al.* (2009). Classifications were downloaded and a third script was used to link the classifications back to the original cluster files. The taxonomic results presented here were generated from the RDP OTUs at 95% similarity. We chose to use this method for analysis because the V4 region performs best with the infernal aligner used by RDP (Nawrocki *et al.*, 2009) and less stringent clustering values have been

shown to minimize overestimates of diversity (White *et al.*, 2010). Selected sequences representing clusters that could not be classified by the RDP classifier were further examined by BLAST searches against the GenBank's non-redundant database (Benson *et al.*, 2009), aligning sequences in ARB (Ludwig *et al.*, 2004) and inserting them into the Silva-96 reference tree (Pruesse *et al.*, 2007) using the quick add function. When possible, clusters were then given a taxonomic classification based on published nomenclature otherwise a generic identifier (e.g., Unclassified Archaea A) was used to track OTUs between samples.

For OTU-based beta-diversity assessments, abundance matrices were imported into Primer v6. Bray-Curtis similarities were calculated on matrices that had been normalized to total and transformed via square root while Sørensen similarities were calculated directly from abundance matrices. Distance matrices were also generated for both archaeal and bacterial communities using the phylogeny-based metric UniFrac (Lozupone *et al.*, 2006; Hamady *et al.*, 2010). First, for each of the Bacteria and Archaea global datasets we grouped the sequences in OTU clusters using either 97% or 95% sequence similarity levels, using the RDP Pyrosequencing Pipeline. We then extracted one sequence from each OTU cluster to construct hydrothermal vent reference datasets for either Bacteria (811 sequences at 97% and 648 sequences at 95% sequence similarity, respectively) or Archaea (310 sequences at 97% and 229 sequences at 95% sequence similarity, respectively). For tree rooting, we added the SSU rRNA sequences of either *Nanoarchaeum equitans* (Genbank AJ318041) (Archaea dataset) or *Hydrogenobaculum* sp. (GenBank AY861719) (Bacteria dataset), trimmed to

correspond to the sequenced V4 region followed by aligning using the RDP aligner. Maximum likelihood rooted phylogenetic trees were then constructed using RAxML-7.0.4 (Stamatakis, 2006) using the GTRGAMMA parameter and 100 independent searches for the best tree. After assigning of each individual sequence from the global datasets to their closest representatives in the reference datasets using local BLAST, the UniFrac sample ID mapping file was generated using a python script, according to the Fast UniFrac data analysis flow. The online Fast UniFrac pipeline was used for the subsequent analysis, including generation of the UniFrac distance matrix. The same results were obtained using either the 97% or the 95% sequence similarity datasets. The presented figures are based on the 97% sequence similarity trees and matrices. In parallel, we also used the Greengenes core sequence dataset and tree that are available as part of the online FastUnifrac for mapping and preliminary analysis, with similar results (not shown). Similarity and distance matrices were analyzed using principal coordinates analysis (PCoA) (not shown), non-metric multi-dimensional scaling (MDS), and tested for significance using ANOSIM. We chose to use MDS instead of other ordination methods like PCoA because it is more flexible in converting (dis)similarity to distances and preserving these relationships in low-dimensional space (Clarke and Gorley, 2006). Similarities/distances were averaged within and between vent sites and tested for significance using a one-tailed T-test. All distance matrix analyses except PCoA was performed with PRIMER v6 (Clarke and Gorley, 2006).

SIMPER analysis

To help identify which organisms were responsible for the differences observed in community composition, we used SIMPER (“similarity percentages”) in PRIMER v6 after classifying each OTU to the genus level (when possible) (Clarke and Gorley, 2006). The top 50 archaeal OTUs across samples were classified, imported into PRIMER v6, normalized by abundance in each sample, square-root transformed and then analyzed with SIMPER. The top 100 bacterial OTUs were treated similarly with the exception that data were transformed to a presence/absence matrix to account for low abundant taxa.

Quantitative PCR

Quantitative PCR was performed according to manufacturer’s instructions using the Quantitect SYBR green PCR kit (Qiagen, Inc., Valencia, CA) and 0.8 μ M final primer concentration, with melting curves performed at the end of each reaction to ensure product specificity. For total archaeal numbers, the protocol outlined by Reysenbach *et al.* (2006) was followed. For quantification of methanogens and sulfate reducers, qPCR with primers specific for the methyl coenzyme M reductase (*mcrA*) and the dissimilatory sulfite reductase (*dsrB*) genes was performed according to published methods (Wilson *et al.*, 2010). Gene copy numbers presented here were normalized by the amount of material in grams extracted.

Nucleotide sequence accession numbers

Nucleotide sequences generated in this study have been deposited to the NCBI Sequence Read Archive (SRP005280) (454 pyrosequencing) and in GenBank under accession numbers HQ893885-HQ894378 (clone libraries). Trimmed 454 sequences are also available at <http://alrlab.research.pdx.edu/projects/MAR2008>.

Contributions

For this project, I collected and processed samples, extracted genomic DNA used for pyrosequencing, qPCR and clone libraries, constructed, analyzed and interpreted clone libraries with a high school student in the laboratory (Josh Steinberg), analyzed and interpreted qPCR data, analyzed and interpreted pyrosequencing data, and wrote the manuscript for publication. In doing so, I also developed a pipeline for analysis of pyrosequencing data with Jennifer Meneghin in the Reysenbach laboratory as these types of data were new to us. Geochemical modeling was performed by Margaret K. Tivey. Hydrothermal fluid composition was determined by Jeff Seewald. qPCR assays were performed by Julie Kirshtein. Pyrosequencing was performed by Mircea Podar, James Campbell and Zamin Yang.

Chapter 3: Microbial Community Structure of Six Hydrothermal Vent Fields From the Lau Back-Arc Basin

Abstract

In this study, we characterized the archaeal and bacterial communities of over 30 hydrothermal deposits from six vent fields located along the Eastern Lau Spreading Center (ELSC) in the Lau Basin. Using bar-coded pyrosequencing of the variable region 4 (V4) of the 16S rRNA gene, we addressed two fundamental questions: 1) are the microbial communities in back-arc basins different than those from mid-ocean ridges, and 2) are the microbial communities in the ELSC different from one another? Results show that at higher taxonomic levels, the bacterial and archaeal communities of deposits from the ELSC are similar to other active vent deposits with a rich diversity of *Epsilonproteobacteria* and thermophilic *Archaea*. However, the bacterial and archaeal communities from the southernmost vent field, Mariner, were very different from the other vent fields along the ELSC. At Mariner, the bacterial genus *Nautilia* and the archaeal family *Thermococcaceae* were prevalent in most deposits, while *Lebetimonas* and *Thermofilaceae* were more abundant at the other vent fields. These differences appear to be driven by the higher concentrations of magmatic volatiles in the Mariner fluids and show that differences in geologic processes in back-arc basins can influence microbial diversity at the vent field scale.

Introduction

Marine hydrothermal vent deposits form as acidic, metal-rich, reduced hydrothermal fluids meet cold, alkaline and oxygenated seawater (Tivey, 2007). These porous deposits are characterized by steep physicochemical gradients that provide a range of microhabitats for colonizing microbes. Numerous Archaea and Bacteria that grow over a wide range of physical and chemical conditions have been isolated and characterized from vent deposits (e.g., Takai and Horikoshi, 2000b; Takai *et al.*, 2000; Götz *et al.*, 2002; Takai *et al.*, 2002; Inagaki *et al.*, 2003; Takai *et al.*, 2003; Inagaki *et al.*, 2004; Takai *et al.*, 2004a; Nakagawa *et al.*, 2005a; Nakagawa *et al.*, 2005b; Takai *et al.*, 2005; Reysenbach *et al.*, 2006; Imachi *et al.*, 2008; Takai *et al.*, 2008). Several cultivation-independent studies employing 16S rRNA gene cloning have also been conducted in order to describe the archaeal and bacterial communities associated with actively venting structures (e.g., Takai and Horikoshi, 1999; Reysenbach *et al.*, 2000; Corre *et al.*, 2001; Takai *et al.*, 2001; Nercessian *et al.*, 2003; Schrenk *et al.*, 2003; Nakagawa *et al.*, 2005d; Page *et al.*, 2008; Takai *et al.*, 2008; Voordeckers *et al.*, 2008; Nunoura and Takai, 2009; Zhou *et al.*, 2009; Kato *et al.*, 2010). Results of these studies have identified the *Epsilonproteobacteria* as being the dominant bacterial lineage associated with vent deposits (Campbell *et al.*, 2006), while other bacterial groups like the *Aquificales*, *Thermales*, *Thermotogales*, *Deltaproteobacteria* and *Thermodesulfobacteriaceae* are also commonly observed. Most Archaea associated with active vent deposits from cultivated lineages are thermophilic and belong to the *Archaeoglobales*, *Thermococcales*, *Aciduliprofundales* (DHVE2), *Methanococcales* and

Desulfurococcales. However, numerous uncultivated archaeal lineages are also commonly observed.

While past studies have provided valuable information about the physiological potential and phylogenetic diversity of microbial communities associated with active vent deposits, we still have a limited understanding of factors that control the diversity and distribution patterns of microbes in these systems. As marine hydrothermal environments are found in diverse geological settings, it is important to characterize the microbial communities from a variety of these settings in order to determine such factors. Thus far, the majority of studies have been conducted along mid-ocean ridges (MOR) where oceanic plates diverge and basaltic lavas erupt forming the seafloor. Along convergent plate boundaries, oceanic crust is consumed as it is subducted beneath a continental plate, leading to the generation of andesitic island-arc volcanoes (Martinez *et al.*, 2007). Adjacent to the island-arcs on the opposite side of the subducting slab, back-arc basins (BAB) form. Back-arc basins are extensional basins that are geologically diverse due to the presence of both convergent and divergent plate boundaries. The spreading centers generated here support hydrothermal environments that are in many ways similar to MORs. However, the composition of hydrothermal fluids in BABs are generally more variable than those from MORs due to differences in magma composition, heterogeneity of island-arc crust versus oceanic crust, and from inputs of the subducting slab (Gamo *et al.*, 2006).

The Eastern Lau Spreading Center (ELSC) is a 397-km segment that includes the Valu Fa Ridge (VFR) of the southernmost part of the back-arc spreading axis in the

Lau Basin (Ferrini *et al.*, 2008; Mottl *et al.*, 2011). Located along this segment are several hydrothermal vent fields that exhibit systematic changes in spreading rate, magma source, subduction influence and host-rock composition from north to south (Figure 3.1). Generally, the northern vent fields are similar to typical MORs as they are more heavily influenced by the diverging plates. In contrast, the southern vent fields are influenced more by the converging plates as they are closer to the Tonga Trench. Hydrothermal fluids from four of the vent fields (Kilo Moana, Tow Cam, ABE and Tui Malila) are similar to fluids from other basalt-hosted MOR systems of similar temperature (Von Damm, 1995; German and Von Damm, 2004; Mottl *et al.*, 2011). Fluids from these four vent fields exhibit a systematic decrease in temperature and an increase in pH from north to south (Mottl *et al.*, 2011). This north-south trend is also generally true for concentrations of metabolically important compounds like aqueous hydrogen (H_2), hydrogen-sulfide (H_2S) and iron (Fe) (Table 3.1). The north-south trend is reversed at the Mariner vent field (Figure 3.1). Fluids from Mariner are quite different than those elsewhere along the ELSC as they contain substantially higher concentrations of CO_2 , Fe, and transition metals and are hotter and more acidic relative to the northern vents. Many of the differences in Mariner fluids are attributed to increased volatile inputs from an actively degassing magma chamber beneath this field (Mottl *et al.*, 2011).

Because the geologic diversity along the ELSC provides an ideal setting for exploring factors that may influence patterns of microbial diversity associated with active vent deposits, we characterized the archaeal and bacterial communities of over 30

deposits from six vent fields using bar-coded pyrosequencing. Results show that the unique geologic setting of the ELSC and BABs in general, can influence both archaeal and bacterial diversity at the vent field scale.

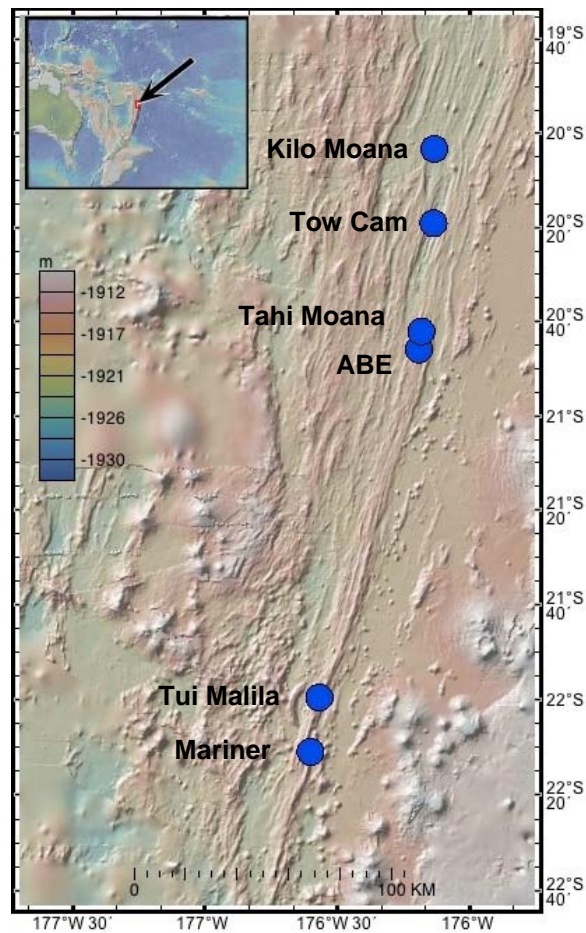


Figure 3.1. Location of hydrothermal vent fields along the Eastern Lau Spreading Center in the western Pacific Ocean.

Table 3.1. Range of physico-chemical characteristics of end-member hydrothermal fluids from different vent fields along the Eastern Lau Spreading Center.

Feature	Kilo Moana	Tow Cam	Tahi Moana	ABE	Tui Malila	Mariner	Seawater
Temp (°C)							
2004§						179-365	
2005¥	293-333	287-328		269-309	229-312	240-363	
2009‡	290-304	320	286-311	297-317	284-315	338-359	2
pH							
2004						2.4-2.7	
2005	2.9-4.0	3.7-4.1		4.3-4.6	4.2-5.7	2.5-2.7	
2009	3.9-4.1	3.6	3.3-3.9	3.9-4.0	3.8-4.2	2.2-2.4	7.6
H ₂ (µm/kg)							
2004						44.9-95.5	
2005	220-498	108-198		54-101	35-135	33-179	
2009							<0.001
H ₂ S (mm/kg)							
2004						6.9-9.0	
2005	5.4-6.4	3.7-5.2		2.6-3.6	1.2-2.5	4.2-9.3	
2009	3.5-3.9	4.8	3.1-4.1			8.9-18	<0.0001
CH ₄ (µm/kg)							
2004						7.2-8.0	
2005	28-33	44-48		42-57	31-43	5.1-7.7	
2009							<0.001
CO ₂ (mm/kg)							
2004						41.2-71.7	
2005	7.5-8.5	10.5-11.5		5.1-6.9	11.7-13.8	32.3-71.4	
2009							2.3
Fe (µm/kg)							
2004						11.1-12.8*	
2005	2,485-3,836	267-368		158-374	143-255	10.5-13.0*	
2009	534-592	205	248-332			11.6-13.1*	0.001
Mn (µm/kg)							
2004						4.9-6.0*	
2005	512-733	332-407		273-468	332-441	4.9-6.3*	
2009	193-213	326	302-468			3.9-5.2*	0.005

§from Takai *et al.* (2008)

¥from Mottl *et al.*, (2011), except H₂ values (Seewald, pers.com.).

‡this study

*Fe and Mn values for Mariner are in mm/kg

Methods

Sample collection

Hydrothermal vent deposits were obtained from six different vent fields along the ELSC in June/July 2009 during the TN236 cruise aboard the RV Thomas G. Thompson. Samples were collected using the robotic manipulators of the remotely operated vehicle (ROV) *Jason II*. Upon collection, samples were placed in sealed, custom made bioboxes to minimize contamination from surrounding seawater. Once shipboard, samples were subsampled as described previously (Götz *et al.*, 2002; Reysenbach *et al.*, 2006; Flores *et al.*, 2011). Homogenized samples were stored in cryovials at -80°C for subsequent DNA extraction. In total, 35 different deposits were used in this study (Figure 3.2, Table 3.2).

Site descriptions

The basalt-hosted Kilo Moana (KM) vent field (176°08.03'W, 20°03.15'S) is at the northern end of the ELSC at depths between 2606-2640 meters where the spreading rate is fast and the crust is relatively thin (Figure 3.1) (Ferrini *et al.*, 2008; Mottl *et al.*, 2011). Hydrothermal activity here occurs in three areas that extends north to south over approximately 130 m (Tivey *et al.*, 2005; Ferrini *et al.*, 2008). Dominant minerals present in KM deposits include cubic cubanite, chalcopyrite, and wurtzite, with pyrite and marcasite more prevalent in deposit exteriors (Tivey, pers. comm.). The Tow Cam (TC) vent field (176°08.2'W, 20°19.0'S, 2690-2728 m) is located 29-km to the south of

KM and is also hosted on basaltic substrate (Ferrini *et al.*, 2008). A newly discovered site, named Tahi Moana (TaM) (176°10.5'W, 20°40.3'S), was also sampled. This site is also basalt-hosted and is at a depth of 2214-2260 m. Fifty kilometers to the south of TC (and ~10 km from Tahi Moana) where spreading rate, crustal thickness and depth have intermediate values, is the ABE vent field (176°11.5'W, 20°45.8'S; 2104-2163 m). ABE is hosted atop basaltic-andesites (Mottl *et al.*, 2011) and hydrothermal activity here extends 600 m along the NE-SW trending fault that dominates this region (Ferrini *et al.*, 2008). Dominant minerals in ABE deposits include chalcopyrite and wurtzite with minor amounts of pyrite and barite, and trace amounts of galena (Tivey, 2007 and Tivey, pers. comm.). Approximately 140 km south of ABE on the VFR, is the Tui Malila (TuM) (176°34.06'W, 21°59.35'S, 1839-1928 m) vent field (Ferrini *et al.*, 2008). Although TuM is on a different spreading segment than ABE, both vent fields are hosted atop basaltic-andesites and are crosscut by NE-SW faults. Hydrothermal activity at TuM extends approximately 350 m north-to-south. Twenty-five kilometers south of TuM on the VFR is the Mariner (176°36.09'W, 22°10.82'S; 1877-1951 m) vent field. Like TuM and ABE, Mariner is hosted on basaltic-andesite, but dacites and rhyolites also lie close to the vents at Mariner (Mottl *et al.*, 2011). Mariner deposits are lined with chalcopyrite, and bornite, with trace amounts of tennentite observed in mid- and exterior layers. Some structures are also barite-rich. Deposits collected from each vent field are summarized in Table 3.2.

Table 3.2. Hydrothermal deposits collected from the Eastern Lau Spreading Center used for microbial community characterization.

Sample Name	Rock number	Longitude	Latitude	Depth (m)	# of bacterial pyrotags	# of archaeal pyrotags
KM-1	J2-434-1-R1	176.13362 W	20.054029 S	2622	-	3368
KM-2	J2-434-2-R1	176.133639 W	20.053795 S	2621.9	5932	4669
KM-35	J2-436-2-R1	176.133515 W	20.054093 S	2616.9	11242	4318
KM-36	J2-436-4-R1	176.133763 W	20.053234 S	2611	8159	6239
TC-26	J2-443-6-R2	176.136593 W	20.316307 S	2721	7061	1159
TC-27	J2-443-4-R1	176.136554 W	20.316497 S	2717	-	4023
TC-46	J2-443-2-R1	176.136516 W	20.316524 S	2710	7757	2801
TC-61	J2-451-1-R1	176.13665 W	20.316316 S	2717	11201	1694
TC-62	J2-451-3-R1	176.136459 W	20.316497 S	2709.7	9842	4035
TaM-29	J2-445-5-R1	176.180099 W	20.673876 S	2258	-	2876
TaM-47	J2-444-22-R1	176.183584 W	20.684679 S	2214.3	8688	5814
TaM-48	J2-444-23-R1	176.18343 W	20.684552 S	2216.7	9108	1118
TaM-49	J2-444-23-R2	176.18343 W	20.684552 S	2216.7	6309	2836
TaM-50	J2-444-4-R1	176.182643 W	20.681743 S	2230	6907	5759
TaM-51	J2-445-4-R1	176.18007 W	20.673894 S	2258	9242	-
TaM-52	J2-445-6-R1	176.180109 W	20.673876 S	2257	11334	1710
ABE-3	J2-435-1-R1	176.190398 W	20.761274 S	2141	4884	2863
ABE-5	J2-435-10-R1	176.193079 W	20.766332 S	2128	8607	3226
ABE-6	J2-435-18-R1	176.191964 W	20.762719 S	2127	6823	3935
ABE-7	J2-435-9-R1	176.192743 W	20.766043 S	2134	7051	3731
ABE-33	J2-435-11-R2a	176.193098 W	20.766214 S	2128.6	6098	4019
ABE-34	J2-435-20-R1	176.190533 W	20.761219 S	2163	11143	2788
TuM-17 ^y	J2-442-12-R2	176.56885 W	21.990663 S	1853	8490	3580
TuM-21 ^y	J2-442-10-R1	176.56885 W	21.990699 S	1855	10875	-
TuM-30 [†]	J2-447-4-R1	176.569082 W	21.99059 S	1842	10078	4799
TuM-31 [†]	J2-447-4-R1	176.569082 W	21.99059 S	1842	-	3740
Mariner-12	J2-437-7-R1	176.600977 W	22.180414 S	1919.2	7715	5085
Mariner-14	J2- 439-3-R1	176.601782 W	22.18045 S	1919	12136	2967
Mariner-15	J2- 439-13-R2	176.601248 W	22.180089 S	1918.1	7626	1321
Mariner-37	J2-437-10-R1	176.60119 W	22.179953 S	1911	-	717
Mariner-38	J2-437-14-R1	176.601045 W	22.179989 S	1912	-	3033
Mariner-39	J2-437-16-R1	176.60087 W	22.180107 S	1917	8577	3151
Mariner-40	J2-437-3-R2	176.601743 W	22.180558 S	1922.9	7694	443
Mariner-42	J2- 439-5-R1	176.600928 W	22.180107 S	1914	8553	412
Mariner-58	J2-448-4-R1	176.601704 W	22.18073 S	1921	7682	1086
Mariner-59	J2-448-9-R1	176.601966 W	22.180612 S	1925.5	21728	962

^yIndicates samples that were collected from the same structure at different times.

[†]Indicates sub-samples that were collected from the same sample.

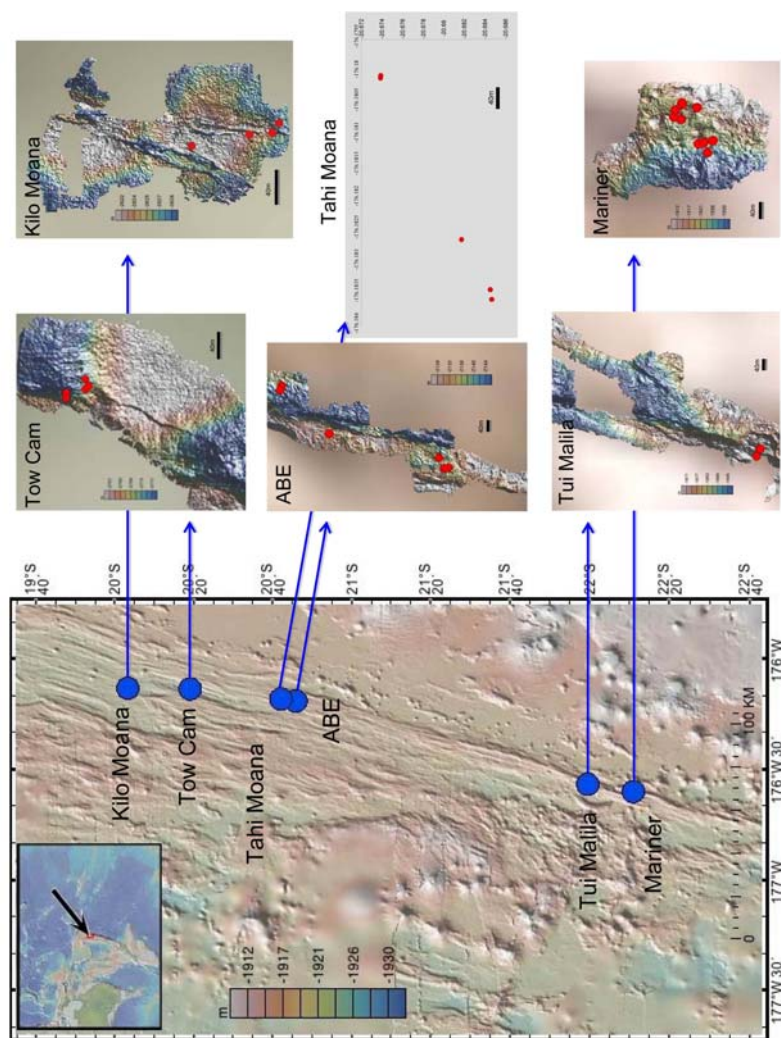


Figure 3.2. Location of deposits collected from each hydrothermal vent field along the Eastern Lau Spreading Center.

DNA extraction, pyrosequencing and sequence analysis

DNA was extracted from homogenized samples ($\approx 1.6 - 3.2$ grams) using the Ultra Clean Soil DNA Isolation Kit (MoBio Laboratories) as previously described (Reysenbach *et al.*, 2006). Pyrosequencing of the variable region 4 (V4) of the 16S rRNA gene was conducted as previously described (Flores *et al.*, 2011).

Raw sequences were initially processed using the RDP-pyrosequencing pipeline (Cole *et al.*, 2009) where sequences less than 200 bp, containing ambiguous nucleotides (N's), with any mismatches to the forward or reverse primers and with a quality score < 20 were discarded (Flores *et al.*, 2011). The resulting sequences were filtered using custom perl scripts to include sequences less than 275 bp and 250 bp for Archaea and Bacteria, respectively. Trimmed sequences were then subjected to a pre-classification step using the RDP-classifier (Wang *et al.*, 2007) in which unclassified sequences (not Archaea or Bacteria) or sequences classified to the incorrect domain (e.g., Bacteria in the archaeal data set) were removed. Quality sequences were then aligned and clustered using the SLP/PW-AL pipeline (Huse *et al.*, 2010) at a 97% similarity cutoff. The resulting cluster files were converted to a format suitable for the RDP-pipeline to generate rarefaction curves (Colwell and Coddington, 1994) and Chao1 richness estimators (Chao and Bunge, 2002) for each sample. Taxonomic classifications were assigned as previously described (Flores *et al.*, 2011) for representative sequences of each cluster.

Pyrosequencing data was analyzed using a combination of OTU-based (Bray-Curtis, Sørensen) and phylogeny-based (UniFrac) (Lozupone *et al.*, 2006; Hamady *et*

al., 2010) beta-diversity metrics as previously described (Flores *et al.*, 2011). Similarity and distance matrices were visualized using non-metric multi-dimensional scaling (MDS), and tested for significance using ANOSIM with PRIMER v6 (Clarke and Gorley, 2006). Only the Bray-Curtis results are presented.

In addition to the routine denoising efforts described above, the archaeal libraries of four deposits were processed using a recently described AmpliconNoise denoising pipeline (Quince *et al.*, 2011). Comparison of the denoising results for the four libraries with and without AmpliconNoise is shown in Table 3.3.

Results

Bacterial community composition

A total of 268,542 high-quality partial 16S rRNA gene sequences were generated from the 30 hydrothermal vent samples for an average of 8,951 sequences per sample (4,884-21,728 sequences per sample) (Table 3.2). From these sequences, 1,699 unique operational taxonomic units (OTUs) (97% sequence similarity, 79-400 OTUs per sample) were identified with 42% (715) being singleton OTUs (Figure 3.3). The most abundant OTU (20.24% of all sequences) was related to *Sulfurovum* and was found in all 30 deposits. *Nitratifractor* (4.20%), *Desulfobulbus* (3.02%) and *Hippea* (0.47%) were the only other OTUs observed in all deposits. Rarefaction analysis (Figure 3.4) and Chao1 richness estimators (Figure 3.3) revealed that more bacterial

diversity may exist for many of the samples surveyed. Bacterial diversity was also generally higher than archaeal diversity for most samples (Figure 3.5).

Table 3.3. Results of AmpliconNoise analysis of four archaeal pyrosequencing libraries from vent deposits of the Eastern Lau Spreading Center. Sequences were put through the AmpliconNoise program as described by Quince *et al.*, (2011) without removal of potential chimeras with Perseus. Resulting sequences were aligned and clustered using two methods as described by Flores *et al.* (2011). Results obtained without AmpliconNoise are provided for comparison.

Sample	# of Sequences	RDP – 95%		SLP/PW-AL – 97%	
		OTUs observed	Chao1 (95% CI)	OTUs observed	Chao1 (95% CI)
Lau09-15 (AN) [§]	1455	18	19 (18-29)	17	19 (17-32)
Lau09-15	1321 [*]	25	30 (26-57)	19	21 (19-34)
Lau09-33 (AN)	4402	44	50 (45-71)	48	55 (50-80)
Lau09-33	4019	60	67 (62-88)	50	57 (52-78)
Lau09-34 (AN)	2657	78	122 (95-188)	87	141 (110-216)
Lau09-34	2788	105	144 (122-194)	89	136 (109-201)
Lau09-35 (AN)	4158	27	35 (28-70)	31	43 (34-85)
Lau09-35	4318 ⁺	39	46 (41-71)	34	56 (40-121)

[§]AmpliconNoise

^{*}59 of these sequences were not in the 1455 sequences resulting from the AmpliconNoise analysis (52 of 59 are unique). From these 59 sequences, four singleton OTUs were generated within the sample but only one of these OTUs was not observed in another sample.

⁺216 of these sequences were not in the 4158 sequences resulting from the AmpliconNoise analysis (174 of 216 are unique). From these 216 sequences, only three unique OTUs were observed.

With the exception of KM-2 and Mariner-12, the majority (> 50%) of sequences detected in all the samples were classified as *Epsilonproteobacteria* (Figure 3.6a). *Caminibacter*, *Lebetimonas*, *Nautilia*, *Nitratifractor*, *Nitratiruptor*, *Sulfurimonas* and *Sulfurovum* were associated with most deposits although the dominant genera varied between samples and in the case of Mariner, by vent field, as the *Nautilia* were more prevalent here (Figure 3.6a). Other taxa commonly observed included thermophilic and non-thermophilic lineages such as the *Alphaproteobacteria*, *Aquificales*, *Caldisericia*, *Chloroflexi*, *Deferribacteres*, *Deinococcus/Thermus*, *Deltaproteobacteria*, *Firmicutes*, *Gammaproteobacteria*, *Thermodesulfobacteria* and *Thermotogae* (Figure 3.6b).

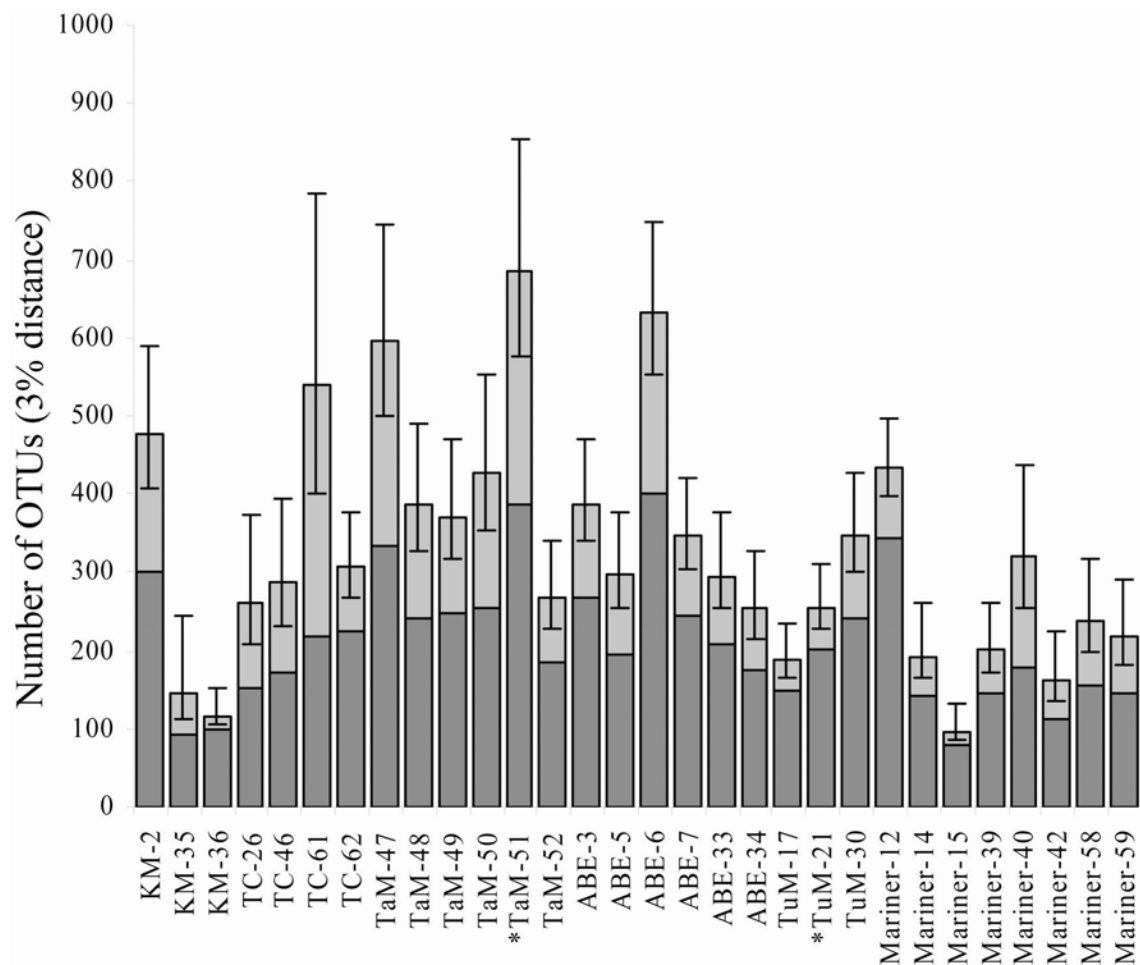


Figure 3.3. OTU richness (dark grey bars) and Chao1 diversity estimates (light grey bars) of bacterial diversity for each vent deposits characterized from the Eastern Lau Spreading Center. Error bars indicate the 95% confidence interval of the Chao1 estimator. Asterisks denote samples for which corresponding archaeal data was not obtained.

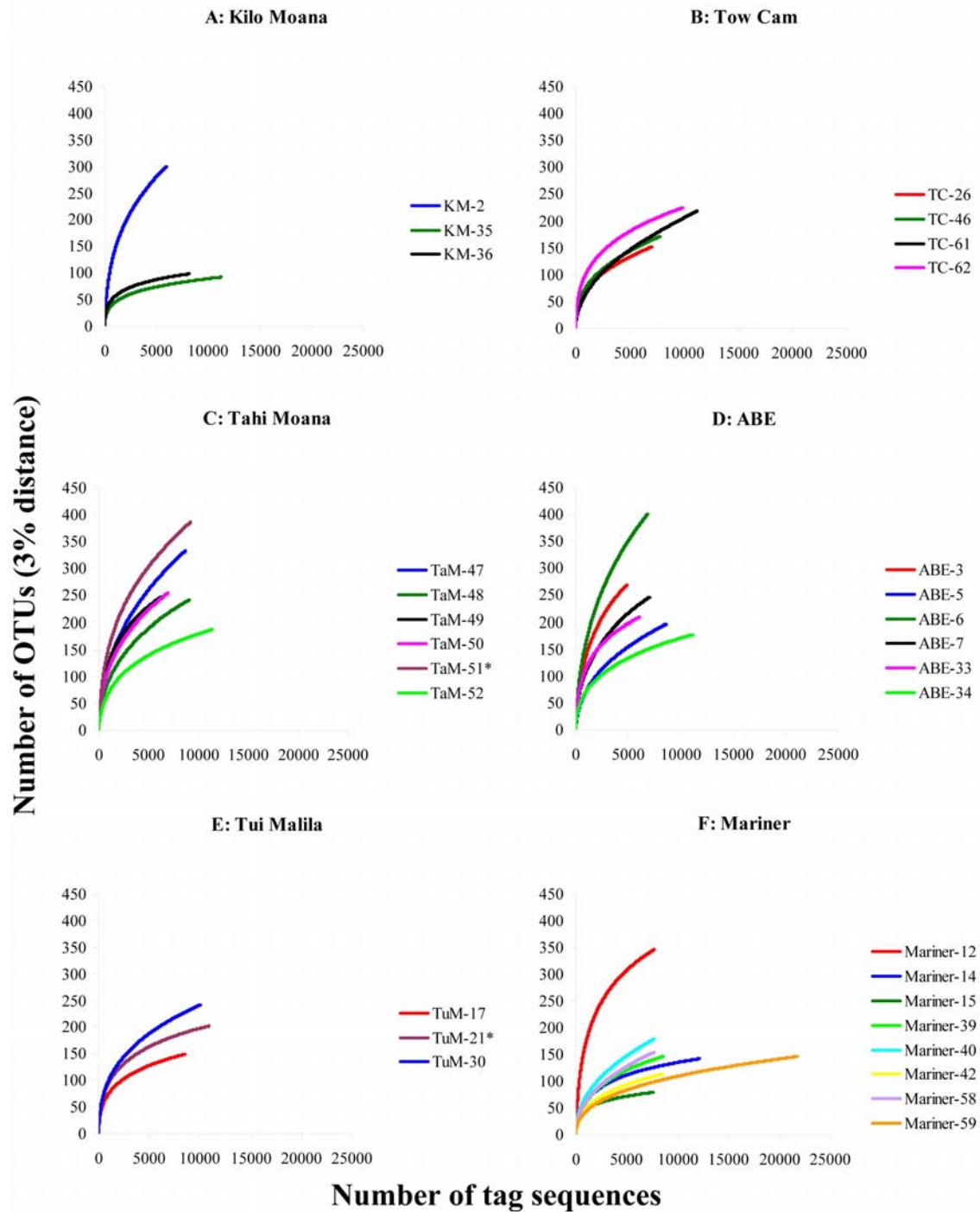


Figure 3.4. Rarefaction curves for bacterial communities of hydrothermal vent deposits from different vent fields along the Eastern Lau Spreading Center.

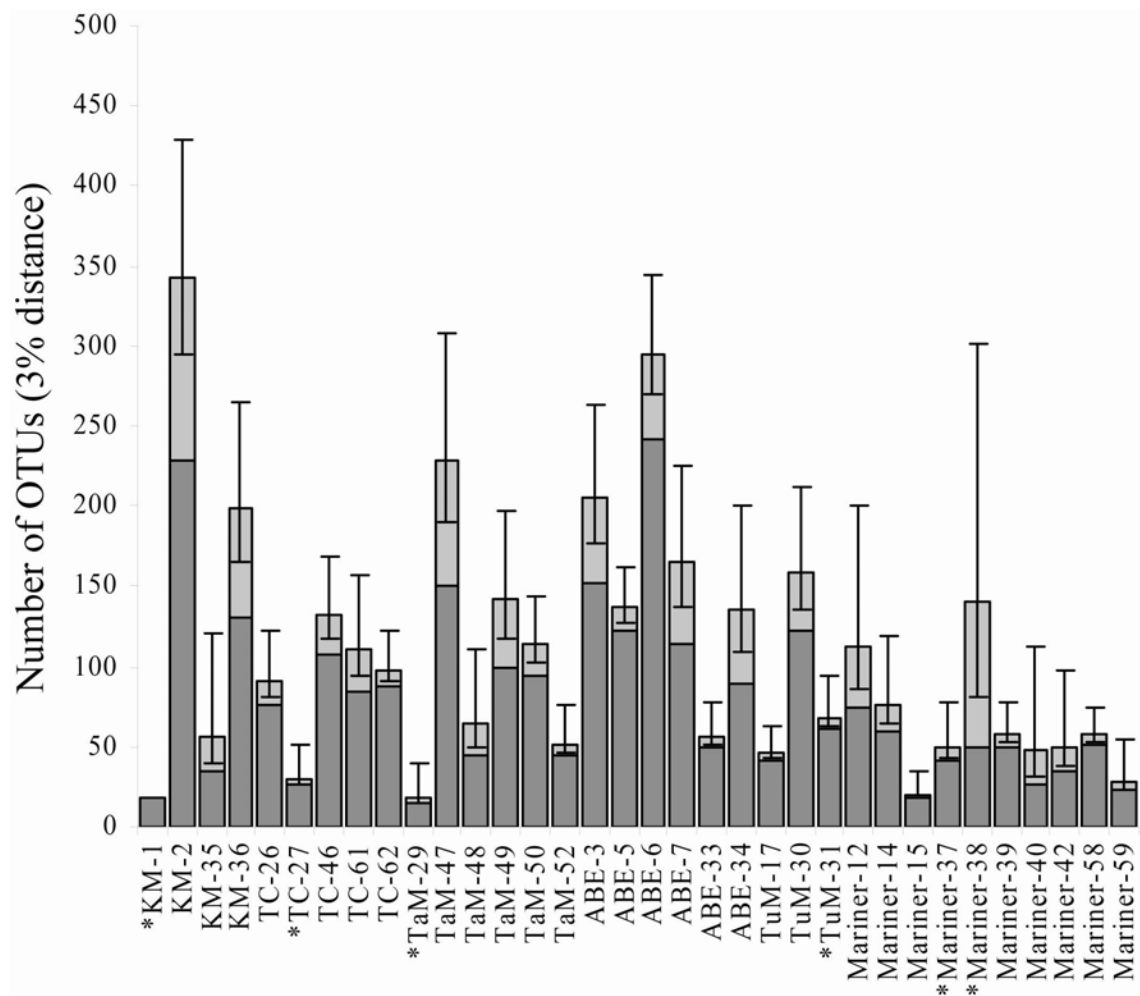


Figure 3.5. OTU richness (dark grey bars) and Chao1 diversity estimates (light grey bars) of archaeal diversity for each vent deposits characterized from the Eastern Lau Spreading Center. Error bars indicate the 95% confidence interval of the Chao1 estimator. Asterisks denote samples for which corresponding bacterial data was not obtained.

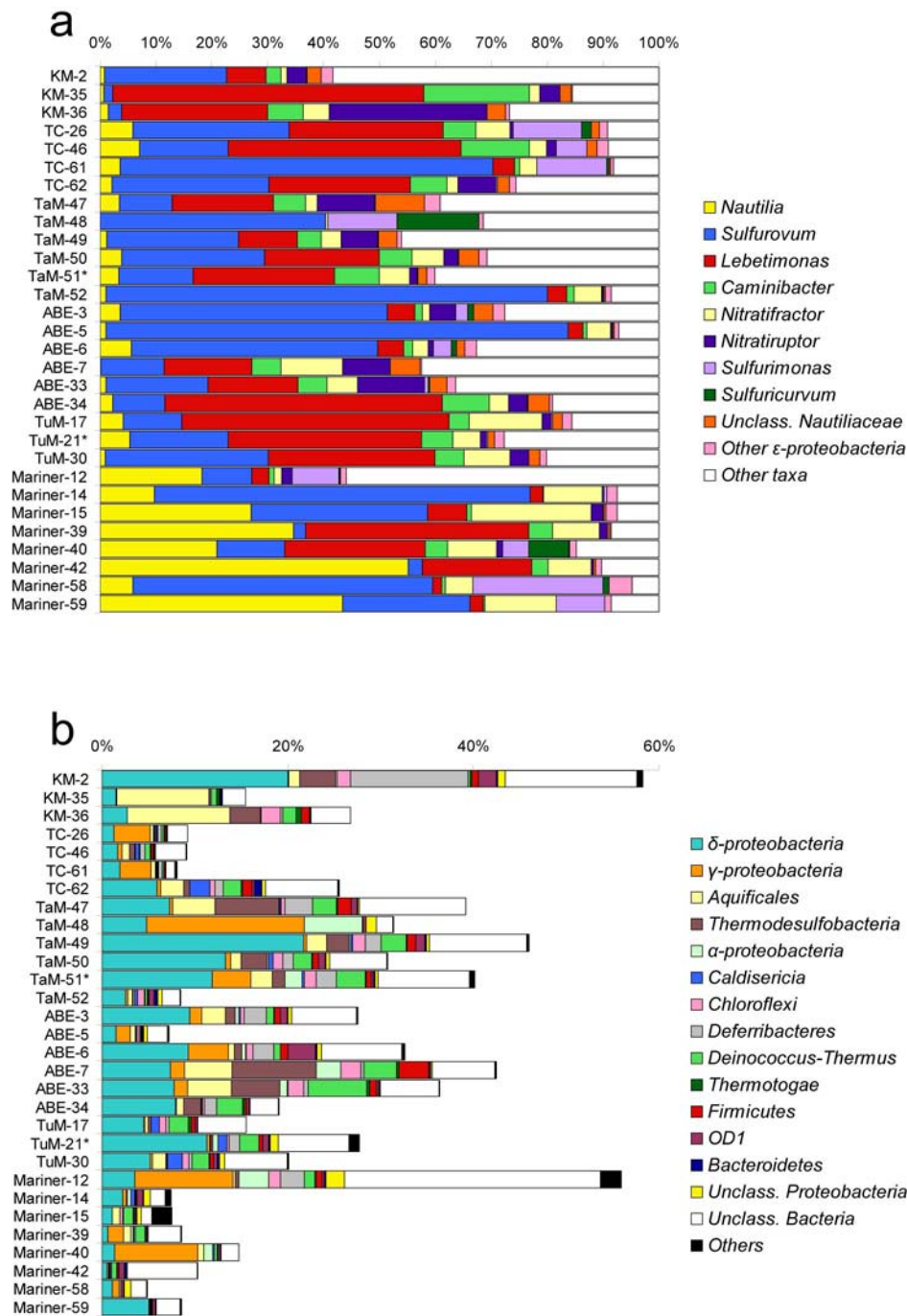


Figure 3.6. Relative abundance of epsilonproteobacterial genera (**a**) and other bacterial taxa (**b**) observed in hydrothermal vent deposits collected from the Eastern Lau Spreading Center. Asterisks denote deposits for which corresponding archaeal data was not obtained.

Interfield bacterial community comparisons

Results of a one-way ANOSIM test comparing the bacterial communities from the different vent fields showed that the communities associated with Mariner deposits were distinct as all pairwise comparisons were statistically significant ($P < 0.05$) (Table 3.4). Only one other pairwise comparison (KM vs. TC) was statistically significant ($R = 0.463$, $P = 0.029$). Non-metric multidimensional scaling (MDS) plots support these observations as communities from Mariner cluster together to the exclusion of deposits from other vent fields, and the communities from KM do not overlap with those from TC (Figure 3.7a). Overall, these results indicate that the bacterial communities from Mariner are different from the other vent fields in the Lau Basin.

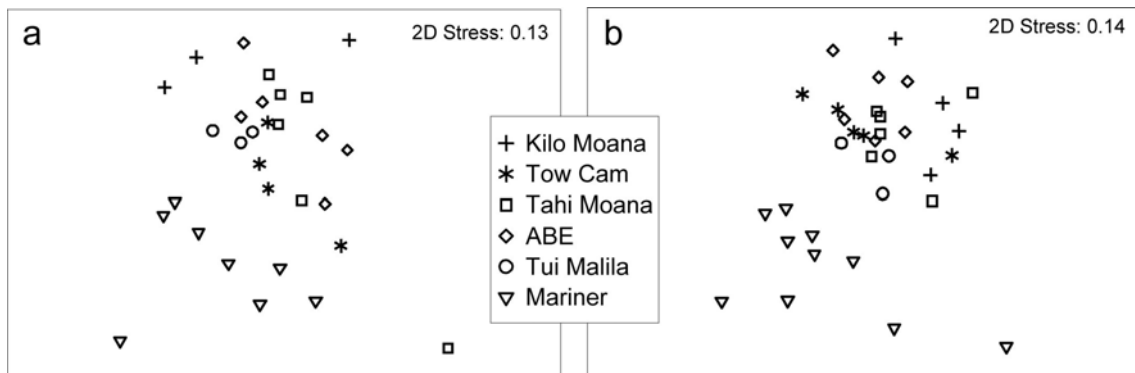


Figure 3.7. Non-metric multidimensional scaling plots (MDS) based on Bray-Curtis similarities of the bacterial (a) and archaeal (b) communities of hydrothermal vent deposits from the Eastern Lau Spreading Center.

Table 3.4. Results of pairwise comparisons of bacterial communities from different vent fields along the Eastern Lau Spreading Center using the ANOSIM test in Primer v6. *R*- and *p*-values (parentheses) are shown for each comparison. Values in italics indicate those that are statistically significant at a *p*-value ≤ 0.05 .

	Kilo Moana	Tow Cam	Tahi Moana	ABE	Tui Malila
Kilo Moana					
Tow Cam	<i>0.463</i> (0.029)				
Tahi Moana	0.204 (0.19)	0.159 (0.148)			
ABE	0.364 (0.083)	0.194 (0.114)	-0.039 (0.645)		
Tui Malila	0.37 (0.10)	0.537 (0.057)	0.031 (0.405)	0.154 (0.226)	
Mariner	<i>0.806</i> (0.006)	<i>0.381</i> (0.012)	<i>0.463</i> (0.001)	<i>0.594</i> (0.0007)	<i>0.411</i> (0.048)
Summary	6/15 pairwise comparisons are statistically significant ($p < 0.05$)				

Archaeal community composition

The archaeal communities of 34 vent deposits were characterized generating 104,277 partial 16S rRNA gene sequences (412-6,239 sequences per sample) (Table 3.2). A total of 656 unique OTUs (97% sequence similarity, 15-242 OTUs per sample) were identified with approximately 17% (114) containing only one sequence (Figure 3.5). The single most abundant OTU (17.6% of all sequences) was classified as *Thermofilum* and was found in 28 of 34 deposits. The six deposits that did not contain this OTU were all from the Mariner vent field. *Thermococcus* (13.2% of all sequences) was the only OTU detected in all deposits. Unlike for the bacterial communities, much

of the diversity of the archaeal communities appeared to be captured as many of the rarefaction curves were asymptotic (Figures 3.8).

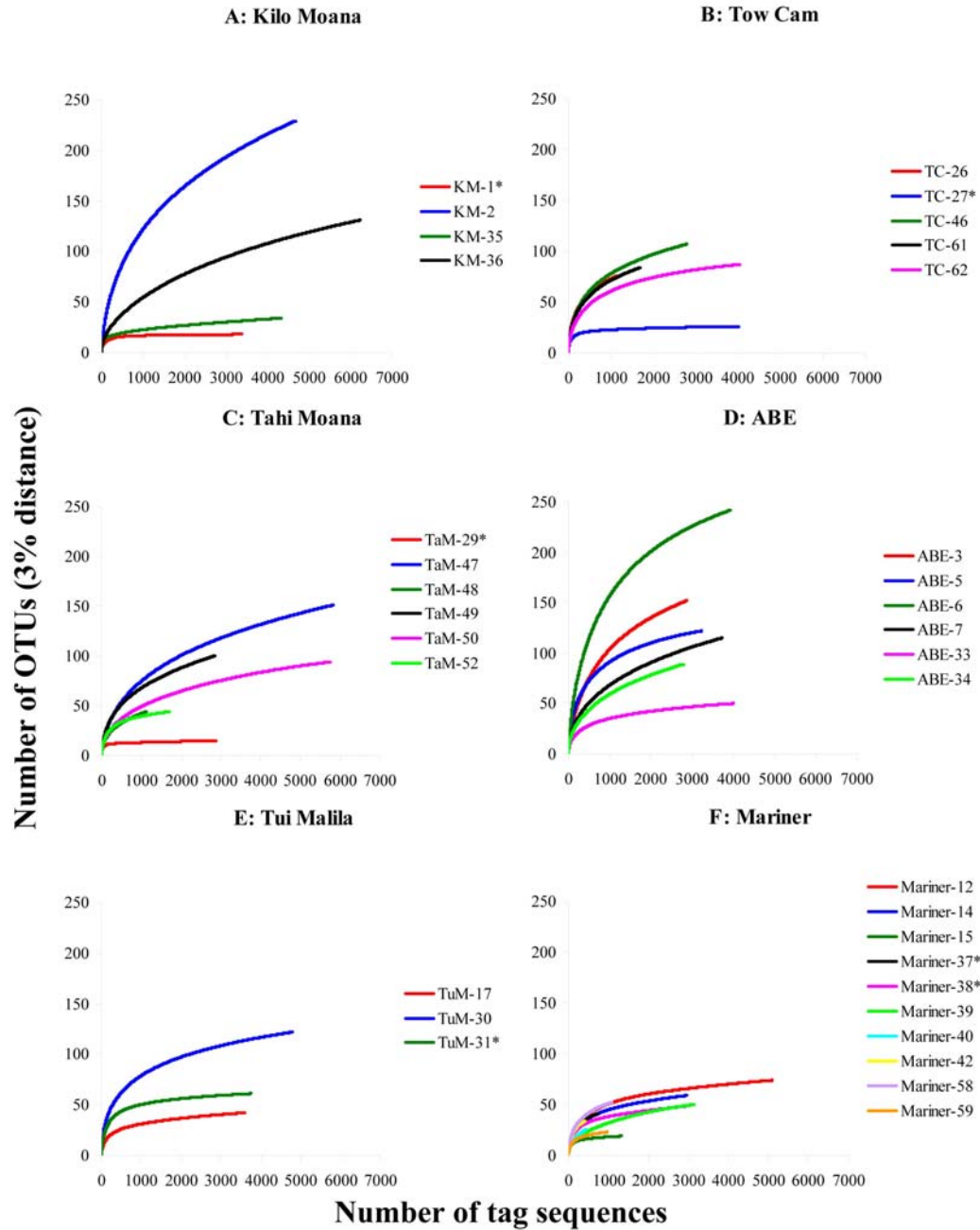


Figure 3.8. Rarefaction curves for archaeal communities of hydrothermal vent deposits from different vent fields along the Eastern Lau Spreading Center.

The *Crenarchaeota* were most abundant in 24 of the 34 deposits (Figure 3.9a). Within the *Crenarchaeota*, the *Desulfurococcaceae*, *Thermofilaceae* and *Thermoproteaceae* were abundant in most deposits except those from Mariner. Deposits from Mariner had, on average, a lower proportion of crenarchaeotal sequences than the other vent fields but did harbor some unique lineages not commonly observed in marine hydrothermal environments (Figure 3.9a, b). For example, one deposit from Mariner, Mariner-12, had a significant number of *Caldisphaeraceae*. There were many crenarchaeotal sequences that could not be classified beyond the class (*Thermoprotei*) or order (*Desulfurococcales* and *Thermoproteales*) levels (Figure 3.9a; unclassified *Crenarchaeota*). Of the ten samples not dominated by *Crenarchaeota*, nine had mostly euryarchaeotal sequences (mostly in the *Thermococcaceae*, DHVE2 and *Archaeoglobaceae*) and one had over 40% nanoarchaeotal sequences. The *Thermococcaceae* dominated most deposits from Mariner (Figure 3.9b). Methanogens (*Methanocaldococcaceae* and *Methanococcaceae*) were relatively rare in most deposits, especially those from Mariner (Figure 3.9b). Several unclassified lineages like the DHVE5 and the unclassified *Euryarchaeota* A (Flores *et al.*, 2011) were also frequently detected (Figure 3.9a). The *Nanoarchaeota* and *Korarchaeota* were observed in 27 and 24 of the 34 deposits, respectively.

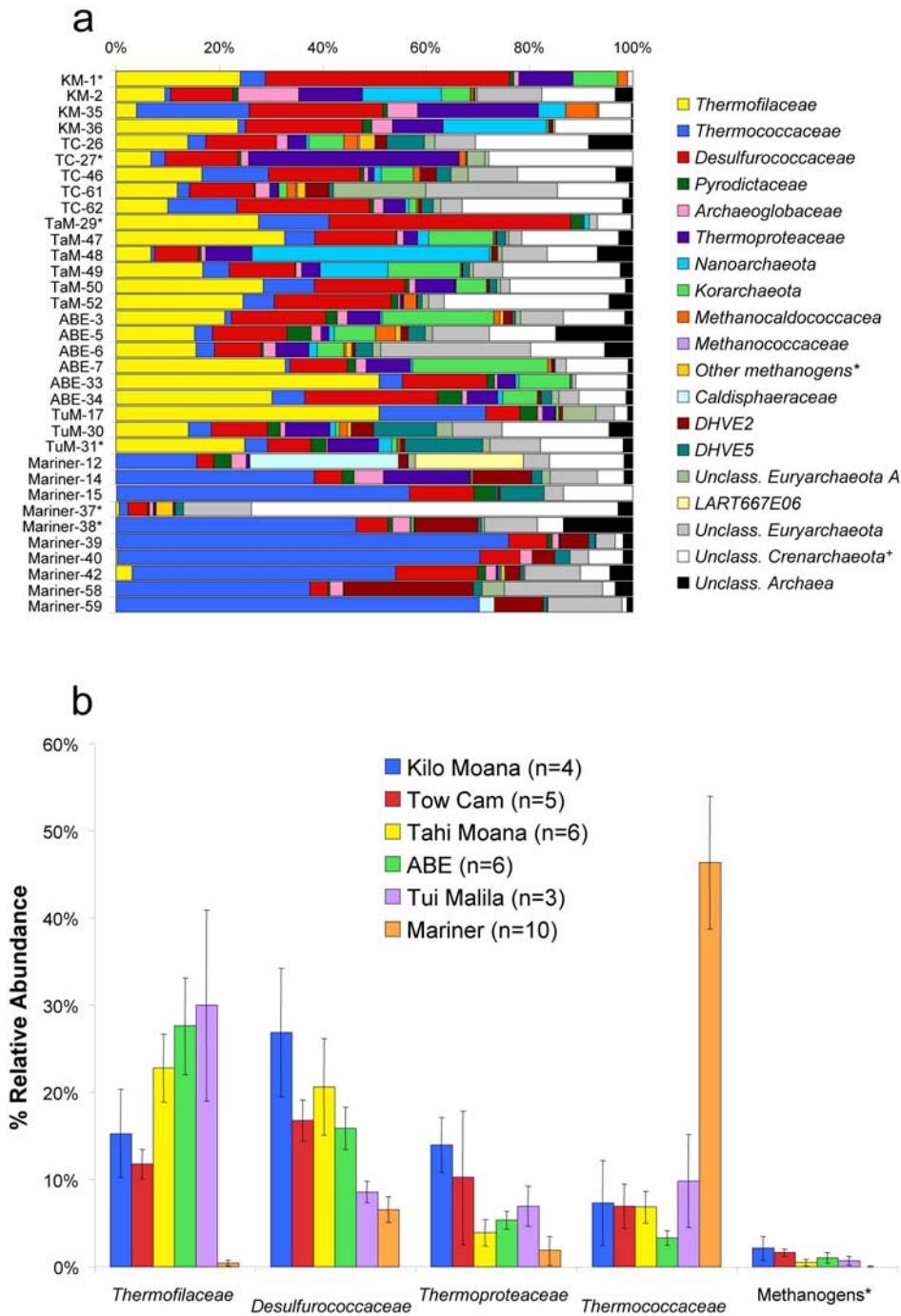


Figure 3.9. Relative abundance of archaeal families (**a**) observed in individual deposits and average abundance of discriminating archaeal families (**b**) observed in deposits within individual vent fields along the Eastern Lau Spreading Center. Asterisks in **a** denote deposits for which corresponding bacterial data was not obtained. Error bars in **b** indicate ± 1 standard error of the mean (SEM).

Interfield archaeal community comparisons

As was observed with the bacterial ANOSIM test, all pairwise comparisons involving Mariner were statistically significant ($P < 0.05$) (Table 3.5 & Figure 3.7b). Unlike with the bacterial communities, however, several other pairwise comparisons including all involving ABE and 4/5 involving KM were also statistically significant ($P < 0.05$) (Table 3.5). Overall, these results suggest that the archaeal communities from the six vent fields, particularly KM, ABE and Mariner, are unique.

Table 3.5. Results of pairwise comparisons of archaeal communities from different vent fields along the Eastern Lau Spreading Center using the ANOSIM test in Primer v6. *R*- and *p*-values (parentheses) are shown for each comparison. Values in italics indicate those that are statistically significant at a *p*-value ≤ 0.05 .

	Kilo Moana	Tow Cam	Tahi Moana	ABE	Tui Malila
Kilo Moana					
Tow Cam	<i>0.444</i> (0.032)				
Tahi Moana	0.087 (0.238)	0.077 (0.169)			
ABE	<i>0.563</i> (0.01)	<i>0.416</i> (0.002)	<i>0.146</i> (0.041)		
Tui Malila	<i>0.463</i> (0.029)	0.395 (0.071)	0.179 (0.214)	<i>0.346</i> (0.048)	
Mariner	<i>0.734</i> (0.002)	<i>0.591</i> (0.001)	<i>0.598</i> (0.0001)	<i>0.699</i> (0.0001)	<i>0.422</i> (0.045)
Summary	11/15 pairwise comparisons are statistically significant ($p \leq 0.05$)				

Discussion

The microbial communities of active hydrothermal vent deposits from six vent fields located along the ELSC were characterized using bar-coded pyrosequencing in order to broaden our understanding of the spatial diversity of deep-sea vent microbial communities. The results presented provide valuable insight into the diversity of microorganisms that inhabit hydrothermal vent deposits and begin to illustrate the impact different geologic settings can have on microbial community composition and structure.

Bacterial communities

Overall, the bacterial communities associated with active hydrothermal deposits in the Lau Basin resemble those from other hydrothermal vent sites with diverse *Epsilonproteobacteria* dominating most deposits. *Epsilonproteobacteria* are considered the most ecologically important microorganisms in marine hydrothermal environments where they are involved in carbon, nitrogen and sulfur cycling at low and high temperatures, and in both oxic and anoxic habitats (Campbell *et al.*, 2006). Most of the deposits had a mix of mesophilic (*Sulfurovum* and *Nitratifractor*) and thermophilic (*Lebetimonas*, *Caminibacter* and *Nautilia*) genera illustrating the steep thermal gradients that exist in vent deposits (Figure 3.6). The prevalence of *Lebetimonas* in most deposits, however, was unexpected as our previous work had shown them to be a minor component of the bacterial communities in deposits from the Mid-Atlantic Ridge (MAR) (Flores *et al.*, 2011). Instead, the closely related *Caminibacter* (both are part of

the *Nautiliaceae*) was the dominant genus of *Epsilonproteobacteria* in most samples from the MAR. While *Caminibacter* are widespread along the ELSC as well, they are generally lower in abundance than *Lebetimonas*. The only described *Lebetimonas* isolate was obtained near the ELSC and is a moderate acidophile capable of oxidizing H₂ and reducing sulfur (Takai *et al.*, 2005). *Caminibacter* are also H₂-oxidizers but have been isolated from the East Pacific Rise (EPR) (Alain *et al.*, 2002) and MAR (Miroshnichenko *et al.*, 2004; Voordeckers *et al.*, 2005). While it is possible that classification of *Lebetimonas* is an artifact of the RDP-classifier, we combined our MAR and ELSC data sets and the dominant *Lebetimonas* OTU at the ELSC (11.03% of all sequences) is not present along the MAR (data not shown). Also, *Lebetimonas* were not detected in 16S rRNA gene clone libraries from deposits along a different back-arc spreading center also in the western Pacific Ocean (Southern Mariana Trough – SMT) (Kato *et al.*, 2010). In that study, depth was thought to be an important factor in epsilonproteobacterial biogeography. Although our study also covers a depth gradient, the vent fields examined here are deeper than those considered by Kato *et al.* (2010). Overall, these results continue to demonstrate the importance of the *Epsilonproteobacteria* in bacterial biogeography of deep-sea vents but also provide intriguing areas for future studies as to why certain genera are more prevalent in different geologic and geographic settings.

Besides the *Epsilonproteobacteria*, genera of *Deltaproteobacteria* were also frequently abundant in most deposits. One genus observed in all samples, albeit at relatively low numbers, was *Hippea*. Recently, several novel *Hippea* species were

found to be thermoacidophiles similar to the archaeal DHVE2 (Flores *et al.*, in review) (Reysenbach *et al.*, 2006). Acidic habitats are generated in deposits by the conductive cooling of hydrothermal fluids or by diffusion of hydrothermal fluids outwards across the wall of a deposit without any mixing of seawater (Tivey, 2004). Just as the presence of mesophilic and thermophilic *Epsilonproteobacteria* illustrated the steep temperature gradients in vent deposits, the presence of thermoacidophiles in all deposits highlights the steep pH gradients that also exist in vent deposits.

The statistical differences observed in the bacterial communities from the Mariner deposits are most evident by the shift in the abundance of *Nautilia* (Figure 3.6a). *Nautilia* are moderately thermophilic, mixotrophic anaerobes (Campbell *et al.*, 2001; Miroshnichenko *et al.*, 2002; Smith *et al.*, 2008). What distinguishes *Nautilia* from other thermophilic *Epsilonproteobacteria* like *Caminibacter* and *Lebetimonas*, is their ability to oxidize formate (Campbell *et al.*, 2006). The concentration of formate in fluids from the ELSC is unknown. However the concentration of formate varies as a function of total carbon, the redox state of the fluids and temperature (Seewald *et al.*, 2006). The CO₂ concentrations at Mariner are generally three to five times higher than the other vent fields due to active degassing of a subsurface magma chamber which also results in more acidic, metal-rich fluids (Table 3.1) (Mottl *et al.*, 2011). With higher CO₂ concentrations in the fluids, formate concentrations may also be higher relative to the other vent fields. Formate is also produced biologically by fermentative Archaea like the DHVE2 (Reysenbach *et al.*, 2006). As total carbon and the DHVE2 are generally more abundant at Mariner, the prevalence of *Nautilia* here may be related to

the availability of formate. Interestingly, several species of *Thermococcus*, which are also abundant at Mariner (see below), have also recently been found to oxidize formate (Kim *et al.*, 2010).

Archaeal communities

As with the bacterial communities, the archaeal communities of the ELSC are generally similar to other deep-sea hydrothermal vent fields with a rich diversity of thermophilic *Euryarchaeota* and *Crenarchaeota*, and the occasional detection of the *Korarchaeota* and *Nanoarchaeota*. The abundance of the *Crenarchaeota* in most deposits (other than Mariner), however, is somewhat unusual as the majority of other 16S rRNA gene based studies of vent deposits have typically recovered a higher proportion of euryarchaeotal sequences (e.g., Takai and Horikoshi, 1999; Takai *et al.*, 2001; Schrenk *et al.*, 2003; Kormas *et al.*, 2006; Voordeckers *et al.*, 2008; Nunoura and Takai, 2009). Unfortunately, many crenarchaeotal lineages observed in the deep-sea are uncultivated, and those with cultivated organisms are represented by only one or a few isolates (Boone *et al.*, 2001). As a result, we know relatively little about the physiological and metabolic capabilities of many of the groups we are now detecting. As it is now recognized that Archaea are not just extremophiles, it is possible that some of these groups could occupy lower temperature niches where they compete with mesophilic Bacteria. These observations highlight the need for more targeted cultivation efforts or the use of single cell genomics techniques to help describe many of these novel lineages.

Regardless of the lack of cultivable diversity, it is clear that the low abundance of *Crenarchaeota* coupled with the high abundance of *Thermococcaceae*, discriminates the Mariner communities from the other vent fields (Figures 3.7 and 3.9). Cultivated members of the *Thermococcaceae* are generally sulfur-reducing heterotrophs (Reysenbach *et al.*, 2002). However, recent genomic analyses of multiple *Thermococcus* species from different deep-sea hydrothermal environments have revealed several species with the potential to oxidize CO to CO₂ (carboxydotrophy) (Lee *et al.*, 2008; Zivanovic *et al.*, 2009; Vannier *et al.*, 2011). Several *Thermococcus* species, including one isolated from KM, have also recently been shown to conserve energy through the anaerobic oxidation of formate coupled with H₂ production (Kim *et al.*, 2010). As with the *Nautilia* discussed above, the abundance of *Thermococcaceae* at Mariner may be related to single-carbon compounds originating from the degassing magma chamber or from other fermentative organisms. Further studies are needed to evaluate the importance of single-carbon compounds in the ecology of this ubiquitous deep-sea archaeon.

The relatively low abundance of methanogens (*Methanocaldococcaceae* and *Methanococcaceae*) at all vent fields continues to demonstrate the importance of H₂ concentrations in structuring the archaeal communities of deep-sea hydrothermal environments (Takai *et al.*, 2006b; McCollom, 2007; Perner *et al.*, 2007; Takai and Nakamura, 2010; Flores *et al.*, 2011). Recently, we characterized the archaeal communities associated with two vent fields at either end of the spectrum with regards to H₂ concentrations and found that methanogens were absent in deposits from the vent

field with extremely low H₂ concentrations while methanogens were abundant when H₂ concentrations were high (Flores *et al.*, 2011). Fluids from the vent fields surveyed in this current study all have H₂ concentrations that are between these two extremes but are much closer to the low end of the spectrum (Table 3.1). It is therefore not surprising that methanogens were observed at relatively low abundance in these vent fields.

Integrating our observations with the known geochemistry of different vent fields should allow for predictions of the occurrence and abundance of methanogens in future studies.

Clear differences in the archaeal communities from deposits within the same vent field were also commonly observed. For example, the archaeal (and bacterial) communities associated with Mariner-12 were very different from any other deposit (Figure 3.9). This same structure was sampled in 2005 and yielded the first obligate thermoacidophile from the deep-sea in pure culture (Reysenbach *et al.*, 2006). Other archaeal lineages identified from the Mariner-12 deposit during our study may also represent novel acidophilic deep-sea lineages. Specifically, the *Caldisphaeraceae* are a thermoacidophilic crenarchaeotal lineage that has only been cultivated from terrestrial hydrothermal environments (Prokofeva *et al.*, 2000; Itoh *et al.*, 2003; Prokofeva *et al.*, 2009) and, to our knowledge, has not previously been detected in the deep-sea. Also, sequences related to the LART667E06 (DQ451876) clone that hinted at an acidophilic lifestyle of the DHVE2 are closely related to acidophilic *Thermoplasmales* isolated from terrestrial environments (Reysenbach *et al.*, 2006). Besides Mariner, deposits within other vent fields also varied from one another. For example, the *Nanoarchaeota*

were abundant in two samples from TaM (TaM-48, TaM49), while they were relatively rare in the 4 other deposits from this vent field. Other researchers have observed variable communities associated with deposits within a vent field and have attributed it to phase separation of the fluids (Nakagawa *et al.*, 2005d; Nunoura and Takai, 2009). As co-collected fluid samples were not obtained for most of our samples, we do not know if our observations are also related to phase separation. However, fluid temperatures from vent fields in the Lau Basin other than Mariner are well below the two-phase boundary indicating that if phase separation occurred, fluids must have cooled prior to reaching the seafloor (Mottl *et al.*, 2011). Therefore, other factors, like fluid mixing styles, deposit mineralogy and age of the deposit, are likely helping to shape within vent field variability in the archaeal communities.

Conclusion

Results of this study show that at higher taxonomic levels, the bacterial and archaeal communities of active hydrothermal deposits from the ELSC are similar to those from other vent fields. However, at finer taxonomic scales differences in the dominant lineages are apparent both between globally distributed vent fields and within vent fields of the ELSC. Whether the global differences are shaped primarily by environmental factors or are due to the island-like nature of vent fields which would promote allopatry remains to be determined. Using this same approach to characterize the communities of several more vent fields from geographically and geologically distinct locations, along with more fine-scale geochemical, mineralogical and

physiological characterizations will help to disentangle the role of these non-exclusive factors in shaping deep-sea vent microbial biogeography.

Contributions

My role in this project was to collect and process samples, extract genomic DNA for pyrosequencing, analyze and interpret pyrosequencing data, and to write the manuscript for publication. Pyrosequencing was conducted by Mircea Podar and his laboratory.

**Chapter 4: *Hipaea jasoniae* sp. nov. and *Hipaea alviniae* sp. nov.,
Thermoacidophilic *Deltaproteobacteria* Isolated From Deep-Sea Hydrothermal
Vent Deposits.**

Flores, GE, Hunter, RC, Liu, Y and Reysenbach, A-L (in review) *International Journal of Systematic and Evolutionary Microbiology*.

Summary

Thirteen novel, obligately anaerobic, thermoacidophilic bacteria were isolated from deep-sea hydrothermal vent sites. Four of the strains, designated EP5-r^T, KM1, Mar08-272r^T and Mar08-368r, were selected for metabolic and physiological characterization. With the exception of EP5-r^T, all strains were short rods that grew between 40 and 72°C, with optimal growth at 60 to 65°C. Strain EP5-r^T was more ovoid in shape and grew between 45 and 75°C, with optimum at 60°C. The pH range for growth of all isolates was between 3.5 and 5.5 (optimum 4.5 to 5.0). Strain Mar08-272r^T could only grow up to pH 5.0. Elemental sulfur was required for heterotrophic growth on acetate, succinate, Casamino acids and yeast extract. Strains EP5-r^T, Mar08-272r^T and Mar08-368r could also use fumarate, while EP5-r^T, KM1 and Mar08-272r^T could also use propionate. All isolates were able to grow chemolithotrophically on H₂, CO₂, sulfur and vitamins. Phylogenetic analysis of 16S rRNA gene sequences placed the isolates within the *Desulfurellaceae* of the *Deltaproteobacteria*, with the closest cultured relative being *Hipaea maritima* MH₂^T (~95-98% sequence similarity).

Phylogenetic analysis also identified several isolates with at least one intervening sequence within the 16S rRNA gene. The genomic G+C content of strains EP5-r^T, KM1, Mar08-272r^T and Mar08-368r were 37.1, 42.0, 35.6 and 37.9 mol%, respectively. The new isolates differed most significantly from *H. maritima* MH₂^T in their phylogenetic placement and in that they are obligate thermoacidophiles. Based on these phylogenetic and phenotypic properties, the following two new species are proposed: *Hippea jasoniae* sp. nov. Mar08-272r^T and *Hippea alviniae* sp. nov. EP5-r^T.

Members of the class *Deltaproteobacteria* are physiologically diverse with eight described orders and thermophiles isolated from at least three of the orders (Boone *et al.*, 2001). The order *Desulfurellales*, however, is the only order whose members are exclusively thermophiles. There is one family within this order, the *Desulfurellaceae*, represented by two genera, *Desulfurella* and *Hippea*. Four species of *Desulfurella* have been formally described from terrestrial thermal environments. All are neutrophiles that grow optimally between 52 to 60°C, and conserve energy by sulfur or thiosulfate respiration or by pyruvate fermentation (Miroshnichenko *et al.*, 1998). *Hippea*, on the other hand, is currently represented by one described species, *Hippea maritima* MH₂^T, which was isolated from a shallow marine vent off the coast of Papua New Guinea (Miroshnichenko *et al.*, 1999). *H. maritima* MH₂^T is neutrophilic to moderately acidophilic (pH 5.7-6.5) and requires salt, yeast extract and sulfur for growth. Electron donors used for growth include molecular hydrogen and acetate. On average, *H. maritima* MH₂^T shares 87% 16S rRNA gene sequence similarity with members of the

genus *Desulfurella*. Here, we describe the first deep-sea vent relatives of *Hippea*, that are phylogenetically distinct and obligately thermoacidophilic.

Enrichment cultures targeting thermoacidophilic microorganisms were initiated from several deep-sea hydrothermal sulfide deposits that were collected with the *HOV Alvin* or *ROV Jason II* during research cruises to the East Pacific Rise (EPR) in 2004 and 2007, the Eastern Lau Spreading Center (ELSC) in 2005 and 2009, the Mid-Atlantic Ridge (MAR) in 2008 and the Guaymas Basin (GB) in 2009 (Table 4.1). Once shipboard, individual samples were processed and stored anaerobically as previously described (Götz *et al.*, 2002; Moussard *et al.*, 2004; Reysenbach *et al.*, 2006).

The medium used for enrichments was identical to that used by Reysenbach *et al.* (2006) and was prepared anaerobically under an atmosphere of N₂:CO₂ (80:20, v/v, 100kPa). The pH was adjusted to 4.5 with sulfuric acid prior to autoclaving at 105°C for 1 hour to avoid melting the sulfur. Cysteine or sulfide (0.5 g l⁻¹) was added as a reducing agent from sterile stock solutions after autoclaving. For initial enrichments, 5 ml of medium was inoculated with 0.5 ml of sulfide-deposit slurry and incubated at 70°C. Growth was detected after 2-3 days of incubation. Two different cell morphologies, small cocci (~1 µm in diameter) and short, motile rods (~1-3 µm in length) were observed in most enrichments when viewed using phase-contrast microscopy (Olympus BX60). The cocci were subsequently isolated and identified as *Aciduliprofundum* spp. (Reysenbach *et al.*, 2006) through 16S rRNA gene sequencing (Chapter 5). Because “*Aciduliprofundum*” spp. utilize peptides (Reysenbach and Flores, 2008), they were selected against by transferring the enrichments into medium

lacking yeast extract and peptone but supplemented with acetate (as $\text{NaC}_2\text{H}_3\text{O}_2$; 15 mM) and 10 ml l^{-1} vitamins (DSMZ medium 141). Pure cultures of the rods were obtained by at least two rounds of dilution to extinction or with the roll-tube method using gelrite. Isolated colonies were small (~1-2 mm in diameter), translucent and spreading. Purity of all isolates was verified by routine observations using phase-contrast microscopy and sequencing of the 16S rRNA gene. A total of 13 pure cultures were obtained with six from the MAR, four from ELSC, two from EPR and one from GB (Table 4.1). Upon isolation, cultures were maintained on the acetate/vitamin medium supplemented with 0.01% (w/v) yeast extract and grown at pH 4.5-5.0 and 65°C.

The 16S rRNA gene of each isolate was amplified, purified and sequenced as described previously (Reysenbach *et al.*, 2000). As 906F failed to amplify the 16S rRNA gene of the isolates, we used 1100R and 1114F for sequencing instead (Lane, 1991). Nearly complete 16S rRNA gene sequences were assembled using the software SeqMan and were compared to the NCBI non-redundant database using BLAST (Altschul *et al.*, 1990). Results of the BLAST search indicated that all 13 isolates were related to the marine thermophile, *Hipaea maritima* MH₂^T (Miroshnichenko *et al.*, 1999). Assembled sequences have been deposited in GenBank under accession numbers FR754496 – FR754508.

Table 4.1. Location of hydrothermal vent fields where novel thermoacidophilic bacteria were isolated.

Strain name	Vent field	Year sampled	Location	Depth (m)	Fluid temp. (°C)	Deposit type
<i>Mar08-272r^T</i>	Lucky Strike – MAR ^a	2008	37° 17.5240'N 32° 16.5085'W	1624	200	Chimney
Mar08-307r	Lucky Strike – MAR	2008	37° 17.5250'N 32° 16.5058'W	1624	70	Flange
Mar08-361r	Lucky Strike – MAR	2008	37° 17.4528'N 32° 16.9161'W	1730	ND	Flange
<i>Mar08-368r</i>	Lucky Strike – MAR	2008	37° 17.4998'N 32° 16.6715'W	1721	177	Chimney
Mar08-598r	TAG ^b – MAR	2008	26° 8.2078'N 44° 49.5297'W	3621	≈ 46 (?)	Chimney
Mar08-641r	TAG – MAR	2008	26° 8.2043'N 44° 49.5283'W	3621	ND	Chimney
<i>EP5-r^T</i>	“A” vent 9° N – EPR ^c	2004	9° 46.5003'N 104° 16.8100'W	2520	240	Chimney
EPR07-159r	“P” vent 9° N – EPR	2007	9° 50.2876'N 104° 17.4721'W	2507	365	Chimney
Guay09-253r	Guaymas Basin	2009	27° 00.405'N 111° 24.567'W	2007	229	Chimney
Lau09-781r	Mariner – VFR ^d	2009	22° 11.2751'S 176° 36.0755'W	1919	ND	Chimney
Lau09-1128r	Tui Malila – ELSC ^e	2009	22° 0.1708'S 176° 34.1066'W	1883	ND	Flange
<i>KM1</i>	Kilo Moana – ELSC	2005	20° 3.1827'S 176° 8.0241'W	2619	302	Chimney
LR3-DR	NELSC ^f	2009	15° 2.334'S 174° 17.022'W	1530	160	Chimney

Organisms in italics were selected for metabolic and physiologic characterization.

ND = not determined

^a Mid-Atlantic Ridge

^b Trans-Atlantic Geotraverse

^c East Pacific Rise

^d Valu Fa Ridge

^e Eastern Lau Spreading Center

^f North-Eastern Lau Spreading Center

While the 16S rRNA gene sequence similarity between *H. maritima* MH₂^T and the isolates appeared relatively high, several of the isolates had large insertions that were not considered in BLAST and similarity analyses. Importing the sequences into

ARB (Ludwig *et al.*, 2004) and aligning them according to secondary structure constraints, revealed that many of the isolates had at least one intervening sequence (IVSs) in two distinct regions of their 16S rRNA genes. Isolates Mar08-272r^T, Mar08-307r, Mar08-598r and Mar08-641r had two different IVSs, one beginning at *Escherichia coli* nucleotide positions 1025 (H1025) and another at 1448 (H1448) (Table 4.2). KM1 had one IVS at H1025, while Mar08-361r and Mar08-368r had one at H1448. No IVSs were detected in LR3-DR, Lau09-781r, Lau09-1128r, EP5-r^T, Epr07-159r or Guay09-253r. *H. maritima* MH₂^T had an IVS in a different region of its 16S rRNA gene (H184) that was not reported in the initial characterization of this organism (Miroshnichenko *et al.*, 1999). An environmental clone sequence (AM712337), previously detected at Brothers Seamount off the coast of New Zealand, also had two IVSs, one at H184 and another at H1448. Secondary structure predictions of the IVSs were made using mfold (<http://mfold.bioinfo.rpi.edu/cgi-bin/rna-form1.cgi>) and drawn using XRNA (<http://rna.ucsc.edu/rnacenter/xrna/>). Structure models of the IVSs revealed likely stem-loop conformations with predicted free energy values between -49.80 and -58.90 kcal/mol for the various IVSs of the different organisms (Figure 4.1). The G+C content of the IVSs were found to be significantly lower than for the remainder of the 16S rRNA genes (Table 4.2). Intervening sequences have most commonly been observed in 23S rRNA genes, although they have been observed in 16S rRNA genes of several Archaea and Bacteria (Baker *et al.*, 2003; Teyssier *et al.*, 2003; Dewhirst *et al.*, 2005; Villemur *et al.*, 2007; Bautista-Zapanta *et al.*, 2009; Tazumi *et al.*, 2009; Tazumi *et al.*, 2010). In some Archaea, IVSs function as small nucleolar

RNAs (snoRNAs) and guide rRNA processing (Omer *et al.*, 2000; Dieci *et al.*, 2009). Others have suggested that IVSs in the H184 region may be involved in interactions with ribosomal proteins (Teyssier *et al.*, 2003). However, the exact role of IVSs in *Hippea* species is unknown and beyond the scope of this study.

Neighbor-joining (Olsen correction, 500 bootstrap replicates) and maximum-likelihood (default parameters, 100 bootstrap replicates) analyses were conducted in ARB (Ludwig *et al.*, 2004) and MEGA5 (Tamura *et al.*, 2007), respectively. Results from these analyses placed the isolates within the genus *Hippea* (Figure 4.2). The 16S rRNA gene sequence similarity of all isolates to *H. maritima* MH₂^T was ~95-98% when the IVSs were masked from the analysis and when only homologous nucleotide positions were compared (1364 bp) (Table 4.3). When the IVSs were included, sequence similarity was significantly lower and ranged from ~81-93%. Isolates from the same oceanic region (Atlantic, Eastern Pacific and Western Pacific) clustered together to form distinct biogeographical clades (Figure 4.2). Nested within each clade were sub-clades that formed based on the specific vent field of isolation. *H. maritima* MH₂^T falls within the Western Pacific Ocean clade and shares 97.9% (93.3% with H184 insert of *H. maritima* MH₂^T) sequence similarity to its closest relative, strain Lau09-1128r. Similar biogeographic patterns have been seen for other thermophilic microorganisms from terrestrial environments using a variety of phylogenetic markers (Papke *et al.*, 2003; Whitaker *et al.*, 2003).

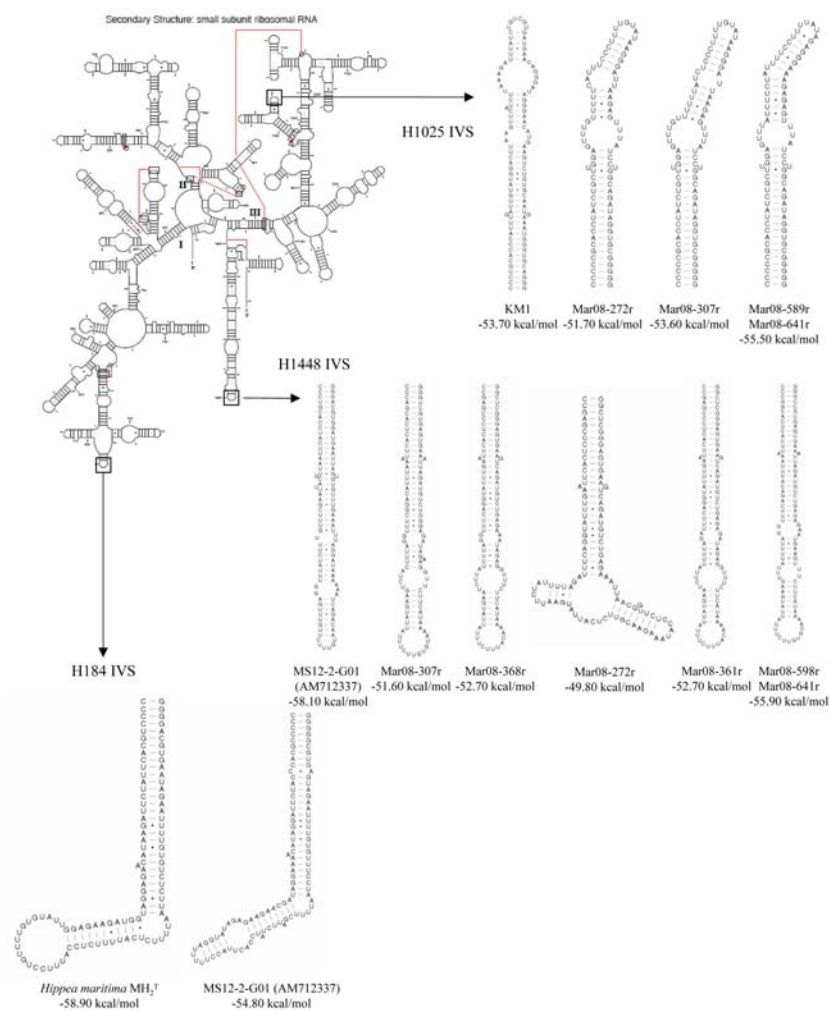


Figure 4.1. Predicted secondary structure of intervening sequences in the 16S rRNA of several of the new isolates and close relatives. The secondary structure of the 16S rRNA of *E. coli* is presented for reference to location and numbering of inserts. Structures were predicted in mfold and drawn with XRNA. Only the most energetically favorable conformations are presented.

Table 4.2. Several of the new isolates and other *Deltaproteobacteria* have intervening sequences (IVSs) in their 16S rRNA genes. The G+C content of the IVSs were very different than that of the full gene.

Strain name	Total sequence length - bp (%G+C)	Sequence length w/out IVSs – bp (%G+C)	H184 ^a – bp (%G+C)	H1025 ^b – bp (%G+C)	H1448 ^c – bp (%G+C)
<i>Mar08-272r^T</i>	1670 (56.53)	1475 (58.31)	-	87 (47.13)	108 (39.81)
Mar08-307r	1680 (56.31)	1484 (58.22)	-	87 (47.13)	109 (37.61)
Mar08-361r	1603 (56.89)	1495 (58.33)	-	-	108 (37.04)
<i>Mar08-368r</i>	1609 (56.93)	1501 (58.36)	-	-	108 (37.04)
Mar08-598r	1635 (56.39)	1440 (58.54)	-	86 (46.51)	109 (35.78)
Mar08-641r	1640 (56.46)	1445 (58.62)	-	86 (46.51)	109 (35.78)
<i>EP5-r^T</i>	1509 (58.71)	-	-	-	-
EPR07-159r	1511 (58.70)	-	-	-	-
Guay09-253r	1501 (58.76)	-	-	-	-
Lau09-781r	1508 (60.01)	-	-	-	-
Lau09-1128r	1482 (58.19)	-	-	-	-
<i>KM1^T</i>	1597 (57.67)	1490 (58.72)	-	107 (42.99)	-
LR3-Dr	1482 (59.92)	-	-	-	-
<i>H. maritima</i> MH ₂ ^T	1607 (56.81)	1499 (58.17)	108 (37.96)	-	-
MS12-2-G01	1712 (53.04)	1498 (55.14)	107 (42.06)	-	107 (34.58)

Organisms in italics were selected for metabolic and physiologic characterization.

^a H184 corresponds *E. coli* nucleotide 184 of the 16S rRNA gene

^b H1025 corresponds *E. coli* nucleotide 1025 of the 16S rRNA gene

^c H1448 corresponds *E. coli* nucleotide 1448 of the 16S rRNA gene

Four of the isolates representing three different geographic and geological settings (MAR (Mar08-272r^T and Mar08-368r), EPR (EP5-r^T) and ELSC (KM1)) were selected for physiological and metabolic characterization (Table 4.1). All four isolates

except Mar08-272r^T and Mar08-368r shared less than 97% 16S rRNA gene sequence similarity with one another when IVSs are masked from the analysis (Figure 4.2). The DNA G+C content of strains EP5-r^T, KM1, Mar08-272r^T and Mar08-368r were 37.1, 42.0, 35.6 and 37.9 mol%, respectively, as determined by thermal denaturation (Table 4.3) (Marmur and Doty, 1962). Unless stated otherwise, all characterization experiments were conducted in triplicate at pH 4.5-5.0 and 65°C in sealed 25 ml Balch tubes containing 5 ml of media inoculated from fresh overnight cultures at 2.5-5% (v/v). The influence of temperature on growth was determined by direct cell counts using a Petroff-Hauser counting chamber.

Strains Mar08-272r^T, Mar08-368r and KM1 all grew at temperatures between 40 and 72°C with growth optima between 60 and 65°C (Table 4.3). Strain EP5-r^T had a slightly higher temperature range for growth of 45 to 75°C with optimal growth at 60°C. Doubling times observed at optimal growth conditions ranged from 66-167 min. The pH range for growth was the same for all isolates at 3.5 to 5.5 except for strain Mar08-272r^T which could only grow up to pH 5.0. No growth was observed at pH 3.0 or 6.0. The optimal pH for growth for all strains was 4.5 to 5.0. NaCl was required for growth at 1-6% (w/v) for Mar08-272r^T and Mar08-368r, while KM1 and EP5-r^T grew on 1- 5% (w/v) NaCl.

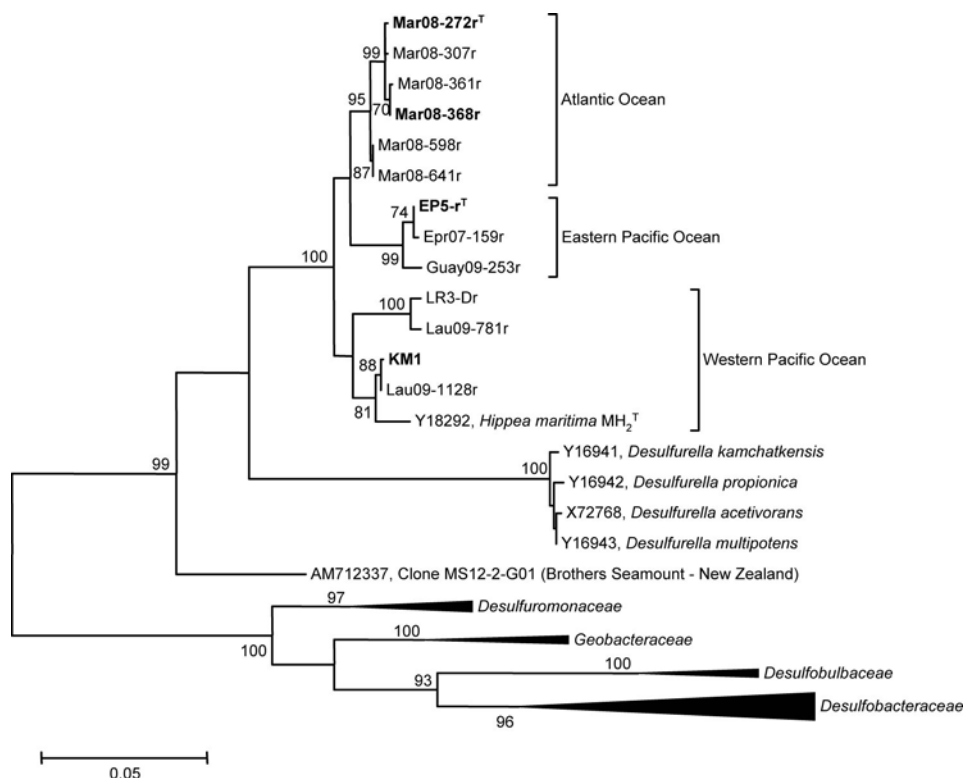


Figure 4.2. Maximum-likelihood tree based on 16S rRNA gene sequence comparisons of thirteen novel thermoacidophilic *Desulfurellaceae* and other families of the *Deltaproteobacteria*. The tree was generated considering only unambiguously aligned nucleotide position (n=1364). Isolates shown in bold were selected for characterization. Bootstrap values greater than or equal to 70 are shown at the base of nodes and were based on 100 replicates. The scale bar represents 0.05 changes per nucleotide position. Accession numbers of organisms used to generate phylogenetic tree that are not indicated in the tree are below: *Desulfuromonas acetoxidans* (AAEW02000008), *Desulfuromonas thiophila* (Y11560), *Pelobacter carbinolicus* (CP000142), *Geobacter thiogenes* (AF223382), *Geobacter bremensis* (U96917), *Geobacter metallireducens* (L07834), *Desulfobulbus propionicus* (AY548789), *Desulfobulbus elongatus* (X95180), *Desulfobulbus japonicus* (AB110549), *Desulfosarcina variabilis* (M34407), *Desulfobacterium indolicum* (AJ237607), *Desulfobacterium vacuolatum* (AF418178), *Desulfobacterium autotrophicum* (AF418177), *Desulfobacula toluolica* (AJ441316), *Desulfobacula phenolica* (AJ237606), *Desulfobacter postgatei* (AF418180), *Desulfobacter curvatus* (AF418175) and *Desulfobacter vibrioformis* (U12254). The tree was rooted with *Aquifex pyrophilus* (M83548) (not shown). Topology of the neighbor-joining tree was identical to that presented here (not shown).

Table 4.3. Comparison of physiological traits of four new isolates with *Hippea maritima* MH₂^T. Strains: 1, EP5-r^T; 2, KM1; 3, Mar08-272r^T; 4, Mar08-368r; 5, *Hippea maritima* MH₂^T (Miroshnichenko *et al.*, 1999). +, positive; (+), weakly positive; -, negative; ND = not determined.

Characteristic	1	2	3	4	5
Origin of isolation	9°N, East Pacific Rise	Kilo Moana vent field, Eastern Lau Spreading Center	Lucky Strike vent field, Mid-Atlantic Ridge	Lucky Strike vent field, Mid-Atlantic Ridge	Matupi Harbor, Papua New Guinea
Cell size (µm) (length x width)	0.7-1.5 x 0.3-0.6	2.0-3.0 x 0.5-1.0	2.0-3.5 x 0.5-0.7	2.0-3.0 x 0.5-1.05	1.0-3.0 x 0.4-0.8
DNA G + C content (mol %)	37.1	41.1	35.6	37.3	40.4
16S rRNA gene sequence similarity to <i>H. maritima</i> MH ₂ ^T (%)	95.4	97.6	95.6	95.6	N/A
Temperature range (°C) (optimum)	45-75 (60)	40-72 (60-65)	40-72 (60-65)	40-72 (60)	40-65 (52-54)
Doubling time at optimal temperature and pH (min)	166	167	96	66	ND
Average cell density at temperature and pH optima (cells/ml)	8.88 x 10 ⁷	7.03 x 10 ⁷	7.90 x 10 ⁷	8.06 x 10 ⁷	ND
pH range (optimum)	3.5-5.5 (4.5-5.0)	3.5-5.5 (4.5-5.0)	3.5-5.0 (4.5-5.0)	3.5-5.5 (4.5-5.0)	5.7-6.5 (5.8-6.2)
NaCl range (% w/v)	1-5	1-5	1-6	1-6	2-3*
Substrates utilized:					
Fumarate	+	-	+	+	(+)
Succinate	+	+	+	+	-
Propionate	+	+	+	-	-
Casamino acids	+	+	+	+	ND
Ethanol	-	-	-	-	+
Yeast extract	+	+	+	+	ND

*Range tested not reported.

Other electron donors utilized by all strains include acetate and hydrogen. All strains also require elemental sulfur as an electron acceptor.

Isolates were tested for their ability to reduce a variety of inorganic electron acceptors with acetate (15 mM) acting as the electron donor. Electron acceptors tested included elemental sulfur (1 %, w/v), O₂ (1-5 %, v/v), sulfate (as Na₂SO₄; 0.1% w/v), thiosulfate (0.1%, w/v), nitrate (as NaNO₃; 0.1%, w/v), Fe³⁺ (as ferric citrate; 5 mM) and arsenate (as Na₂HAsO₄.7H₂O; 5mM). All characterized isolates were strictly anaerobic and only able to use elemental sulfur as an electron acceptor (Table 4.3).

Isolates were tested for their ability to utilize a variety of organic carbon sources with and without CO₂ (N₂, 100%) in the headspace and sulfur acting as the sole electron acceptor. Vitamins were provided in all carbon substrate tests. Substrates were added at 0.1 and 0.02% (w/v; v/v for liquids) and included yeast extract, Bacto peptone, Casamino acids, glucose, starch, acetate, butyrate, formate, fumarate, lactate, succinate, propionate, pyruvate, ethanol, methanol and benzoate. All strains could use acetate, succinate, yeast extract, and Casamino acids. Strains KM1, EP5-r^T and Mar08-272r^T could use propionate while EP5-r^T and the two MAR strains (Mar08-272r^T and Mar08-368r) could also use fumarate (Table 4.3). No difference in growth was observed at the different concentrations of carbon substrates (0.1 and 0.02%). Isolates were not able to grow on yeast extract and Casamino acids without elemental sulfur indicating that they are not fermentative. Yeast extract was not required for growth if medium was supplemented with vitamins. All isolates were also capable of autotrophic growth with H₂, CO₂, sulfur and vitamins.

For morphological analysis by thin-section transmission electron microscopy (TEM), cells were prepared as previously described (Hunter and Beveridge, 2005). For

negatively-stained whole mounts, 20 μ L drops of culture were allowed to adsorb onto the copper grids for 2 min and were subsequently post-stained in 2% uranyl acetate. Mar08-272r^T (Figure 4.3a), Mar08-368r (Figure 4.3b), and KM1 (Figure 4.3c) were rod shaped, while EP5-r^T was more ovoid in shape (Figure 4.3d). Cell dimensions of each isolate varied (Table 4.3). Strains were all Gram-negative and the peptidoglycan sacculi were often difficult to visualize (white arrow, Figure 4.3d). No intracellular membrane structures were observed, however strains Mar08-272r^T, Mar08-368r, and KM1 contained electron dense intracellular granules adjacent to the cytoplasmic membrane (black arrows, Figure 4.3). These inclusions closely resemble intracellular mixed-valence iron granules formed by *Shewanella putrefaciens* CN32 under anaerobic conditions (Glasauer *et al.*, 2007). Consistent with this observation, when these strains were centrifuged for DNA extraction, small black precipitates were observed in cell pellets. Negative stains of each isolate revealed polar flagella extending from the surfaces of most cells (Figures 4.3e, f).

The physiological and phylogenetic characteristics of the newly described isolates are distinct from *H. maritima* MH₂^T and each other. Unlike *H. maritima* which was isolated from shallow (<40m) marine thermal environments, our strains were all isolated from deep-sea vents (>1500m). All new strains have very different pH and temperature ranges for growth from *H. maritima* MH₂^T which grows at pH 5.7 to 6.5 and 40 to 65°C (Miroshnichenko *et al.*, 1999). In contrast, the newly described isolates are obligately acidophilic growing at pH 3.5 to 5.5 (Mar08-272^T only up to pH 5.0) and temperatures between 40 and 72°C (EP5-r^T grows between 45 and 75°C). The new

isolates also differ from *H. maritima* MH₂^T and each other, in their ability to utilize succinate and propionate (EP5-r^T, KM1, Mar08-272r^T), and in their inability to utilize ethanol (EP5-r^T, KM1, Mar08-272r^T and Mar08-368r) and fumarate (KM1). Genomic G+C content also varies amongst all isolates and *H. maritima* MH₂^T but are all within ± 5%. Additionally, based on their 16S rRNA phylogenies, two of the isolates are distinct species (~95% 16S rRNA gene sequence similarity) (Table 4.3).

Based on the phenotypic (primarily acidophily, carbon substrate utilization and temperature range for growth) and phylogenetic differences between the new isolates and *H. maritima* MH₂^T, we propose emending the description of the genus *Hippea* and designating two new species, namely, *Hippea jasoniae* sp. nov. strain Mar08-272r^T and *Hippea alviniae* sp. nov. strain EP5-r^T.

Emended description of the genus Hippea

Cells are Gram-negative rods or ovoid in shape. Moderate thermophiles. Neutrophiles to obligate acidophiles. Obligate anaerobes. Metabolize by reduction of elemental sulfur. Substrates utilized include: H₂, volatile fatty acids, fatty acids and alcohols. Growth products are CO₂ and H₂S. The G+C content of the type strain of the type species is 40 mol%. Inhabits shallow to deep submarine hydrothermal vents. The type species is *Hippea maritima*.

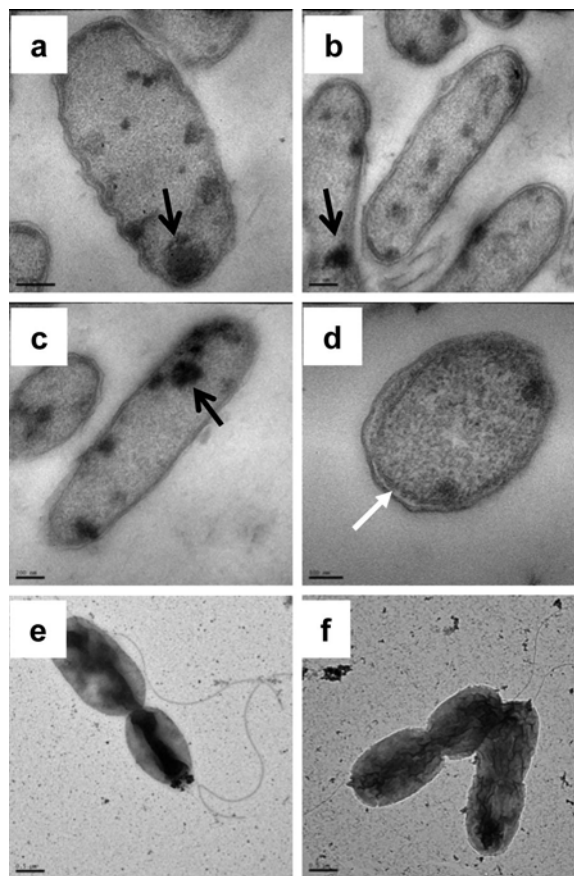


Figure 4.3. Thin section electron micrographs of strains Mar08-272rT (**a**), Mar08-368r (**b**), KM1T (**c**) and EP5rT (**d**). Negatively stained cells of strain Mar08-368r (**e**) and EP5rT (**f**) show flagella. Black arrows in **a**, **b** and **c** point to areas where electron dense granules are evident. The white arrow in **d** shows where the peptidoglycan sacculus is visible. Scale bar in **a**, **b** and **c** corresponds to 200 nm, while **d** is 100 nm. The scale bar in **e** and **f** is 500 nm.

Description of *Hippea jasoniae* sp. nov.

Hippea jasoniae (ja.so.ni'a.e. N.L. fem. gen. n. *jasoniae* of Jason, named in honor of the *ROV Jason II* which collected the samples harboring this strain and has been essential in the exploration of deep-sea hydrothermal environments).

Cells are motile, Gram-negative rods, 2.0-3.5 μm long and 0.5-0.7 μm wide. Moderate thermophiles (40-72°C, optimal 60-65°C). Obligate acidophiles (pH 3.5-5.0, optimal pH 4.5-5.0). Obligate anaerobes. Requires NaCl (1-6% w/v) for growth. Metabolize by reduction of elemental sulfur. Growth substrates are H_2/CO_2 , acetate, fumarate, succinate, propionate (not all strains), Casamino acids and yeast extract. Yeast extract is not required for growth if vitamins are provided. The G+C content of the genomic DNA of the type strain is 35.6 mol%.

The type strain, Mar08-272r^T (=DSM24585^T) was isolated from the Lucky Strike (37° 17.5240'N, 32° 16.5085'W, 1624 m depth) hydrothermal vent field along the Mid-Atlantic Ridge in the Atlantic Ocean.

Description of *Hippea alviniae* sp. nov.

Hippea alviniae (al.vi.ni'a.e. N.L. fem. gen. n. *alviniae* of Alvin, named in honor of the *HOV Alvin* which collected the samples harboring this strain).

Cells are motile, Gram-negative ovoid rods, 0.7-1.5 μm long and of 0.3-0.6 μm wide. Moderate thermophiles (45-75°C, optimal 60°C). Obligate acidophiles (pH 3.5-5.5, optimal pH 4.5-5.0). Obligate anaerobes. Requires NaCl (1-5 % w/v) for growth. Metabolize by reduction of elemental sulfur. Growth substrates are H_2/CO_2 , acetate, fumarate, succinate, propionate, Casamino acids and yeast extract. Yeast extract is not required for growth if vitamins are provided. The G+C content of the genomic DNA of the type strain is 37.1 mol%.

The type strain, EP5-r^T (=DSM 24586^T), was isolated from “A” vent (9° 46.5003'N, 104° 16.8100'W, 2520 m depth) along the East Pacific Rise in the eastern Pacific Ocean.

Contributions

For this project, I enriched and isolated organisms with Yitai Liu, performed characterization experiments, performed all molecular and phylogenetic analyses of isolates, generated secondary structure models, interpreted all data and wrote the manuscript for publication. Electron microscopy was performed by Ryan Hunter.

Chapter 5: Biogeography of the Thermoacidophilic Deep-Sea Hydrothermal Vent Euryarchaeota 2 (DHVE2).

Abstract

The first cultivated thermoacidophile from deep-sea hydrothermal environments, *Aciduliprofundum boonei* T469^T, belongs to the deep-sea hydrothermal vent euryarchaeota 2 (DHVE2) lineage that, based on 16S rRNA gene surveys, is widespread at deep-sea hydrothermal vents. However, relatively little is known about the overall distribution and phylogenetic diversity of this important lineage. In this study, we examined the distribution, relative abundance, co-occurrence patterns and cultivable diversity of thermoacidophilic DHVE2 in deposits from several geochemically distinct vent fields. Quantitative polymerase chain reaction (qPCR) assays with primers specific for the DHVE2 and most Archaea were employed to determine the occurrence and relative abundance of the DHVE2 in native vent deposits. Mining of pyrosequencing data was conducted to look for correlations in the distribution of the DHVE2 with other Archaea. Deposits from numerous vent sites were also used as inocula for enrichment cultures targeting the DHVE2. Results from this study demonstrate the ubiquity of the DHVE2 at the vent field scale and suggest that they are significant members of the archaeal communities of most mature vent deposits, especially horizontal flange structures. Furthermore, using local similarity analysis (LSA), the occurrence of the DHVE2 was positively correlated with other

Euryarchaeota and negatively correlated with mostly *Crenarchaeota* in pyrosequencing data from several vent fields. Targeted cultivation efforts resulted in the isolation of 15 new isolates from six different vent fields expanding the cultivable diversity of this lineage to vents along the East Pacific Rise and Mid-Atlantic Ridge. Overall, this study increases our understanding of the biogeography of the DHVE2 and identifies factors that may influence thermoacidophily in deep-sea hydrothermal environments.

Introduction

The diversity of Archaea associated with marine hydrothermal vent habitats is unrivaled in any other ecosystem on Earth (Auguet *et al.*, 2009). Much of this diversity resides within the *Euryarchaeota* where numerous cultivated and uncultivated lineages appear to be endemic to the deep-sea. One such lineage is the deep-sea hydrothermal vent euryarchaeota 2 (DHVE2) (Takai and Horikoshi, 1999). Our knowledge of the distribution and diversity of the DHVE2 is based primarily on cultivation-independent studies (Table 5.1). These studies established that the DHVE2 are widespread and can account for up to 15% of the archaeal diversity, suggesting that they are important components of deep-sea hydrothermal ecosystems (Reysenbach *et al.*, 2006).

Table 5.1. Summary of 16S rRNA gene sequences previously detected in marine hydrothermal environments. All listed sequences are greater than 600 bp in length and share greater than 94% sequence similarity with *Aciduliprofundum boonei* T469^T.

Accession Number	Clone Name	Vent Field	Reference
AB247823	pLM14A-5	Mariner – Eastern Lau Spreading Center	unpublished
AB052986	pPACMA-Q	Manus Basin	(Takai <i>et al.</i> , 2001)
AB052983	pPACMA-M	Manus Basin	(Takai <i>et al.</i> , 2001)
AB052990	pPACMA-W	Manus Basin	(Takai <i>et al.</i> , 2001)
AB052985	pPACMA-P	Manus Basin	(Takai <i>et al.</i> , 2001)
AB366574	SSM040-14	Suiyo Seamount, Izu-Ogasawara Arc	(Kimura <i>et al.</i> , 2010)
AB019740	pSSMCA108	Suiyo Seamount, Izu-Ogasawara Arc	(Takai and Horikoshi, 1999)
AB019739	pMC2A10	Myojin Knoll, Izu-Ogasawara Arc	(Takai and Horikoshi, 1999)
AB019741	pISA12	Iheya Basin, Middle Okinawa Trough	(Takai and Horikoshi, 1999)
AB019742	pISA42	Iheya Basin, Middle Okinawa Trough	(Takai and Horikoshi, 1999)
AB175593	IACC-11	Iheya Basin, Middle Okinawa Trough	(Nakagawa <i>et al.</i> , 2005d)
AB197209	IAP6.5m-12	Iheya Basin, Middle Okinawa Trough	unpublished
AB302005	P816_a_1.07	Yonaguni Knoll, Southern Okinawa Trough	(Nunoura <i>et al.</i> , 2010)
AB235350	pYK04-8A-26	Yonaguni Knoll, Southern Okinawa Trough	(Nunoura <i>et al.</i> , 2010)
AB611429	HTM1039Pn-A31	Hatoma Knoll – Okinawa Trough	unpublished
AB611418	HTM1039Pn-A12	Hatoma Knoll – Okinawa Trough	unpublished
AB611448	HTM1036Pn-A103	Hatoma Knoll – Okinawa Trough	unpublished
AB611404	HTM871W-A1	Hatoma Knoll – Okinawa Trough	unpublished
AB611358	HTM873S-A1	Hatoma Knoll – Okinawa Trough	unpublished
AB611414	HTM1039Pn-A8	Hatoma Knoll – Okinawa Trough	unpublished
AB611339	HTM866S-A3	Hatoma Knoll – Okinawa Trough	unpublished
AB611424	HTM1039Pn-A24	Hatoma Knoll – Okinawa Trough	unpublished
AB611425	HTM1039Pn-A26	Hatoma Knoll – Okinawa Trough	unpublished
AB611367	HTM873I-A23	Hatoma Knoll – Okinawa Trough	unpublished
AB611430	HTM1039Pn-A32	Hatoma Knoll – Okinawa Trough	unpublished
AB611375	HTM1039S-A21	Hatoma Knoll – Okinawa Trough	unpublished

AB611386	HTM1036S-A21	Trough Hatoma Knoll – Okinawa Trough	unpublished
EU107487	A10	Snail surface – Okinawa Trough	unpublished
AB167485	TOTO-A6-1	Toto Cladera – Mariana Arc	(Nakagawa <i>et al.</i> , 2006)
AB167482	TOTO-A1-28	Toto Cladera – Mariana Arc	(Nakagawa <i>et al.</i> , 2006)
AB167498	TOTO-ISCS-A45	Toto Cladera – Mariana Arc	(Nakagawa <i>et al.</i> , 2006)
AB167486	TOTO-A6-12	Toto Cladera – Mariana Arc	(Nakagawa <i>et al.</i> , 2006)
AB293232	Pcsc1A26	Southern Mariana Trough	(Kato <i>et al.</i> , 2010)
AB293231	Pcsc1A25	Southern Mariana Trough	(Kato <i>et al.</i> , 2010)
AB293234	Pcsc1A38	Southern Mariana Trough	(Kato <i>et al.</i> , 2010)
EU574651	CPA_17	Northern Mariana Backarc	unpublished
AM749972	854e_arc05A	Kermadec Arc – New Zealand	(Stott <i>et al.</i> , 2008)
AB177273	ODP1251A15.24	Cascadia Margin Sediments	(Inagaki <i>et al.</i> , 2006)
AF355838	33-P120A99	Juan de Fuca Ridge	(Huber <i>et al.</i> , 2002b)
DQ118404	Fosmid Alv-FOS4	13°N East Pacific Rise	(Moussard <i>et al.</i> , 2006b)
DQ082975	FOS2	13°N East Pacific Rise	(Moussard <i>et al.</i> , 2006a)
DQ082976	FOS3	13°N East Pacific Rise	(Moussard <i>et al.</i> , 2006a)
DQ082980	metF2	13°N East Pacific Rise	(Moussard <i>et al.</i> , 2006a)
DQ082964	met50	13°N East Pacific Rise	(Moussard <i>et al.</i> , 2006a)
DQ082953	met21	13°N East Pacific Rise	(Moussard <i>et al.</i> , 2006a)
DQ082954	met24	13°N East Pacific Rise	(Moussard <i>et al.</i> , 2006a)
DQ082969	metF8	13°N East Pacific Rise	(Moussard <i>et al.</i> , 2006a)
DQ082955	met43	13°N East Pacific Rise	(Moussard <i>et al.</i> , 2006a)
DQ118403	Fosmid Alv-FOS1	13°N East Pacific Rise	(Moussard <i>et al.</i> , 2006b)
AF526965	pEPR193	13°N East Pacific Rise	(Nercessian <i>et al.</i> , 2003)
AF526964	pEPR159	13°N East Pacific Rise	(Nercessian <i>et al.</i> , 2003)
AF526963	pEPR122	13°N East Pacific Rise	(Nercessian <i>et al.</i> , 2003)
AF526962	pEPR719	13°N East Pacific Rise	(Nercessian <i>et al.</i> , 2003)
AF526961	pEPR707	13°N East Pacific Rise	(Nercessian <i>et al.</i> , 2003)
AY672495	CH8_7a_Arc	9°N East Pacific Rise	(Kormas <i>et al.</i> , 2006)
AF356635	G26-C56	Guaymas Basin	unpublished
AF356637	G26_C73	Guaymas Basin	unpublished
AF068820	VC2.1 Arc13	Snake Pit – Mid-Atlantic Ridge	(Reysenbach <i>et al.</i> , 2000)
AB496479	pMARA06_14	Lucky Strike – Mid-Atlantic Ridge	unpublished
FM863771	T48R	TAG – Mid-Atlantic Ridge (<i>Rimacaris</i> gut)	unpublished
FM863772	T14R	TAG – Mid-Atlantic Ridge (<i>Rimacaris</i> gut)	unpublished
FM863773	T22R	TAG – Mid-Atlantic Ridge (<i>Rimacaris</i> gut)	unpublished
AY251065	FT17A09	Central Indian Ridge	(Hoek <i>et al.</i> , 2003)
AY251064	FT17A03	Central Indian Ridge	(Hoek <i>et al.</i> , 2003)

The first representative of the DHVE2 was obtained in pure culture and represents the first obligate thermoacidophile discovered from deep-sea vents despite the known acidity of most hydrothermal fluids (pH 2.8-4.5) and predictions of acidic microhabitats within the walls of vent deposits (Tivey, 2004; Reysenbach *et al.*, 2006). The organism, *Aciduliprofundum boonei* T469^T, was isolated from the Mariner vent field along the Eastern Lau Spreading Center (ELSC) in the western Pacific Ocean and grows between 55 and 75°C and pH 3.3 to 5.8. The genome of the isolate revealed a specialized metabolism based on peptide fermentation and auxotrophy for several amino acids (Reysenbach and Flores, 2008).

Acidic habitats are generated in vent deposits by conductive cooling of end-member fluids or by transport of hydrothermal fluids outward across deposit walls by diffusion only (Tivey, 2004). However, when hydrothermal fluids and seawater mix, either in the subsurface or by advection across deposit walls, neutrality of the fluids is quickly reached resulting in most marine hydrothermal vent habitats being circumneutral. Therefore, the pH of end-member fluids and the degree of fluid mixing within an individual deposit are likely important factors in controlling the distribution and abundance of thermoacidophilic DHVE2 both within and between vent fields. Factors that influence the pH of hydrothermal fluids are related to the geologic setting and include the presence of organic sediments, which increases the pH of fluids like what occurs in the Guaymas Basin, and inputs of magmatic volatiles like what is observed in the low pH fluid of Mariner (Tivey, 2007). Fluid mixing styles can be influenced by the type of vent structure as hydrothermal fluids associated with

horizontal flanges are conductively cooled with little or no mixing of seawater, while the mixing styles of vertical chimney structures are much more variable (Tivey, 2004).

Assuming other DHVE2 possess similar physiological and metabolic features as *A. boonei* T469^T, then understanding more about the biogeography of this archaeal lineage can begin to identify possible constraints on thermoacidophily in deep-sea hydrothermal ecosystems. Therefore, we investigated the occurrence, abundance and diversity of the DHVE2 in hydrothermal vent deposits from several geochemically distinct vent fields using a combination of cultivation-dependent and -independent approaches. Here we expand the geographic distribution and phylogeny of thermoacidophilic DHVE2, and provide clues to factors that may influence their distribution and abundance.

Materials and Methods

Sample collection

Deep-sea hydrothermal mineral deposits were collected with the *HOV Alvin* or *ROV Jason II* during research cruises to the East Pacific Rise (EPR) in 2007, the Mid-Atlantic Ridge (MAR) in 2008, the Eastern Lau Spreading Center (ELSC) in 2009 and the Guaymas Basin (GB) in 2009. Once shipboard, individual samples were processed and stored anaerobically as previously described (Götz *et al.*, 2002; Reysenbach *et al.*, 2006; Flores *et al.*, 2011).

Quantitative polymerase chain reaction (qPCR)

Nucleic acids from environmental samples were extracted from homogenized samples ($\approx 1.6 - 3.2$ grams) using the Ultra Clean Soil DNA Isolation Kit (MoBio Laboratories) according to the modified protocol of Reysenbach *et al.* (2006).

Quantitative PCR was performed according to manufacturer's instructions using the Quantitect SYBR green PCR kit (Qiagen, Inc., Valencia, CA) and $0.8 \mu\text{M}$ final primer concentration, with melting curves performed at the end of each reaction to ensure product specificity. Primers and thermocycling conditions were followed according to Reysenbach *et al.* (2006). Gene copy numbers presented were normalized by the amount of material in grams (wet weight) extracted.

Local similarity analysis

Pyrosequencing data of the variable region 4 (V4) of archaeal 16S rRNA genes from 57 deposits from the MAR, ELSC and Guyamas Basin were trimmed, aligned and clustered at 97% sequence similarity as previously described (Flores *et al.*, 2011).

DHVE2 operational taxonomic units (OTUs) were identified by first BLASTing (Altschul *et al.*, 1990) a representative sequences of each OTU against the 16S rRNA gene of *A. boonei* T469^T, selecting OTUs with greater than 95% sequence similarity to *A. boonei* T469^T, manually aligning sequences and generating phylogenetic trees in a custom ARB database (Ludwig *et al.*, 2004). For local similarity analysis (LSA), all OTUs with greater than 100 sequences, including three DHVE2 OTUs, were normalized to percent and imported into the LSA compute tool

(<http://meta.cmb.usc.edu/>) using default parameters. LSA explores co-varying relationships of microbial species (or OTUs) to one another and to environmental parameters (Ruan *et al.*, 2006). In this case, we used LSA to look at the relationships between co-varying OTUs as no complementary environmental data was available. Results of LSA were pruned to include only the two most prevalent DHVE2 OTUs (ID#'s 727 and 1148), and other OTUs that were positively and negatively correlated ($P < 0.05$). Visualization of the resulting interaction network was performed using Cytoscape (Shannon *et al.*, 2003). Correlated OTUs were classified to the lowest taxonomic level that had a bootstrap value of $\geq 50\%$ (Claesson *et al.*, 2009) using the RDP-classifier (Wang *et al.*, 2007).

Enrichment culturing and phylogenetic analysis

Medium used for enrichments was identical to that used by Reysenbach *et al.* (2006). The pH was adjusted to 4.5 with sulfuric acid prior to autoclaving at 105°C for 1 hour to avoid melting the sulfur. Cysteine or sulfide (0.5 g l^{-1}) was added as a reducing agent from sterile stock solutions after autoclaving. For initial enrichments, 5 ml of medium was inoculated with 0.5 ml of sulfide-deposit slurry and incubated at 70°C.

Genomic DNA was extracted from isolated cultures using the DNeasy Tissue Kit (Qiagen) following the manufacturer's protocol. The 16S rRNA gene of each isolate was amplified, purified and sequenced as described previously (Reysenbach *et al.*, 2006). Nearly complete 16S rRNA gene sequences (FR865176-FR865190) were

assembled using the software SeqMan, compared to the NCBI non-redundant database using BLAST (Altschul *et al.*, 1990) and aligned in ARB (Ludwig *et al.*, 2004) according to secondary structure constraints. Neighbor-joining (Olsen correction, 500 bootstrap replicates) and maximum-likelihood (default parameters, 100 bootstrap replicates) analyses were conducted in ARB (Ludwig *et al.*, 2004) and MEGA5 (Tamura *et al.*, 2007), respectively, on only unambiguous nucleotide positions (789 nt).

Results and Discussion

Occurrence and relative abundance of the DHVE2

To determine the occurrence and relative abundance of the DHVE2 in deposits from geologically distinct vent fields, 16S rRNA genes were quantified for most Archaea and the DHVE2 using qPCR. Archaeal 16S rRNA genes were successfully amplified from 130 samples with deposits from Tui Malila along the ELSC having, on average, the lowest copy number (8.35×10^4 copies) and TAG along the MAR having the highest copy number (9.78×10^7 copies) (Table 5.2). Although these values cover a wide range, they are similar to archaeal abundances that have been reported from other hydrothermal vent deposits (e.g., Takai *et al.*, 2001; Schrenk *et al.*, 2003; Nakagawa *et al.*, 2005d; Zhou *et al.*, 2009). Using group specific primers, the DHVE2 were observed at all vent fields but in only 60% (78/130) of samples analyzed. At individual vent fields, the DHVE2 were most frequently observed at Mariner (80% of samples), EPR (77.8%) and TAG (75%). In contrast, they were detected in less than 50% of

samples from Tui Malila (37.5%), Tow Cam (42.9%) and the Guaymas Basin (48.1%). While their occurrence varied within an individual vent field, these results clearly illustrate the ubiquity of the DHVE2 and suggest that differences in the geological properties that influence end-member fluid pH over the ranges we examined do not inhibit colonization by the DHVE2 at these vent sites. Assuming all members of the DHVE2 are thermoacidophilic, then thermoacidophily is a common ecological niche in deep-sea hydrothermal ecosystems.

In samples where the DHVE2 were not detected, the average archaeal abundance was significantly lower at 3.64×10^5 copies/gram than in deposits where the DHVE2 were observed, which averaged 3.34×10^7 copies/gram ($P = 0.002$, one-tailed T-test) (Tables 5.3-5.6). Also, deposits where the DHVE2 were absent were typically younger, thin-walled structures without an obvious biofilm on the exterior of the deposit. Previous work had demonstrated that, while Archaea are typically the initial colonizers of newly formed vent deposits, they are primarily autotrophic with later colonization by heterotrophs (Page *et al.*, 2008). Consequently, the occurrence of the DHVE2 in an individual deposit may be dependent upon the presence of a mature microbial community from which to scavenge fermentable peptides (Reysenbach and Flores, 2008). Older deposits also generally have more defined walls and fluid conduits that would help isolate the hydrothermal fluids from seawater allowing for more conductive cooling of the fluids.

Table 5.2. Results of qPCR assays to determine the occurrence and relative abundance of the DHVE2 in hydrothermal vent deposits from several different vent fields.

	Average archaeal 16S rRNA gene copies per gram of deposit (s.e.m.) [‡]	Average DHVE2 16S rRNA gene copies per gram of deposit (s.e.m.)	Average proportion of DHVE2 16S rRNA gene copies (%) [†]
Eastern Lau Spreading Center			
Kilo Moana (n=8, 62.5%)*	2.86×10^7 (1.25×10^7)	1.74×10^5 (1.50×10^5)	0.38
Tow Cam (n=7, 42.9%)	1.91×10^7 (1.08×10^7)	5.39×10^5 (3.32×10^5)	1.21
Tahi Moana (n=11, 63.6%)	1.51×10^7 (7.58×10^6)	5.65×10^5 (2.02×10^5)	2.39
ABE (n=11, 63.6%)	7.25×10^6 (2.78×10^6)	1.58×10^5 (6.17×10^4)	1.39
Tui Malila (n=16, 37.5%)	8.35×10^4 (2.59×10^4)	2.30×10^4 (9.22×10^3)	12.88
Mariner (n=15, 80.0%)	3.14×10^6 (2.11×10^6)	1.62×10^5 (7.53×10^4)	12.69
Mid-Atlantic Ridge			
Lucky Strike (n=10, 70%)	6.41×10^5 (4.22×10^5)	1.34×10^5 (5.96×10^4)	14.74
Rainbow (n=12, 66.7%)	2.15×10^7 (7.68×10^6)	4.49×10^4 (1.27×10^4)	0.14
TAG (n=4, 75.0%)	9.78×10^7 (5.98×10^7)	5.19×10^5 (5.04×10^5)	0.57
Guaymas Basin (n=27, 48.1%)	5.36×10^7 (2.37×10^7)	1.52×10^6 (5.03×10^5)	1.36
East Pacific Rise (n=9, 77.8%)	4.08×10^5 (1.62×10^5)	2.71×10^4 (1.96×10^4)	7.26

[‡]s.e.m. = standard error of the mean

[†]Average proportion of DHVE2 was calculated for only samples with positive amplification for both Archaea and the DHVE2.

*Numbers in parentheses indicate the total number of samples with positive archaeal amplification and the percentage of those with positive amplification of the DHVE2.

Quantitative PCR was also used to determine the proportion of the DHVE2 in the archaeal communities. Within individual vent fields, the proportion of DHVE2 16S rRNA gene copies ranged from 0.14% at Rainbow to 14.74% at Lucky Strike. Deposits

from Mariner (12.69%), Tui Malila (12.88%) and EPR (7.26%) also had, on average, a high proportion of DHVE2 sequences within their archaeal communities (Table 5.2). This level of relative abundance implies that, when the DHVE2 are present, they can be a significant component of the archaeal community. However, it is difficult to compare their relative abundance to other archaeal groups from previous studies because of differences in the methods employed to determine abundances (e.g., FISH, MPN culturing).

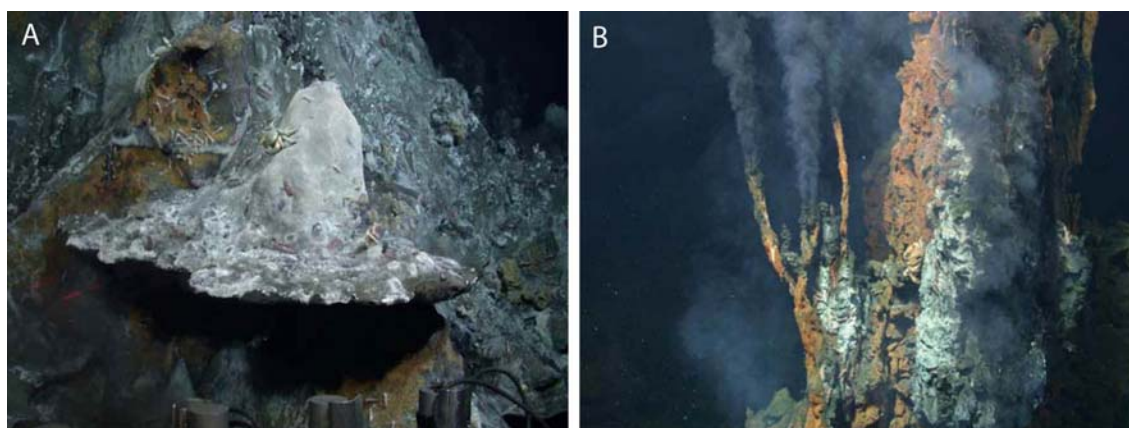


Figure 5.1. Photographs of a horizontal flange deposit (A) and vertical chimneys (B) from the Eastern Lau Spreading Center.

Individual samples having the highest proportion of DHVE2 gene copies were typically flanges (Tables 5.3-5.6). Flanges are horizontal, shelf-like structures that form in some hydrothermal systems (Figure 5.1) (Tivey, 2007). Hydrothermal fluids associated with flanges are conductively cooled by seawater with very little mixing of the fluids (Tivey, 2004). As a result, these fluids remain acidic as they cool to hospitable temperatures ($<120^{\circ}\text{C}$) and percolate vertically through the structure generating relatively larger thermoacidic zones than what is present in vertical chimney

structures. In a recent study, the microbial community of a flange deposit from the Yonaguni Knoll IV hydrothermal field in the western Pacific Ocean was characterized using 16S rRNA gene cloning (Nunoura and Takai, 2009). Results showed that the DHVE2 accounted for nearly 46% (16/35) of the archaeal clones in one subsample further supporting the observation that flanges can be “hot-spots” for the DHVE2 and likely, other thermoacidophiles.

Table 5.3. Results of qPCR assays to determine the occurrence and relative abundance of the DHVE2 in hydrothermal vent deposits from the East Pacific Rise (EPR). Values are the average of two replicates unless otherwise noted. Lower case letters next to sample names indicate paired samples.

	Archaeal 16S rRNA gene copies per gram of deposit (s.e.m.) [‡]	DHVE2 16S rRNA gene copies per gram of deposit (s.e.m.)	Proportion of DHVE2 16S rRNA gene copies (%)	Deposit type – sample location
EPR07-15	7.18 x 10 ⁵ (7.32 x 10 ⁴)	1.44 x 10 ⁵ (3.39 x 10 ²)	20.01	Chimney – outer
EPR07-20	1.47 x 10 ⁵ (1.12 x 10 ⁴)	3.64 x 10 ³ (4.86 x 10 ²)	2.49	Chimney – outer
EPR07-45	3.64 x 10 ⁴ (1.75 x 10 ³)	BDL [§]	-	Chimney – outer
EPR07-64	6.10 x 10 ⁴ (6.87 x 10 ³)	2.66 x 10 ³ (4.12 x 10 ²)	4.37	Chimney – inner
EPR07-70a	2.63 x 10 ⁵ (3.55 x 10 ⁴)	1.23 x 10 ⁴ (2.34 x 10 ³)	4.68	Chimney – outer
EPR07-75a	8.12 x 10 ³ (1.14 x 10 ²)	3.36 x 10 ³ (4.41 x 10 ²)	41.34	Chimney – inner
EPR07-138	1.03 x 10 ⁶ (2.52 x 10 ³)	BDL	-	Chimney – outer
EPR07-155	1.05 x 10 ⁵ (8.21 x 10 ³)	2.12 x 10 ⁴ (1.02 x 10 ³)	19.58	Chimney – outer
EPR07-174	1.31 x 10 ⁶ (9.91 x 10 ⁴)	2.74 x 10 ³ (3.26 x 10 ²)	0.21	Chimney – outer & inner

[‡]s.e.m. = standard error of the mean

[§]BDL = below detection limit

Table 5.4. Results of qPCR assays to determine the occurrence and relative abundance of the DHVE2 in hydrothermal vent deposits from the Guaymas Basin. Values are the average of two replicates unless otherwise noted. Lower case letters next to sample names indicate paired samples.

	Archaeal 16S rRNA gene copies per gram of deposit (s.e.m.) [‡]	DHVE2 16S rRNA gene copies per gram of deposit (s.e.m.)	Proportion of DHVE2 16S rRNA gene copies (%)	Deposit type – sample location
Guay09-1	2.59×10^5 (6.56×10^3)	BDL [§]	-	Flange – top/lip
Guay09-31	1.92×10^7 (1.64×10^5)	1.47×10^5 (1.01×10^4)	0.76	Flange – top/lip
Guay09-56	1.95×10^8 (1.43×10^7)	2.63×10^6 (1.89×10^5)	1.35	Chimney – outer
Guay09-45	8.13×10^7 (1.60×10^7)	3.10×10^5 (5.47×10^3)	0.38	Chimney – outer
Guay09-70	6.66×10^4 (4.80×10^3)	BDL	-	Chimney – outer
Guay09-99	4.88×10^4 (1.02×10^4)	BDL	-	Chimney – outer
Guay09-146	2.84×10^4 (2.77×10^3)	BDL	-	Flange – whole
Guay09-173	1.27×10^7 (4.00×10^6)	6.99×10^5 (1.43×10^5)	5.50	Chimney – outer
Guay09-205	4.13×10^7 (1.08×10^7)	3.42×10^6 (7.05×10^5)	8.27	Chimney – outer
Guay09-127	1.54×10^4 (1.25×10^3)	BDL	-	Flange – whole
Guay09-138	1.93×10^4 (4.87×10^2)	BDL	-	Flange – whole
Guay09-190	4.84×10^7 (1.49×10^7)	1.27×10^5 (9.27×10^4)	0.26	Chimney – outer
Guay09-159	3.74×10^6 (1.45×10^5)	2.50×10^4 (4.32×10^3)	0.67	Chimney – whole
Guay09-228	1.23×10^4 (2.96×10^3)	BDL	-	Chimney – whole
Guay09-244	2.50×10^7 (1.59×10^6)	1.42×10^6 (6.05×10^4)	5.68	Chimney – outer
Guay09-237	4.38×10^8 (1.13×10^8)	1.85×10^6 (1.44×10^5)	0.42	Chimney – outer
Guay09-258a	7.57×10^7 (1.03×10^7)	5.89×10^6 (5.08×10^6)	7.78	Pagoda – outer

Guay09-264a	2.99×10^7 (2.17×10^6)	3.17×10^6 (1.71×10^5)	10.58	Flange of Pagoda – top/lip
Guay09-327	5.72×10^3 (8.84×10^2)	BDL	-	Flange – whole
Guay09-314	1.52×10^5 (2.02×10^3)	BDL	-	Flange – top
Guay09-302	1.52×10^4 (2.85×10^2)	BDL	-	Flange – whole
Guay09-289	3.75×10^6 (2.08×10^4)	7.35×10^3 (1.02×10^3)	0.20	Flange – top
Guay09-363	3.86×10^5 (5.87×10^4)	BDL	-	Chimney – outer
Guay09-439	1.87×10^4 (NA)*	BDL	-	Chimney – outer
Guay09-441b	4.73×10^8 (1.73×10^7)	3.05×10^4 (4.87×10^3)	0.01	Chimney – outer brown
Guay09-442b	3.06×10^4 (2.21×10^3)	BDL	-	Chimney – outer white
Guay09-452	1.46×10^5 (4.86×10^3)	BDL	-	Flange – top

[¶]s.e.m. = standard error of the mean

[§]BDL = below detection limit

*Denotes samples for which only one replicate had successful amplification.

Table 5.5. Results of qPCR assays to determine the occurrence and relative abundance of the DHVE2 in hydrothermal vent deposits from the Mid-Atlantic Ridge. Values are the average of two replicates unless otherwise noted. Lower case letters next to sample names indicate paired samples.

	Archaeal 16S rRNA gene copies per gram of deposit (s.e.m.) [‡]	DHVE2 16S rRNA gene copies per gram of deposit (s.e.m.)	Proportion of DHVE2 16S rRNA gene copies (%)	Deposit type – sample location
Rainbow-2a	4.13 x 10 ⁷ (3.34 x 10 ⁶)	1.06 x 10 ⁵ (4.71 x 10 ³)	0.26	Chimney – outer
Rainbow-3a	5.16 x 10 ⁶ (6.23 x 10 ⁴)	3.84 x 10 ⁴ (1.63 x 10 ⁴)	0.74	Chimney – inner
Rainbow-103	2.60 x 10 ⁵ (4.39 x 10 ⁴)	BDL [§]	-	Chimney – whole
Rainbow-158	3.67 x 10 ⁵ (3.32 x 10 ⁵)	BDL	-	Chimney – inner
Rainbow-165	4.74 x 10 ⁶ (4.71 x 10 ⁵)	4.48 x 10 ³ (1.50 x 10 ²)	0.09	Chimney – outer
Rainbow-177b	5.14 x 10 ⁷ (1.31 x 10 ⁵)	3.00 x 10 ⁴ (1.23 x 10 ³)	0.06	Chimney – outer
Rainbow-183b	2.70 x 10 ⁵ (7.10 x 10 ⁴)	BDL	-	Chimney – inner
Rainbow-5c	7.99 x 10 ⁶ (1.59 x 10 ⁵)	2.09 x 10 ⁴ (1.27 x 10 ³)	0.26	Chimney – outer
Rainbow-6c	4.54 x 10 ⁷ (1.05 x 10 ⁶)	9.41 x 10 ⁴ (2.06 x 10 ⁴)	0.21	Chimney – inner
Rainbow-217	1.82 x 10 ⁷ (2.58 x 10 ⁶)	3.91 x 10 ⁴ (1.08 x 10 ⁴)	0.21	Chimney – whole
Rainbow-231d	8.03 x 10 ⁷ (7.60 x 10 ⁷)	2.60 x 10 ⁴ (2.38 x 10 ³)	0.03	Chimney – outer
Rainbow-241d	2.28 x 10 ⁶ (3.33 x 10 ⁵)	BDL	-	Chimney – inner
Lucky Strike-7	4.33 x 10 ⁶ (6.40 x 10 ⁵)	3.60 x 10 ⁵ (3.28 x 10 ²)	8.33	Chimney – outer
Lucky Strike-304	1.00 x 10 ⁶ (4.99 x 10 ⁴)	3.60 x 10 ⁵ (2.96 x 10 ⁴)	35.91	Flange – bottom
Lucky Strike-333	5.34 x 10 ⁴ (3.69 x 10 ³)	6.51 x 10 ³ (5.41 x 10 ²)	12.20	Chimney – outer
Lucky Strike-8	2.61 x 10 ⁵ (2.52 x 10 ³)	1.03 x 10 ⁵ (9.24 x 10 ³)	39.48	Flange – bottom
Lucky Strike-365	5.40 x 10 ⁵ (3.60 x 10 ⁴)	4.17 x 10 ⁴ (9.84 x 10 ¹)	7.72	Chimney – outer

Lucky Strike-371	1.45×10^4 (4.72×10^3)	BDL	-	Chimney – outer
Lucky Strike-11	2.86×10^4 (1.37×10^4)	BDL	-	Chimney – whole
Lucky Strike-449	2.93×10^4 (4.27×10^2)	9.14×10^3 (1.45×10^3)	31.24	Flange – bottom
Lucky Strike-460	6.95×10^3 (2.21×10^3)	BDL	-	Chimney – outer
Lucky Strike-12	1.50×10^5 (7.22×10^3)	5.83×10^4 (3.01×10^3)	38.79	Flange – lip/edge
TAG-593	3.99×10^6 (8.86×10^4)	9.52×10^3 (8.88×10^2)	0.03	Chimney – outer
TAG-604	1.37×10^6 (1.24×10^5)	1.86×10^4 (6.38×10^2)	1.36	Chimney – whole
TAG-625	2.09×10^5 (2.52×10^4)	BDL	-	Chimney – outer
TAG-635	2.70×10^8 (3.04×10^7)	1.53×10^6 (NA)*	0.57	Chimney – outer

*s.e.m. = standard error of the mean

§BDL = below detection limit

*Denotes samples for which only one replicate had successful amplification.

Table 5.6. Results of qPCR assays to determine the occurrence and relative abundance of the DHVE2 in hydrothermal vent deposits from the Eastern Lau Spreading Center. Values are the average of two replicates unless otherwise noted. Lower case letters next to sample names indicate paired samples.

	Archaeal 16S rRNA gene copies per gram of deposit (s.e.m.) [‡]	DHVE2 16S rRNA gene copies per gram of deposit (s.e.m.)	Proportion of DHVE2 16S rRNA gene copies (%)	Deposit type
Kilo Moana-3	9.79 x 10 ⁷ (3.17 x 10 ⁵)	7.74 x 10 ⁵ (5.25 x 10 ³)	0.79	Flange – top
Kilo Moana-19	4.18 x 10 ⁴ (1.63 x 10 ³)	BDL	-	Flange – top
Kilo Moana-358	4.80 x 10 ⁷ (3.13 x 10 ⁶)	3.39 x 10 ³ (1.85 x 10 ²)	0.01	Flange – top/lip
Kilo Moana-36	3.01 x 10 ⁷ (3.47 x 10 ⁶)	7.70 x 10 ⁴ (8.68 x 10 ³)	0.26	Chimney – outer
Kilo Moana-371	7.51 x 10 ³ (2.76 x 10 ²)	BDL	-	Array+
Kilo Moana-399	1.16 x 10 ⁶ (3.31 x 10 ⁵)	1.04 x 10 ⁴ (1.50 x 10 ³)	0.90	Chimney – outer
Kilo Moana-413	1.97 x 10 ⁶ (3.78 x 10 ⁵)	BDL	-	Flange – top
Kilo Moana-54	4.98 x 10 ⁷ (1.11 x 10 ⁷)	6.98 x 10 ³ (1.11 x 10 ³)	0.01	Flange – top
Tow Cam-1134	4.17 x 10 ⁷ (1.09 x 10 ⁷)	1.40 x 10 ⁵ (1.44 x 10 ⁴)	0.34	Chimney – outer
Tow Cam-1146	3.78 x 10 ⁴ (3.60 x 10 ³)	BDL	-	Chimney – outer
Tow Cam-1175	1.73 x 10 ⁵ (2.33 x 10 ³)	BDL	-	Chimney – whole
Tow Cam-1195	2.07 x 10 ⁵ (1.04 x 10 ⁴)	BDL	-	Chimney – outer
Tow Cam-1768	7.34 x 10 ⁷ (2.42 x 10 ⁶)	1.20 x 10 ⁶ (2.33 x 10 ⁵)	1.63	Chimney – outer
Tow Cam-1774	4.39 x 10 ³ (1.29 x 10 ³)	BDL	-	Chimney – whole
Tow Cam-1789	1.85 x 10 ⁷ (5.65 x 10 ⁵)	2.80 x 10 ⁵ (2.63 x 10 ³)	1.51	Chimney – outer
Tahi Moana-1255	1.12 x 10 ⁴ (3.33 x 10 ²)	BDL	-	Flange – top
Tahi Moana-1274	7.31 x 10 ⁶ (2.70 x 10 ⁵)	7.10 x 10 ⁵ (1.13 x 10 ⁵)	9.71	Chimney – outer

Tahi Moana-1350	7.66×10^7 (2.43×10^6)	1.33×10^6 (1.64×10^5)	1.74	Chimney – outer
Tahi Moana-1360	4.95×10^7 (5.04×10^6)	7.42×10^5 (5.22×10^4)	1.50	Chimney – outer
Tahi Moana-1371	1.38×10^7 (9.10×10^5)	1.05×10^6 (7.57×10^4)	7.61	Chimney – outer
Tahi Moana-1381	8.50×10^5 (2.32×10^5)	1.22×10^4 (3.44×10^3)	1.44	Flange – top
Tahi Moana-1388	1.61×10^7 (9.25×10^5)	9.95×10^4 (4.79×10^3)	0.62	Chimney – outer
Tahi Moana-1403	2.80×10^3 (1.62×10^2)	BDL	-	Flange – top
Tahi Moana-1464	1.37×10^4 (2.52×10^1)	BDL	-	Chimney – whole
Tahi Moana-1476	1.05×10^6 (2.67×10^5)	9.16×10^3 (2.29×10^3)	0.87	Flange – top
Tahi Moana-1758	7.63×10^5 (2.77×10^5)	BDL	-	Chimney – outer
ABE-139	1.86×10^7 (4.09×10^6)	1.34×10^5 (1.85×10^4)	0.72	Chimney – outer
ABE-180	2.49×10^4 (4.92×10^3)	BDL	-	Chimney – whole
ABE-194	9.70×10^3 (3.45×10^3)	BDL	-	Chimney – whole
ABE-206	2.31×10^4 (1.73×10^3)	BDL	-	Chimney – whole
ABE-220	1.12×10^7 (2.11×10^6)	4.13×10^5 (1.55×10^4)	3.69	Chimney – outer
ABE-231a	1.84×10^7 (2.63×10^4)	3.61×10^5 (1.24×10^4)	1.97	Chimney on flange
ABE-233a	2.09×10^6 (6.16×10^5)	4.68×10^4 (8.86×10^2)	2.24	Chimney on flange – outer
ABE-250	4.56×10^6 (6.80×10^5)	1.07×10^5 (1.45×10^4)	2.35	Chimney – outer
ABE-309	5.49×10^5 (1.74×10^4)	2.89×10^3 (1.29×10^3)	0.53	Chimney – outer
ABE-91	3.40×10^3 (2.46×10^3)	BDL	-	Chimney – outer
ABE-283	2.44×10^7 (1.28×10^6)	3.97×10^4 (3.16×10^3)	0.16	Chimney – outer
Tui Malila-1021	2.52×10^5 (3.88×10^4)	2.76×10^4 (3.38×10^3)	10.95	Chimney – whole

Tui Malila-1041	3.19×10^5 (6.11×10^4)	7.59×10^3 (3.50×10^2)	2.38	Flange – lip edge
Tui Malila-1059b	8.39×10^4 (6.56×10^1)	5.96×10^4 (6.52×10^3)	71.06	Flange – bottom
Tui Malila-1066b	2.41×10^3 (1.68×10^2)	BDL	-	Flange – lip/edge
Tui Malila-1093	1.66×10^5 (2.23×10^4)	3.65×10^4 (6.56×10^2)	21.96	Flange – top
Tui Malila-1123	4.24×10^3 (8.30×10^2)	BDL	-	Flange – top
Tui Malila-1540c	5.14×10^3 (3.85×10^3)	BDL	-	Flange – bottom
Tui Malila-1556c	2.77×10^4 (1.71×10^3)	2.46×10^3 (5.86×10^2)	8.87	Flange – lip/edge
Tui Malila-1570	5.67×10^4 (4.09×10^3)	BDL	-	Chimney – whole
Tui Malila-1600	2.24×10^5 (7.89×10^4)	4.47×10^3 (1.34×10^3)	1.99	Chimney – outer
Tui Malila-1623	9.80×10^3 (1.06×10^3)	BDL	-	Chimney – outer
Tui Malila-1636	3.22×10^4 (9.98×10^3)	-	-	Array
Tui Malila-828	1.28×10^5 (2.35×10^3)	BDL	-	Chimney – outer
Tui Malila-833	1.17×10^3 (NA)*	BDL	-	Chimney – whole
Tui Malila-858	4.92×10^3 (8.89×10^2)	BDL	-	Flange – bottom/lip
Tui Malila-976	1.86×10^4 (6.20×10^3)	BDL	-	Flange – bottom
Mariner-466	1.93×10^6 (1.73×10^5)	3.00×10^5 (1.03×10^4)	15.53	Chimney – outer
Mariner-496	8.85×10^4 (1.64×10^4)	5.30×10^4 (2.47×10^3)	59.88	Flange – top
Mariner-542	2.69×10^6 (2.96×10^5)	1.39×10^5 (1.77×10^3)	5.19	Chimney – outer
Mariner-568	1.90×10^4 (1.89×10^3)	BDL	-	Chimney – outer
Mariner-576	2.64×10^5 (1.91×10^4)	4.23×10^3 (3.55×10^2)	1.60	Chimney – outer
Mariner-621	5.40×10^4 (7.97×10^3)	2.82×10^3 (6.42×10^2)	5.23	Flange – top

Mariner-646	3.18×10^7 (4.06×10^6)	ND	-	Flange – top
Mariner-672	9.23×10^5 (3.59×10^4)	7.81×10^4 (1.30×10^3)	8.46	Flange – top
Mariner-719	2.01×10^4 (4.22×10^3)	BDL	-	Chimney – outer
Mariner-729	5.69×10^4 (6.74×10^3)	4.00×10^3 (5.75×10^2)	7.03	Chimney – outer
Mariner-1493	3.82×10^4 (8.35×10^3)	2.08×10^3 (6.68×10^2)	5.45	Flange – top
Mariner-1652	1.23×10^6 (1.52×10^4)	4.66×10^5 (6.38×10^4)	37.93	Chimney – outer
Mariner-1684	6.58×10^4 (1.54×10^4)	4.06×10^4 (7.80×10^3)	61.76	Flange – top
Mariner-1704	2.26×10^4 (8.43×10^3)	4.89×10^3 (6.35×10^2)	21.61	Flange – top
Mariner-1718	8.00×10^6 (2.11×10^6)	8.53×10^5 (1.34×10^5)	10.66	Chimney – outer

*s.e.m. = standard error of the mean

§BDL = below detection limit

*Denotes samples for which only one replicate had successful amplification.

For most of the deposits we collected, only the outer few millimeters were sampled as this is where the majority of microorganisms are found (Takai *et al.*, 2001; Schrenk *et al.*, 2003; Nakagawa *et al.*, 2005d; Kormas *et al.*, 2006; Nunoura and Takai, 2009). However, for some of the deposits, we sampled exterior and interior sections of chimneys and, for flanges, different spatial areas on the top, bottom and lip/edge. (Tables 5.3-5.6). As a result of this sampling strategy, we have paired samples from a few deposits that illustrate the spatial variability of the DHVE2 within individual deposits. Spatial variability on a deposit is perhaps best illustrated by a flange structure collected from the Tui Malila vent field along the ELSC. On the bottom of this deposit, the DHVE2 comprised over 70% of the archaeal 16S rRNA gene sequences detected (Tui Malila-1059) while they were undetectable on the lip/edge (Tui Malila-1066).

These observations illustrate the spatial variability of the DHVE2 in individual deposits. Spatial variability on/in a deposit can be shaped by a number of factors including heterogeneous wall thickness, deposit mineralogy and fluid flow rate.

Co-occurrence patterns of the DHVE2

In previous studies, bar-coded pyrosequencing was used to characterize the archaeal communities of numerous vent deposits from geochemically and geographically distinct hydrothermal vent fields (MAR, Guaymas Basin, ELSC) (Flores *et al.*, 2011). These large data sets provided an ideal resource to examine the co-occurrence of the DHVE2 with other archaeal lineages using Local Similarity Analysis (LSA). In total, three OTUs were identified as the DHVE2 (ID#'s 727, 1148 and 1137) and contained 3557, 1389 and 120 sequences, respectively (Table 5.7). OTUs 727 and 1148 were present in 89% and 65% of samples, respectively, while 1137 was present in only 10% of samples. Using LSA, we found that the occurrence of clusters 727 and 1148 were positively correlated with one another but not with 1137 (Figure 5.2). Due to the low abundance, relatively rare occurrence and lack of correlation with the other DHVE2, results of LSA including cluster 1137 are not presented. An additional ten OTUs were positively correlated with both 727 and 1148, while five were negatively correlated (Figure 5.2). Interestingly, all negatively correlated OTUs were relatively abundant (≥ 1371 sequences) and observed in most samples (present in 68 to 91% of deposits) while the positively correlated OTUs were generally less abundant (≤ 2204) and rarer (present in 7 to 70% of deposits) (Table 5.8).

Table 5.7. Results of local similarity analysis illustrating the co-occurrence of the DHVE2 with other archaeal OTUs.

	Number of sequences	Percentage of deposits	Lowest taxonomic classification with a bootstrap value greater than 50% (%)
OTUs classified as DHVE2			
727	3557	89.5	<i>Euryarchaeota</i> (98)
1148	1389	65.0	<i>Euryarchaeota</i> (92)
1137	120	10.5	<i>Euryarchaeota</i> (100)
OTUs positively correlated with 727 & 1148			
421	538	38.6	<i>Archaea</i> (85)
544	171	38.6	<i>Ferroglobus</i> (55)
547	190	15.8	<i>Euryarchaeota</i> (93)
593	2204	65.0	<i>Euryarchaeota</i> (93)
648	134	7.0	<i>Euryarchaeota</i> (87)
677	101	29.8	<i>Euryarchaeota</i> (52)
739	101	40.4	<i>Euryarchaeota</i> (91)
927	990	70.2	<i>Thermogymnomonas</i> (55)
1026	145	19.3	<i>Euryarchaeota</i> (72)
1248	535	22.8	<i>Euryarchaeota</i> (65)
OTUs negatively correlated with 727 & 1148			
461	3539	71.9	<i>Archaeoglobus</i> (98)
549	7143	68.4	<i>Thermoproteaceae</i> (84)
594	6680	91.2	<i>Aeropyrum</i> (53)
638	5105	77.2	<i>Desulfurococcales</i> (98)
738	1371	68.4	<i>Staphylothermus</i> (99)

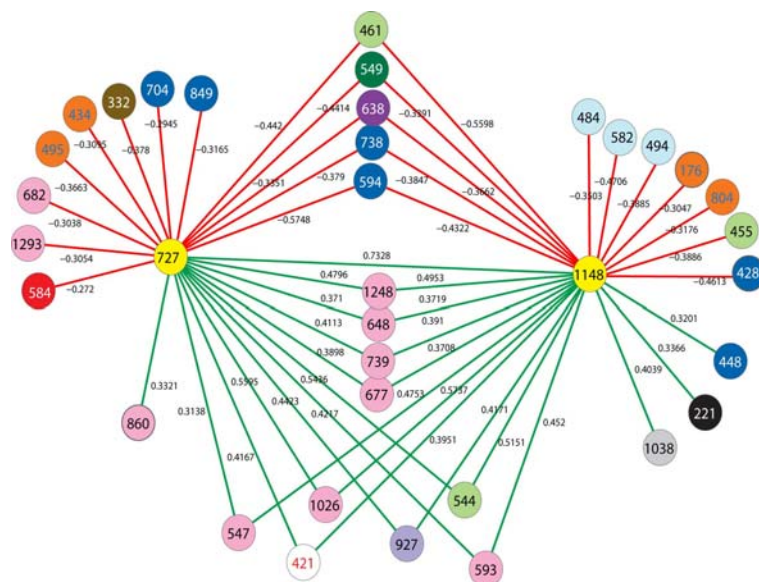


Figure 5.2. Results of local similarity analysis showing OTUs that are negatively (red lines) and positively (green lines) correlated with the DHVE2 (yellow circles). Circles represent OTUs and are colored according to family-level taxonomic classification by the RDP-classifier when possible. Color key is as follows: white = unclassified Archaea, pink = unclassified *Euryarchaeota*, red = unclassified *Crenarchaeota*, orange = *Nanoarchaeota*, purple = unclassified *Desulfurococcales*, lavender = *Thermoplasmatales*, light green = *Archaeoglobaceae*, light blue = *Methanococcaceae*, grey = *Thermococcaceae*, brown = *Thermofilaceae*, black = *Pyrodictaceae*, dark blue = *Desulfurococcaceae*, dark green = *Thermoproteaceae*.

The majority (9/10) of positively correlated OTUs were classified as *Euryarchaeota* (Figure 5.2, Table 5.7). However, most (7/9) could not be classified below the phylum making it difficult to speculate on potential ecological relationships between these OTUs and the DHVE2. Of the OTUs that could be classified beyond phylum, one was classified as *Thermogymnomonas* and the other *Ferroglobus* (Table 5.7). Only one *Thermogymnomonas* species is in culture but, it shares important phenotypic traits, like thermoacidophily, with *A. boonei* T469^T (Itoh *et al.*, 2007). However, the cultured *Thermogymnomonas* species also differs from *A. boonei* T469^T

in many significant ways as it is aerobic, utilizes sugars as carbon substrates and was isolated from a solfatara field in Japan. Whether deep-sea representatives of this lineage are phenotypically similar as the terrestrial isolate is unknown, but acidophily is at least a common trait of the *Thermoplasmatales* to which it belongs. The sole described *Ferroglobus* species, *F. placidus*, can both reduce (Tor *et al.*, 2001) and oxidize (Hafenbradl *et al.*, 1996) iron under different thermophilic conditions. Iron concentrations are generally high in deep-sea hydrothermal environments but are greatest when the pH of the fluids are low due to differences in solubility, suggesting that conditions which favor acidophiles may also favor thermophilic iron-oxidizers. It is therefore likely that these OTUs share the same acidophilic niche with the DHVE2 but utilize different carbon and/or energy sources which allow all to co-exist. These and the other positively correlated OTUs may also be involved in syntrophic relationships with the DHVE2 as others have proposed for fermentative *Thermococcales* (Bonch-Osmolovskaya and Stetter, 1991; Rinker and Kelly, 2000).

In contrast to the positively correlated OTUs, all negatively correlated OTUs were confidently classified to at least the order level and four of five were *Crenarchaeota* (Figure 5.2, Table 5.7). Some of the negatively correlated OTUs were related to organisms requiring oxidants from seawater. For example, the one euryarchaeotal OTU was confidently classified as *Archaeoglobus* which are thermophilic sulfate-reducers (Stetter, 1988; Burggraf *et al.*, 1990; Beeder *et al.*, 1994). Also, one of the crenarchaeotal OTUs was most closely related to *Aeropyrum* which are aerobic thermophiles (Sako *et al.*, 1996). The only source for these oxidants in deep-

sea hydrothermal environments is from seawater which upon mixing with hydrothermal fluids would raise fluid pH, therefore inhibiting acidophiles. Cultivated organisms related to the negatively correlated OTUs are also not acidophilic and tended to have higher optimum growth temperatures than *A. boonei* T469^T (Boone *et al.*, 2001). It appears then, that while the positively correlated OTUs may share the same acidophilic niche of the DHVE2 and are able to co-exist because of different carbon/energy sources, the negatively correlated OTUs require different physical conditions (neutral pH, oxidizing conditions) that do not permit anaerobic thermoacidophiles to grow.

Genetic diversity of cultivable DHVE2

In order to better understand the phylogenetic diversity of the DHVE2, numerous enrichment cultures targeting thermoacidophilic microorganisms were initiated from samples collected in 2006 – 2009. Many of the enrichment cultures discussed above in chapter 4 that yielded thermoacidophilic Bacteria also yielded new DHVE2 isolates (Table 5.8). In total, 15 DHVE2 isolates were obtained with seven from the MAR (five from Lucky Strike, one from Rainbow, one from TAG), six from ELSC (one from Tui Malila, five from Mariner) and two from the EPR (Table 5.8). No isolates were obtained from the Guaymas Basin despite detection of the DHVE2 (by amplification of DHVE2 specific PCR primers) in two enrichments. Manipulations of medium pH, temperature and organic substrates were performed to try and isolate the DHVE2 from Guaymas samples, but were unsuccessful as *Thermococcus* spp. would typically outgrow the DHVE2 under these conditions.

Table 5.8. Hydrothermal vent deposits from which new DHVE2 isolates were obtained.

Isolate name	Vent field of isolation (deposit type)	Location	Depth (m)
Mar08-237a	Rainbow (chimney)	36° 13.75625'N 33° 54.11541'W	2275
Mar08-276	Lucky Strike (chimney)	37° 17.52494'N 32° 16.50738'W	1617
Mar08-307	Lucky Strike (flange)	37° 17.5250'N 32° 16.5058'W	1624
Mar08-339	Lucky Strike (chimney)	37° 17.45770'N 32° 16.91245'W	1730
Mar08-361	Lucky Strike (flange)	37° 17.4528'N 32° 16.9161'W	1730
Mar08-368	Lucky Strike (chimney)	37° 17.4998'N 32° 16.6715'W	1721
Mar08-641	TAG (chimney)	26° 8.2043'N 44° 49.5283'W	3621
EPR07-39	9°N (chimney)	9° 50.31366'N 104° 17.48471'W	2510
EPR07-159	9°N (chimney)	9° 50.2876'N 104° 17.4721'W	2507
Lau09-cd652	Mariner (flange)	22° 10.82942'S 176° 36.10686'W	1919
Lau09-654	Mariner (flange)	22° 10.82942'S 176° 36.10686'W	1919
Lau09-664	Mariner (chimney)	22° 10.80806'S 176° 36.05562'W	1915
Lau09-781	Mariner (chimney)	22° 11.2751'S 176° 36.0755'W	1919
Lau09-1128	Tui Malila (flange)	22° 0.1708'S 176° 34.1066'W	1883
Lau09-cd1713	Mariner (flange)	22° 10.79920'S 176° 36.06771'W	1911

Despite large geographic distances between many of the vent fields, the genetic similarities of the 16S rRNA genes of the isolates were high. With the exception of strain Lau09-1128, all isolates shared greater than 97% 16S rRNA gene sequence similarity with one another and *A. boonei* T469^T (Figure 5.3). This is similar to the diversity of *Thermococcus* species from different vent fields (e.g., Huber *et al.*, 1995; Canganella *et al.*, 1998; Holden *et al.*, 2001; Huber *et al.*, 2006) but quite different than what was observed for thermoacidophilic Bacteria as discussed in Chapter 4. Strain

Lau09-1128 was $\geq 96\%$ similar to all isolates but was most similar ($> 97\%$ similar) to clone sequences (Figure 5.3). Despite the overall high sequence similarity of all organisms, isolates tended to cluster based on the vent field of isolation. Other thermophilic archaeal lineages, most notably the *Sulfolobales* and *Thermococcales*, do not exhibit such clear biogeographical trends using only 16S rRNA gene sequences. Instead, other genes or intergenic regions must be used for biogeographical trends like these to be observed (Whitaker *et al.*, 2003; Huber *et al.*, 2006; Reno *et al.*, 2009).

Conclusion

Results from this study show that the DHVE2 are ubiquitous in deep-sea hydrothermal environments and tend to co-occur with other *Euryarchaeota*. Assuming that all DHVE2 are thermoacidophilic, then thermoacidophily is an important physiological strategy for some microorganisms in these poorly understood ecosystems. Factors that seemed to influence the occurrence and abundance of the DHVE2 within an individual vent field include the age of the vent deposit (as this is indicative of the maturity of the microbial community), fluid mixing style and type of vent structure (chimney vs. flange). Other factors like deposit mineralogy, grazing by eukaryotes and viruses may also be influencing the biogeography of the DHVE2 but were not examined as part of this project.

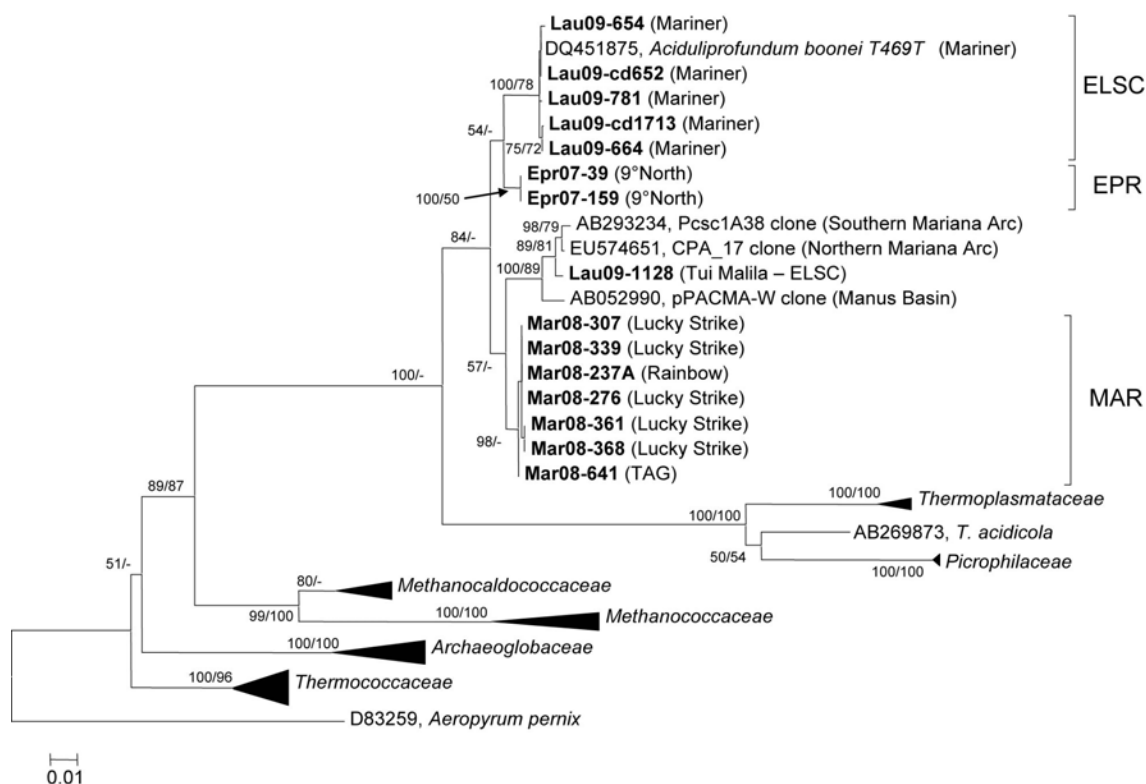


Figure 5.3. Neighbor-joining tree based on 16S rRNA gene sequence comparisons of 15 novel DHVE2 isolates and other archaeal families. Bootstrap percentages above 50% are shown firstly for the neighbor-joining analysis (based on 500 replicates) and secondly for the maximum-likelihood analysis (based on 100 replicates). The tree was generated considering only unambiguously aligned nucleotide position (n=789). New isolates are shown in bold. The scale bar represents 0.01 changes per nucleotide position. *T. acidicola* in tree is *Thermogymnomonas acidicola*.

Contributions

For this project, I enriched and isolated novel members of the DHVE2 with Yitai Liu, performed all molecular and phylogenetic analyses of isolates, performed and analyzed qPCR results, mined pyrosequencing data, interpreted all results and wrote the manuscript for publication.

Chapter 6: Conclusion

It has been nearly 35 years since deep-sea hydrothermal vents were first discovered. Over that time, numerous theoretical, observational and empirical studies have provided valuable information about the physiological potential and phylogenetic diversity of the microbial communities associated with these environments. However, we still have a limited understanding of the factors that control microbial biogeography in these systems. The studies presented in this dissertation aimed to improve our understanding of microbial biogeography of active hydrothermal vent deposits at multiple spatial scales and levels of biological organization.

In Chapter 2, bar-coded pyrosequencing was used to compare the archaeal and bacterial communities of two geochemically different vent fields along the MAR. The vent fields studied, Rainbow and Lucky Strike, are hosted atop different igneous substrates (peridotite vs. basalt) and, as a result, generate contrasting fluid chemistries that were predicted to influence microbial community composition (McCollom, 2007). Results show that the communities are indeed distinct between the two vent fields and the differences appear to be driven primarily by contrasting H₂ concentrations in the hydrothermal fluids (Flores *et al.*, 2011). The observed differences were supported by geochemical modeling that shows oxidizing conditions in the exterior of the H₂-poor Lucky Strike deposits. To my knowledge, this is the first study in deep-sea vent microbial ecology where bar-coded pyrosequencing was used to show differences in both the archaeal and bacterial communities of a relatively large number of deposits from two geologically distinct vent fields. It is also the first to demonstrate a

correlation between subsurface geological processes and microbial community structure at the vent field scale.

For Chapter 3, I extended the same pyrosequencing approach to compare the communities of over 30 deposits from six vent fields along the ELSC. Geologically, back-arc basins are different than mid-ocean ridge systems like the MAR and can generate contrasting fluid chemistries over relatively small geographic areas. Results from this study showed that the southernmost Mariner vent field hosted unique archaeal and bacterial communities. Differences in the Mariner communities were related to increased degassing of magma in the subsurface which results in more acidic, volatile rich fluids. Like the MAR study, this study highlights the coupling of geologic and microbial processes in deep-sea hydrothermal environments and provides an invaluable data-set that can be used to continue to unravel these associations.

While the studies presented in Chapters 2 and 3 identified geologic processes influencing microbial communities at the vent field scale, they also illustrated how many uncultivated lineages still exist in these environments. To help fill in these gaps, a targeted cultivation-based study was conducted in Chapter 4, resulting in the isolation and description of the first obligately thermoacidophilic Bacteria from deep-sea hydrothermal vents. Targeted cultivation efforts like this are becoming less common in microbial ecology as molecular techniques continue to dominate the field. However, as this study proves, numerous surprises remain about the physiological and metabolic potential of environmental microbes and without cultivation-based studies we will never

be able to take full advantage of 16S rRNA gene sequence data or appreciate the true diversity of our planet.

For Chapter 5, the biogeography of an important archaeal lineage, the thermoacidophilic DHVE2, was investigated using a combination of cultivation-dependent and -independent techniques. Results showed that the DHVE2 are ubiquitous in deep-sea hydrothermal environments but their occurrence and abundance within an individual deposit depends on a number of factors. Targeted biogeographical studies like this can help us better understand constraints on certain physiological strategies in deep-sea hydrothermal environments. Furthermore, the use of correlation techniques like LSA could help identify shared niches between cultivated and uncultivated lineages allowing for more informed cultivation strategies targeting the uncultivated. Further detailed genomic analysis of the new isolates will also be able to identify similarities and differences between the biogeographical patterns observed in terrestrial thermoacidophilic Archaea.

In conclusion, deep-sea hydrothermal environments still represent one of the most fascinating and least understood environments on Earth. Future research should continue to build upon what I have presented here by applying similar sampling and sequencing strategies to capture the phylogenetic diversity of different hydrothermal vent environments. At the community level, the next step will be to determine the functional capabilities of these microbial communities through metagenomic and metatranscriptomic approaches. Targeted cultivation efforts and/or single cell sequencing techniques targeting novel lineages will also help to elucidate the functional

capabilities of these communities. Eventually, these data can be integrated with various geological data (e.g., heat flux, fluid flow rates, geochemical composition of fluids, mineralogy, etc.) to provide more quantitative insights of microbial productivity of deep-sea hydrothermal environments in the context of the global ocean system.

References

- Alain, K., Querellou, J., Lesongeur, F., Pignet, P., Crassous, P., Raguenes, G. *et al.* (2002) *Caminibacter hydrogeniphilus* gen. nov., sp. nov., a novel thermophilic, hydrogen-oxidizing bacterium isolated from an East Pacific Rise hydrothermal vent. *Int J Syst Evol Microbiol* **52**: 1317-1323.
- Alt, J.C. (1995) Subseafloor Processes in Mid-Ocean Ridge Hydrothermal Systems. In *Seafloor Hydrothermal Systems: Physical, Chemical, Biological, and Geological Interactions*. Humphris, S.E., Zierenberg, R.A., Mullineaux, L.S., and Thomson, R.E. (eds). Washington, DC: American Geophysical Union, pp. 85-114.
- Altschul, S.F., Gish, W., Miller, W., Myers, E.W., and Lipman, D.J. (1990) Basic local alignment search tool. *J Mol Biol* **215**: 403-410.
- Auguet, J.C., Barberan, A., and Casamayor, E.O. (2009) Global ecological patterns in uncultured Archaea. *The ISME journal* **4**: 182-190.
- Baker, B.J., Hugenholtz, P., Dawson, S.C., and Banfield, J.F. (2003) Extremely acidophilic protists from acid mine drainage host *Rickettsiales*-lineage endosymbionts that have intervening sequences in their 16S rRNA genes. *Appl Environ Microbiol* **69**: 5512-5518.
- Bautista-Zapanta, J.N., Arafat, H.H., Tanaka, K., Sawada, H., and Suzuki, K. (2009) Variation of 16S-23S internally transcribed spacer sequence and intervening

- sequence in rDNA among the three major *Agrobacterium* species. *Microbiol Res* **164**: 604-612.
- Beeder, J., Nilsen, R.K., Rosnes, J.T., Torsvik, T., and Lien, T. (1994) *Archaeoglobus fulgidus* isolated from hot North Sea oil field waters. *Applied and Environmental Microbiology* **60**: 1227.
- Benson, D.A., Karsch-Mizrachi, I., Lipman, D.J., Ostell, J., and Sayers, E.W. (2009) GenBank. *Nucleic Acids Res* **37**: D26-31.
- Bonch-Osmolovskaya, E.A., and Stetter, K.O. (1991) Interspecies hydrogen transfer in cocultures of thermophilic archaea. *Systematic and applied microbiology* **14**: 205-208.
- Boone, D.R., Castenholz, R.W., and Garrity, G.M. (2001) *Bergey's manual of systematic bacteriology* / George M. Garrity, editor-in-chief. New York: Springer.
- Burggraf, S., Jannasch, H., Nicolaus, B., and Stetter, K. (1990) *Archaeoglobus profundus* sp. nov., represents a new species within the sulfate-reducing archaeobacteria. *Systematic and applied microbiology* **13**: 24-28.
- Campbell, B.J., Engel, A.S., Porter, M.L., and Takai, K. (2006) The versatile *epsilon*-*proteobacteria*: key players in sulphidic habitats. *Nat Rev Microbiol* **4**: 458-468.
- Campbell, B.J., Jeanthon, C., Kostka, J.E., Luther, G.W., 3rd, and Cary, S.C. (2001) Growth and phylogenetic properties of novel bacteria belonging to the epsilon subdivision of the *Proteobacteria* enriched from *Alvinella pompejana* and deep-sea hydrothermal vents. *Appl Environ Microbiol* **67**: 4566-4572.

- Canganella, F., Jones, W.J., Gambacorta, A., and Antranikian, G. (1998) *Thermococcus guaymasensis* sp. nov. and *Thermococcus aggregans* sp. nov., two novel thermophilic archaea isolated from the Guaymas Basin hydrothermal vent site. *International Journal of Systematic and Evolutionary Microbiology* **48**: 1181-1185.
- Cavanaugh, C.M., Gardiner, S.L., Jones, M.L., Jannasch, H.W., and Waterbury, J.B. (1981) Prokaryotic Cells in the Hydrothermal Vent Tube Worm *Riftia pachytila* Jones: Possible Chemoautotrophic Symbionts. *Science* **213**: 340-342.
- Chao, A., and Bunge, J. (2002) Estimating the number of species in a stochastic abundance model. *Biometrics* **58**: 531-539.
- Charlou, J., Donval, J., Douville, E., Jean-Baptiste, P., Radford-Knoery, J., Fouquet, Y. *et al.* (2000) Compared geochemical signatures and the evolution of Menez Gwen (37° 50'N) and Lucky Strike (37° 17'N) hydrothermal fluids, south of the Azores Triple Junction on the Mid-Atlantic Ridge. *Chemical Geology* **171**: 49-75.
- Charlou, J.L., Donval, J.P., Fouquet, Y., Jean-Baptiste, P., and Holm, N. (2002) Geochemistry of high H₂ and CH₄ vent fluids issuing from ultramafic rocks at the Rainbow hydrothermal field (36 degrees 14 ' N, MAR). *Chemical Geology* **191**: 345-359.
- Claesson, M.J., O'Sullivan, O., Wang, Q., Nikkila, J., Marchesi, J.R., Smidt, H. *et al.* (2009) Comparative analysis of pyrosequencing and a phylogenetic microarray

- for exploring microbial community structures in the human distal intestine.
PLoS One **4**: e6669.
- Clarke, K., and Gorley, R. (2006) PRIMER v6. *User manual/tutorial Plymouth routine in multivariate ecological research Plymouth Marine Laboratory.*
- Cole, J.R., Wang, Q., Cardenas, E., Fish, J., Chai, B., Farris, R.J. *et al.* (2009) The Ribosomal Database Project: improved alignments and new tools for rRNA analysis. *Nucleic Acids Res* **37**: D141-145.
- Colwell, R.K., and Coddington, J.A. (1994) Estimating terrestrial biodiversity through extrapolation. *Philos Trans R Soc Lond B Biol Sci* **345**: 101-118.
- Corre, E., Reysenbach, A.L., and Prieur, D. (2001) Epsilon-proteobacterial diversity from a deep-sea hydrothermal vent on the Mid-Atlantic Ridge. *FEMS Microbiol Lett* **205**: 329-335.
- De Angelis, M., Lilley, M., and Baross, J. (1993) Methane oxidation in deep-sea hydrothermal plumes of the Endeavour Segment of the Juan de Fuca Ridge. *Deep Sea Research Part I: Oceanographic Research Papers* **40**: 1169-1186.
- Desbruyeres, D., Almeida, A., Biscoito, M., Comtet, T., Khripounoff, A., Le Bris, N. *et al.* (2000) A review of the distribution of hydrothermal vent communities along the northern Mid-Atlantic Ridge: dispersal vs. environmental controls. *Hydrobiologia* **440**: 201-216.
- Desbruyeres, D., Chevaldonné, P., Alayse, A.M., Jollivet, D., Lallier, F., Jouin-Toulmond, C. *et al.* (1998) Biology and ecology of the “Pompeii worm”(Alvinella pompejana Desbruyeres and Laubier), a normal dweller of an

- extreme deep-sea environment: a synthesis of current knowledge and recent developments. *Deep-Sea Research Part II* **45**: 383-422.
- Desbruyeres, D., Biscoito, M., Caprais, J.C., Colaco, A., Comtet, T., Crassous, P. *et al.* (2001) Variations in deep-sea hydrothermal vent communities on the Mid-Atlantic Ridge near the Azores plateau. *Deep-Sea Research Part I-Oceanographic Research Papers* **48**: 1325-1346.
- Dewhirst, F.E., Shen, Z., Scimeca, M.S., Stokes, L.N., Boumenna, T., Chen, T. *et al.* (2005) Discordant 16S and 23S rRNA gene phylogenies for the genus *Helicobacter*: implications for phylogenetic inference and systematics. *J Bacteriol* **187**: 6106-6118.
- Dhillon, A., Lever, M., Lloyd, K.G., Albert, D.B., Sogin, M.L., and Teske, A. (2005) Methanogen diversity evidenced by molecular characterization of methyl coenzyme M reductase A (mcrA) genes in hydrothermal sediments of the Guaymas Basin. *Appl Environ Microbiol* **71**: 4592-4601.
- Dick, G.J., Lee, Y.E., and Tebo, B.M. (2006) Manganese(II)-oxidizing *Bacillus* spores in Guaymas Basin hydrothermal sediments and plumes. *Appl Environ Microbiol* **72**: 3184-3190.
- Dieci, G., Preti, M., and Montanini, B. (2009) Eukaryotic snoRNAs: a paradigm for gene expression flexibility. *Genomics* **94**: 83-88.
- Douville, E., Charlou, J.L., Oelkers, E.H., Bienvenu, P., Colon, C.F.J., Donval, J.P. *et al.* (2002) The rainbow vent fluids (36 degrees 14 ' N, MAR): the influence of

- ultramafic rocks and phase separation on trace metal content in Mid-Atlantic Ridge hydrothermal fluids. *Chemical Geology* **184**: 37-48.
- Edwards, K.J. (2004) Formation and degradation of seafloor hydrothermal sulfide deposits. In *Sulfur Biogeochemistry: Past and Present*. Amend, J.P., Edwards, K.J., and Lyons, T.W. (eds). Boulder, CO: The Geological Society of America, pp. 83-96.
- Edwards, K.J., Bach, W., and McCollom, T.M. (2005) Geomicrobiology in oceanography: microbe-mineral interactions at and below the seafloor. *TRENDS in Microbiology* **13**: 449-456.
- Edwards, K.J., McCollom, T.M., Konishi, H., and Buseck, P.R. (2003a) Seafloor bioalteration of sulfide minerals: results from in situ incubation studies. *Geochimica Et Cosmochimica Acta* **67**: 2843-2856.
- Edwards, K.J., Rogers, D.R., Wirsén, C.O., and McCollom, T.M. (2003b) Isolation and characterization of novel psychrophilic, neutrophilic, Fe-oxidizing, chemolithoautotrophic *alpha*- and *gamma*-proteobacteria from the deep sea. *Appl Environ Microbiol* **69**: 2906-2913.
- Felbeck, H. (1981) Chemoautotrophic Potential of the Hydrothermal Vent Tube Worm, *Riftia pachyptila* Jones (Vestimentifera). *Science* **213**: 336-338.
- Ferrera, I., Longhorn, S., Banta, A.B., Liu, Y., Preston, D., and Reysenbach, A.L. (2007) Diversity of 16S rRNA gene, ITS region and *acI*B gene of the *Aquificales*. *Extremophiles* **11**: 57-64.

- Ferrini, V., Tivey, M., Carbotte, S., Martinez, F., and Roman, C. (2008) Variable morphologic expression of volcanic, tectonic, and hydrothermal processes at six hydrothermal vent fields in the Lau back-arc basin. *Geochemistry Geophysics Geosystems* **9**: Q07022.
- Flores, G.E., Campbell, J.H., Kirshtein, J.D., Meneghin, J., Podar, M., Steinberg, J.I. *et al.* (2011) Microbial Community Structure of Hydrothermal Deposits from Geochemically Different Vent Fields Along the Mid-Atlantic Ridge. *Environ Microbiol.* **13**: no. doi: 10.1111/j.1462-2920.2011.02463.x
- Foustoukos, D., Houghton, J., Seyfried, W., Sievert, S., and Cody, G. (2011) Kinetics of H₂-O₂-H₂O redox equilibria and formation of metastable H₂O₂ under low temperature hydrothermal conditions. *Geochimica Et Cosmochimica Acta.* **75**: 1594-1607.
- Gamo, T., Ishibashi, J., Tsunogai, U., Okamura, K., and Chiba, H. (2006) Unique geochemistry of submarine hydrothermal fluids from arc-back-arc settings of the western Pacific. In *Back-Arc Spreading Systems: Geological, Biological, Chemical, and Physical Interactions*. Christie, D.M., Fisher, C.R., Lee, S.-M., and Givens, S. (eds): American Geophysical Union, pp. 147-161.
- German, C., and Von Damm, K. (2004) Hydrothermal processes In *Treatise on Geochemistry*. Turekian, K.K., and Holland, H.D. (eds). New York, N. Y.: Elsevier, pp. 181-222.

- Glasauer, S., Langley, S., Boyanov, M., Lai, B., Kemner, K., and Beveridge, T.J. (2007) Mixed-valence cytoplasmic iron granules are linked to anaerobic respiration. *Appl Environ Microbiol* **73**: 993-996.
- Götz, D., Banta, A., Beveridge, T.J., Rushdi, A.I., Simoneit, B.R., and Reysenbach, A.L. (2002) *Persephonella marina* gen. nov., sp. nov. and *Persephonella guaymasensis* sp. nov., two novel, thermophilic, hydrogen-oxidizing microaerophiles from deep-sea hydrothermal vents. *Int J Syst Evol Microbiol* **52**: 1349-1359.
- Hafenbradl, D., Keller, M., Dirmeyer, R., Rachel, R., Roßnagel, P., Burggraf, S. *et al.* (1996) *Ferroglobus placidus* gen. nov., sp. nov., a novel hyperthermophilic archaeum that oxidizes Fe^{2+} at neutral pH under anoxic conditions. *Archives of microbiology* **166**: 308-314.
- Hamady, M., Lozupone, C., and Knight, R. (2010) Fast UniFrac: facilitating high-throughput phylogenetic analyses of microbial communities including analysis of pyrosequencing and PhyloChip data. *ISME J* **4**: 17-27.
- Harmsen, H., Prieur, D., and Jeanthon, C. (1997) Distribution of microorganisms in deep-sea hydrothermal vent chimneys investigated by whole-cell hybridization and enrichment culture of thermophilic subpopulations. *Appl Environ Microbiol* **63**: 2876-2883.
- Hoek, J., Banta, A., Hubler, F., and Reysenbach, A. (2003) Microbial diversity of a sulphide spire located in the Edmond deep-sea hydrothermal vent field on the Central Indian Ridge. *Geobiology* **1**: 119-127.

- Holden, J.F., Takai, K., Summit, M., Bolton, S., Zyskowski, J., and Baross, J.A. (2001) Diversity among three novel groups of hyperthermophilic deep-sea *Thermococcus* species from three sites in the northeastern Pacific Ocean. *FEMS Microbiol Ecol* **36**: 51-60.
- Huber, H., Hohn, M., Rachel, R., Fuchs, T., Wimmer, V., and Stetter, K. (2002a) A new phylum of Archaea represented by a nanosized hyperthermophilic symbiont. *Nature* **417**: 63-67.
- Huber, J., Cantin, H., Huse, S., Welch, D., Sogin, M., and Butterfield, D. (2010) Isolated communities of *Epsilonproteobacteria* in hydrothermal vent fluids of the Mariana Arc seamounts. *FEMS microbiology ecology* **73**: 538-549.
- Huber, J., Mark Welch, D., Morrison, H., Huse, S., Neal, P., Butterfield, D., and Sogin, M. (2007) Microbial population structures in the deep marine biosphere. *Science* **318**: 97-100.
- Huber, J.A., Butterfield, D.A., and Baross, J.A. (2002b) Temporal changes in archaeal diversity and chemistry in a mid-ocean ridge seafloor habitat. *Appl Environ Microbiol* **68**: 1585-1594.
- Huber, J.A., Butterfield, D.A., and Baross, J.A. (2006) Diversity and distribution of seafloor *Thermococcales* populations in diffuse hydrothermal vents at an active deep-sea volcano in the northeast Pacific Ocean. *Journal of Geophysical Research-Biogeosciences* **111**: G04016.
- Huber, R., Stöhr, J., Hohenhaus, S., Rachel, R., Burggraf, S., Jannasch, H.W., and Stetter, K.O. (1995) *Thermococcus chitonophagus* sp. nov., a novel, chitin-

- degrading, hyperthermophilic archaeum from a deep-sea hydrothermal vent environment. *Archives of microbiology* **164**: 255-264.
- Humphris, S.E., Fornari, D.J., Scheirer, D.S., German, C.R., and Parson, L.M. (2002) Geotectonic setting of hydrothermal activity on the summit of Lucky Strike Seamount (37 degrees 17 ' N, Mid-Atlantic Ridge). *Geochemistry Geophysics Geosystems* **3**: 1-24.
- Hunter, R.C., and Beveridge, T.J. (2005) High-resolution visualization of *Pseudomonas aeruginosa* PAO1 biofilms by freeze-substitution transmission electron microscopy. *J Bacteriol* **187**: 7619-7630.
- Huse, S., Welch, D., Morrison, H., and Sogin, M. (2010) Ironing out the wrinkles in the rare biosphere through improved OTU clustering. *Environmental microbiology* **12**: 1889-1898.
- Imachi, H., Sakai, S., Hirayama, H., Nakagawa, S., Nunoura, T., Takai, K., and Horikoshi, K. (2008) *Exilispira thermophila* gen. nov., sp. nov., an anaerobic, thermophilic spirochaete isolated from a deep-sea hydrothermal vent chimney. *Int J Syst Evol Microbiol* **58**: 2258-2265.
- Inagaki, F., Takai, K., Nealson, K.H., and Horikoshi, K. (2004) *Sulfurovum lithotrophicum* gen. nov., sp. nov., a novel sulfur-oxidizing chemolithoautotroph within the *epsilon-Proteobacteria* isolated from Okinawa Trough hydrothermal sediments. *Int J Syst Evol Microbiol* **54**: 1477-1482.
- Inagaki, F., Takai, K., Kobayashi, H., Nealson, K.H., and Horikoshi, K. (2003) *Sulfurimonas autotrophica* gen. nov., sp. nov., a novel sulfur-oxidizing epsilon-

- proteobacterium isolated from hydrothermal sediments in the Mid-Okinawa Trough. *Int J Syst Evol Microbiol* **53**: 1801-1805.
- Inagaki, F., Nunoura, T., Nakagawa, S., Teske, A., Lever, M., Lauer, A. *et al.* (2006) Biogeographical distribution and diversity of microbes in methane hydrate-bearing deep marine sediments on the Pacific Ocean Margin. *Proc Natl Acad Sci* **103**: 2815-2820.
- Itoh, T., Yoshikawa, N., and Takashina, T. (2007) *Thermogymnomonas acidicola* gen. nov., sp. nov., a novel thermoacidophilic, cell wall-less archaeon in the order *Thermoplasmatales*, isolated from a solfataric soil in Hakone, Japan. *International Journal of Systematic and Evolutionary Microbiology* **57**: 2557-2561.
- Itoh, T., Suzuki, K., Sanchez, P., and Nakase, T. (2003) *Caldisphaera lagunensis* gen. nov., sp. nov., a novel thermoacidophilic crenarchaeote isolated from a hot spring at Mt Maquiling, Philippines. *International Journal of Systematic and Evolutionary Microbiology* **53**: 1149-1154.
- Jannasch, H.W. (1995) Microbial Interactions with Hydrothermal Fluids. In *Seafloor Hydrothermal Systems: Physical, Chemical, Biological, and Geological Interactions*. Humphris, S.E., Zierenberg, R.A., Mullineaux, L.S., and Thomson, R.E. (eds). Washington, DC: American Geophysical Union, pp. 273-296.
- Jones, M.L. (1981) *Riftia pachyptila* Jones: Observations on the Vestimentiferan Worm from the Galapagos Rift. *Science* **213**: 333-336.

- Juniper, S.K., and Tebo, B.M. (1995) Microbe-Metal Interactions and Mineral Deposition at Hydrothermal Vents. In *The Microbiology of Deep-Sea Hydrothermal Vents*. Karl, D.M. (ed). Boca Raton, FL: CRC Press, pp. 219-253.
- Kallmeyer, J., and Boetius, A. (2004) Effects of temperature and pressure on sulfate reduction and anaerobic oxidation of methane in hydrothermal sediments of Guaymas Basin. *Appl Environ Microbiol* **70**: 1231-1233.
- Karl, D.M. (ed) (1995a) *The Microbiology of Deep-Sea Hydrothermal Vents*. Boca Raton, FL: CRC Press.
- Karl, D.M. (1995b) Ecology of Free-Living, Hydrothermal Vent Microbial Communities. In *The Microbiology of Deep-Sea Hydrothermal Vents*. Karl, D.M. (ed). Boca Raton, FL: CRC Press, pp. 35-124.
- Kato, S., Takano, Y., Kakegawa, T., Oba, H., Inoue, K., Kobayashi, C. *et al.* (2010) Biogeography and biodiversity in sulfide structures of active and inactive vents at deep-sea hydrothermal fields of the Southern Mariana Trough. *Appl Environ Microbiol* **76**: 2968-2979.
- Kelley, D.S., Karson, J.A., Blackman, D.K., Fruh-Green, G.L., Butterfield, D.A., Lilley, M.D. *et al.* (2001) An off-axis hydrothermal vent field near the Mid-Atlantic Ridge at 30 degrees N. *Nature* **412**: 145-149.
- Kim, Y.J., Lee, H.S., Kim, E.S., Bae, S.S., Lim, J.K., Matsumi, R. *et al.* (2010) Formate-driven growth coupled with H₂ production. *Nature* **467**: 352-355.
- Kimura, H., Mori, K., Tashiro, T., Kato, K., Yamanaka, T., Ishibashi, J.I., and Hanada, S. (2010) Culture-Independent Estimation of Optimal and Maximum Growth

- Temperatures of Archaea in Subsurface Habitats Based on the G plus C Content in 16S rRNA Gene Sequences. *Geomicrobiology Journal* **27**: 114-122.
- Kormas, K.A., Tivey, M.K., Von Damm, K., and Teske, A. (2006) Bacterial and archaeal phylotypes associated with distinct mineralogical layers of a white smoker spire from a deep-sea hydrothermal vent site (9 degrees N, East Pacific Rise). *Environ Microbiol* **8**: 909-920.
- Lane, D.J. (1991) 16S/23S rRNA Sequencing. In *Nucleic Acid Techniques in Bacterial Systematics*. Stackebrandt, E., and Goodfellow, M. (eds). Chichester, West Sussex: John Wiley & Sons Ltd., pp. 115-148.
- Langmuir, C., Humphris, S., Fornari, D., VanDover, C., VonDamm, K., Tivey, M.K. *et al.* (1997) Hydrothermal vents near a mantle hot spot: The Lucky Strike vent field at 37 degrees N on the Mid-Atlantic Ridge. *Earth and Planetary Science Letters* **148**: 69-91.
- Lee, H.S., Kang, S.G., Bae, S.S., Lim, J.K., Cho, Y., Kim, Y.J. *et al.* (2008) The complete genome sequence of *Thermococcus onnurineus* NA1 reveals a mixed heterotrophic and carboxydophilic metabolism. *Journal of Bacteriology* **190**: 7491-7499.
- Longnecker, K., and Reysenbach, A. (2001) Expansion of the geographic distribution of a novel lineage of *epsilon-Proteobacteria* to a hydrothermal vent site on the Southern East Pacific Rise. *FEMS Microbiol Ecol* **35**: 287-293.

- Lozupone, C., Hamady, M., and Knight, R. (2006) UniFrac--an online tool for comparing microbial community diversity in a phylogenetic context. *BMC Bioinformatics* **7**: 371.
- Ludwig, W., Strunk, O., Westram, R., Richter, L., Meier, H., Yadhukumar *et al.* (2004) ARB: a software environment for sequence data. *Nucleic Acids Res* **32**: 1363-1371.
- Marmur, J., and Doty, P. (1962) Determination of the base composition of deoxyribonucleic acid from its thermal denaturation temperature. *Journal of Molecular Biology* **5**: 109-118.
- Marques, A.F.A., Barriga, F., Chavagnac, V., and Fouquet, Y. (2006) Mineralogy, geochemistry, and Nd isotope composition of the Rainbow hydrothermal field, Mid-Atlantic Ridge. *Mineralium Deposita* **41**: 52-67.
- Martinez, F., Okino, K., Ohara, Y., Reysenbach, A.-L., and Goffredi, S.K. (2007) Back-arc basins. *Oceanography* **20**: 116-127.
- McCliment, E.A., Voglesonger, K.M., O'Day, P.A., Dunn, E.E., Holloway, J.R., and Cary, S.C. (2006) Colonization of nascent, deep-sea hydrothermal vents by a novel Archaeal and Nanoarchaeal assemblage. *Environ Microbiol* **8**: 114-125.
- McCollom, T.M. (2000) Geochemical constraints on primary productivity in submarine hydrothermal vent plumes. *Deep Sea Research Part I: Oceanographic Research Papers* **47**: 85-101.

- McCollom, T.M. (2007) Geochemical constraints on sources of metabolic energy for chemolithoautotrophy in ultramafic-hosted deep-sea hydrothermal systems. *Astrobiology* **7**: 933-950.
- McCollom, T.M., and Shock, E.L. (1997) Geochemical constraints on chemolithoautotrophic metabolism by microorganisms in seafloor hydrothermal systems. *Geochimica Et Cosmochimica Acta* **61**: 4375-4391.
- Minic, Z., and Herve, G. (2004) Biochemical and enzymological aspects of the symbiosis between the deep-sea tubeworm *Riftia pachyptila* and its bacterial endosymbiont. *Eur J Biochem* **271**: 3093-3102.
- Miroshnichenko, M., Kostrikina, N., L'Haridon, S., Jeanthon, C., Hippe, H., Stackebrandt, E., and Bonch-Osmolovskaya, E. (2002) *Nautilia lithotrophica* gen. nov., sp. nov., a thermophilic sulfur-reducing epsilon-proteobacterium isolated from a deep-sea hydrothermal vent. *International Journal of Systematic and Evolutionary Microbiology* **52**: 1299-1304.
- Miroshnichenko, M.L., and Bonch-Osmolovskaya, E.A. (2006) Recent developments in the thermophilic microbiology of deep-sea hydrothermal vents. *Extremophiles* **10**: 85-96.
- Miroshnichenko, M.L., Rainey, F.A., Rhode, M., and Bonch-Osmolovskaya, E.A. (1999) *Hippea maritima* gen. nov., sp. nov., a new genus of thermophilic, sulfur-reducing bacterium from submarine hot vents. *Int J Syst Bacteriol* **49**: 1033-1038.

- Miroshnichenko, M.L., Rainey, F.A., Hippe, H., Chernyh, N.A., Kostrikina, N.A., and Bonch-Osmolovskaya, E.A. (1998) *Desulfurella kamchatkensis* sp. nov. and *Desulfurella propionica* sp. nov., new sulfur-respiring thermophilic bacteria from Kamchatka thermal environments. *Int J Syst Bacteriol* **48**: 475-479.
- Miroshnichenko, M.L., L'Haridon, S., Schumann, P., Spring, S., Bonch-Osmolovskaya, E.A., Jeanthon, C., and Stackebrandt, E. (2004) *Caminibacter profundus* sp. nov., a novel thermophile of *Nautiliales* ord. nov. within the class 'Epsilonproteobacteria', isolated from a deep-sea hydrothermal vent. *Int J Syst Evol Microbiol* **54**: 41-45.
- Mottl, M., Seewald, J., Wheat, C., Tivey, M., Michael, P., Proskurowski, G. *et al.* (2011) Chemistry of hot springs along the Eastern Lau Spreading Center. *Geochimica Et Cosmochimica Acta* **75**: 1013-1038.
- Moussard, H., Moreira, D., Cambon-Bonavita, M., López-García, P., and Jeanthon, C. (2006a) Uncultured Archaea in a hydrothermal microbial assemblage: phylogenetic diversity and characterization of a genome fragment from a euryarchaeote. *FEMS microbiology ecology* **57**: 452-469.
- Moussard, H., Henneke, G., Moreira, D., Jouffe, V., Lopez-Garcia, P., and Jeanthon, C. (2006b) Thermophilic lifestyle for an uncultured archaeon from hydrothermal vents: evidence from environmental genomics. *Appl Environ Microbiol* **72**: 2268-2271.
- Moussard, H., L'Haridon, S., Tindall, B.J., Banta, A., Schumann, P., Stackebrandt, E. *et al.* (2004) *Thermodesulfator indicus* gen. nov., sp. nov., a novel thermophilic

- chemolithoautotrophic sulfate-reducing bacterium isolated from the Central Indian Ridge. *Int J Syst Evol Microbiol* **54**: 227-233.
- Nakagawa, S., Inagaki, F., Takai, K., Horikoshi, K., and Sako, Y. (2005a) *Thioreductor micantisoli* gen. nov., sp. nov., a novel mesophilic, sulfur-reducing chemolithoautotroph within the *epsilon-Proteobacteria* isolated from hydrothermal sediments in the Mid-Okinawa Trough. *Int J Syst Evol Microbiol* **55**: 599-605.
- Nakagawa, S., Takai, K., Inagaki, F., Horikoshi, K., and Sako, Y. (2005b) *Nitratiruptor tergarcus* gen. nov., sp. nov. and *Nitratifactor salsuginis* gen. nov., sp. nov., nitrate-reducing chemolithoautotrophs of the *epsilon-Proteobacteria* isolated from a deep-sea hydrothermal system in the Mid-Okinawa Trough. *Int J Syst Evol Microbiol* **55**: 925-933.
- Nakagawa, S., Takai, K., Inagaki, F., Hirayama, H., Nunoura, T., Horikoshi, K., and Sako, Y. (2005c) Distribution, phylogenetic diversity and physiological characteristics of *epsilon-Proteobacteria* in a deep-sea hydrothermal field. *Environ Microbiol* **7**: 1619-1632.
- Nakagawa, S., Takai, K., Inagaki, F., Chiba, H., Ishibashi, J., Kataoka, S. *et al.* (2005d) Variability in microbial community and venting chemistry in a sediment-hosted backarc hydrothermal system: Impacts of subseafloor phase-separation. *FEMS Microbiol Ecol* **54**: 141-155.
- Nakagawa, T., Takai, K., Suzuki, Y., Hirayama, H., Konno, U., Tsunogai, U., and Horikoshi, K. (2006) Geomicrobiological exploration and characterization of a

- novel deep-sea hydrothermal system at the TOTO caldera in the Mariana Volcanic Arc. *Environ Microbiol* **8**: 37-49.
- Nawrocki, E.P., Kolbe, D.L., and Eddy, S.R. (2009) Infernal 1.0: inference of RNA alignments. *Bioinformatics* **25**: 1335-1337.
- Nelson, D.C., Wirsén, C.O., and Jannasch, H.W. (1989) Characterization of large, autotrophic *Beggiatoa* spp. abundant at hydrothermal vents of the Guaymas Basin. *Appl Environ Microbiol* **55**: 2909-2917.
- Nercessian, O., Reysenbach, A.L., Prieur, D., and Jeanthon, C. (2003) Archaeal diversity associated with in situ samplers deployed on hydrothermal vents on the East Pacific Rise (13 degrees N). *Environ Microbiol* **5**: 492-502.
- Nunoura, T., and Takai, K. (2009) Comparison of microbial communities associated with phase-separation-induced hydrothermal fluids at the Yonaguni Knoll IV hydrothermal field, the Southern Okinawa Trough. *FEMS Microbiol Ecol* **67**: 351-370.
- Nunoura, T., Oida, H., Nakaseama, M., Kosaka, A., Ohkubo, S.B., Kikuchi, T. *et al.* (2010) Archaeal diversity and distribution along thermal and geochemical gradients in hydrothermal sediments at the Yonaguni Knoll IV hydrothermal field in the Southern Okinawa trough. *Appl Environ Microbiol* **76**: 1198-1211.
- Omer, A.D., Lowe, T.M., Russell, A.G., Ebhardt, H., Eddy, S.R., and Dennis, P.P. (2000) Homologs of small nucleolar RNAs in Archaea. *Science* **288**: 517-522.

- Opatkiewicz, A.D., Butterfield, D.A., and Baross, J.A. (2009) Individual hydrothermal vents at Axial Seamount harbor distinct seafloor microbial communities. *Fems Microbiology Ecology* **70**: 413-424.
- Page, A., Tivey, M.K., Stakes, D.S., and Reysenbach, A.L. (2008) Temporal and spatial archaeal colonization of hydrothermal vent deposits. *Environ Microbiol* **10**: 874-884.
- Papke, R.T., Ramsing, N.B., Bateson, M.M., and Ward, D.M. (2003) Geographical isolation in hot spring cyanobacteria. *Environ Microbiol* **5**: 650-659.
- Perner, M., Kuever, J., Seifert, R., Pape, T., Koschinsky, A., Schmidt, K. *et al.* (2007) The influence of ultramafic rocks on microbial communities at the Logatchev hydrothermal field, located 15 degrees N on the Mid-Atlantic Ridge. *FEMS Microbiol Ecol* **61**: 97-109.
- Prokofeva, M., Miroshnichenko, M., Kostrikina, N., Chernyh, N., Kuznetsov, B., Tourova, T., and Bonch-Osmolovskaya, E. (2000) *Acidilobus aceticus* gen. nov., sp. nov., a novel anaerobic thermoacidophilic archaeon from continental hot vents in Kamchatka. *Int J Syst Evol Microbiol* **50**: 2001.
- Prokofeva, M.I., Kostrikina, N.A., Kolganova, T.V., Tourova, T.P., Lysenko, A.M., Lebedinsky, A.V., and Bonch-Osmolovskaya, E.A. (2009) Isolation of the anaerobic thermoacidophilic crenarchaeote *Acidilobus saccharovorans* sp. nov. and proposal of *Acidilobales* ord. nov., including *Acidilobaceae* fam. nov. and *Caldisphaeraceae* fam. nov. *Int J Syst Evol Microbiol* **59**: 3116-3122.

- Pruesse, E., Quast, C., Knittel, K., Fuchs, B.M., Ludwig, W., Peplies, J., and Glockner, F.O. (2007) SILVA: a comprehensive online resource for quality checked and aligned ribosomal RNA sequence data compatible with ARB. *Nucleic Acids Res* **35**: 7188-7196.
- Quince, C., Lanzen, A., Davenport, R., and Turnbaugh, P. (2011) Removing noise from pyrosequenced amplicons. *BMC Bioinformatics* **12**: 38.
- Ramirez-Llodra, E., Shank, T.M., and German, C.R. (2007) Biodiversity and biogeography of hydrothermal vent species. *Oceanography* **20**: 30-41.
- Reno, M.L., Held, N.L., Fields, C.J., Burke, P.V., and Whitaker, R.J. (2009) Biogeography of the *Sulfolobus islandicus* pan-genome. *Proc Natl Acad Sci U S A* **106**: 8605-8610.
- Reysenbach, A.-L., Götz, D., and Yernool, D. (2002) Microbial diversity of marine and terrestrial thermal springs. In *Biodiversity of Microbial Life*. Staley, J.T., and Reysenbach, A.-L. (eds). New York: Wiley-Liss, Inc., pp. 345-421.
- Reysenbach, A.L., and Flores, G.E. (2008) Electron microscopy encounters with unusual thermophiles helps direct genomic analysis of *Aciduliprofundum boonei*. *Geobiology* **6**: 331-336.
- Reysenbach, A.L., Longnecker, K., and Kirshtein, J. (2000) Novel bacterial and archaeal lineages from an in situ growth chamber deployed at a Mid-Atlantic Ridge hydrothermal vent. *Appl Environ Microbiol* **66**: 3798-3806.

- Reysenbach, A.L., Liu, Y., Banta, A.B., Beveridge, T.J., Kirshtein, J.D., Schouten, S. *et al.* (2006) A ubiquitous thermoacidophilic archaeon from deep-sea hydrothermal vents. *Nature* **442**: 444-447.
- Rinker, K.D., and Kelly, R.M. (2000) Effect of carbon and nitrogen sources on growth dynamics and exopolysaccharide production for the hyperthermophilic archaeon *Thermococcus litoralis* and bacterium *Thermotoga maritima*. *Biotechnology and Bioengineering* **69**: 537-547.
- Rogers, D.R., Santelli, C.M., and Edwards, K.J. (2003) Geomicrobiology of deep sea deposits: estimating community diversity from low temperature seafloor rocks and minerals. *Geobiology* **1**: 109-117.
- Rouxel, O., Fouquet, Y., and Ludden, J.N. (2004a) Copper isotope systematics of the Lucky Strike, Rainbow, and Logatchev sea-floor hydrothermal fields on the Mid-Atlantic Ridge. *Economic Geology and the Bulletin of the Society of Economic Geologists* **99**: 585-600.
- Rouxel, O., Fouquet, Y., and Ludden, J.N. (2004b) Subsurface processes at the Lucky Strike hydrothermal field, Mid-Atlantic Ridge: Evidence from sulfur, selenium, and iron isotopes. *Geochimica Et Cosmochimica Acta* **68**: 2295-2311.
- Ruan, Q., Dutta, D., Schwalbach, M.S., Steele, J.A., Fuhrman, J.A., and Sun, F. (2006) Local similarity analysis reveals unique associations among marine bacterioplankton species and environmental factors. *Bioinformatics* **22**: 2532-2538.

- Sako, Y., Nomura, N., Uchida, A., Ishida, Y., Morii, H., Koga, Y. *et al.* (1996) *Aeropyrum pernix* gen. nov., sp. nov., a novel aerobic hyperthermophilic archaeon growing at temperatures up to 100 degrees C. *International journal of systematic bacteriology* **46**: 1070-1077.
- Sarrazin, J., and Juniper, S.K. (1999) Biological characteristics of a hydrothermal edifice mosaic community. *Marine Ecology-Progress Series* **185**: 1-19.
- Schloss, P. (2010) The effects of alignment quality, distance calculation method, sequence filtering, and region on the analysis of 16S rRNA gene-based studies. *PLoS Comput Biol* **6**: e1000844.
- Schmidt, K., Koschinsky, A., Garbe-Schonberg, D., de Carvalho, L.M., and Seifert, R. (2007) Geochemistry of hydrothermal fluids from the ultramafic-hosted Logatchev hydrothermal field, 15 degrees N on the Mid-Atlantic Ridge: Temporal and spatial investigation. *Chemical Geology* **242**: 1-21.
- Schrenk, M.O., Kelley, D.S., Delaney, J.R., and Baross, J.A. (2003) Incidence and diversity of microorganisms within the walls of an active deep-sea sulfide chimney. *Appl Environ Microbiol* **69**: 3580-3592.
- Seewald, J.S., Zolotov, M.Y., and McCollom, T. (2006) Experimental investigation of single carbon compounds under hydrothermal conditions. *Geochimica Et Cosmochimica Acta* **70**: 446-460.
- Seewald, J.S., Doherty, K.W., Hammar, T.R., and Liberatore, S.P. (2002) A new gas-tight isobaric sampler for hydrothermal fluids. *Deep-Sea Research Part I-Oceanographic Research Papers* **49**: 189-196.

- Seyfried, W., Pester, N.J., Ding, K., and Rough, M. (2011) Vent fluid chemistry of the Rainbow Hydrothermal System (36° N, MAR): Phase equilibria and in-situ pH controls on seafloor alteration processes. *Geochimica Et Cosmochimica Acta* **75**: 1574-1593.
- Seyfried, W.E., Jr., and Mottl, M.J. (1995) Geologic setting and chemistry of deep-sea hydrothermal vents. In *The Microbiology of Deep-Sea Hydrothermal Vents*. Karl, D.M. (ed). Boca Raton, FL: CRC Press, pp. 1-34.
- Shannon, P., Markiel, A., Ozier, O., Baliga, N.S., Wang, J.T., Ramage, D. *et al.* (2003) Cytoscape: a software environment for integrated models of biomolecular interaction networks. *Genome Res* **13**: 2498-2504.
- Shock, E.L., and Holland, M.E. (2004) Geochemical energy sources that support the subsurface biosphere. In *Seafloor biosphere at Mid-Ocean Ridges*. Wilcock, W., Cary, C., DeLong, E., Kelley, D., and Baross, J. (eds). Washington, DC: American Geophysical Union, pp. 153-165.
- Shock, E.L., McCollom, T., and Schulte, M.D. (1995) Geochemical constraints on chemolithoautotrophic reactions in hydrothermal systems. *Origins of Life and Evolution of the Biosphere* **25**: 141-159.
- Singh, S.C., Crawford, W.C., Carton, H., Seher, T., Combier, V., Cannat, M. *et al.* (2006) Discovery of a magma chamber and faults beneath a Mid-Atlantic Ridge hydrothermal field. *Nature* **442**: 1029-1032.
- Smith, J.L., Campbell, B.J., Hanson, T.E., Zhang, C.L., and Cary, S.C. (2008) *Nautilia profundicola* sp. nov., a thermophilic, sulfur-reducing epsilonproteobacterium

- from deep-sea hydrothermal vents. *International Journal of Systematic and Evolutionary Microbiology* **58**: 1598-1602.
- Sogin, M.L., Morrison, H.G., Huber, J.A., Mark Welch, D., Huse, S.M., Neal, P.R. *et al.* (2006) Microbial diversity in the deep sea and the underexplored "rare biosphere". *Proc Natl Acad Sci U S A* **103**: 12115-12120.
- Stamatakis, A. (2006) RAxML-VI-HPC: maximum likelihood-based phylogenetic analyses with thousands of taxa and mixed models. *Bioinformatics* **22**: 2688-2690.
- Stetter, K. (1988) *Archaeoglobus fulgidus* gen. nov., sp. nov.: A new taxon of extremely thermophilic archaebacteria. *Systematic and applied microbiology* **10**: 172-173.
- Stott, M.B., Saito, J.A., Crowe, M.A., Dunfield, P.F., Hou, S., Nakasone, E. *et al.* (2008) Culture-independent characterization of a novel microbial community at a hydrothermal vent at Brothers volcano, Kermadec arc, New Zealand. *Journal of Geophysical Research-Solid Earth* **113**: B08S06.
- Sunamura, M., Higashi, Y., Miyako, C., Ishibashi, J., and Maruyama, A. (2004) Two bacteria phylotypes are predominant in the Suiyo seamount hydrothermal plume. *Appl Environ Microbiol* **70**: 1190-1198.
- Suzuki, M.T., and Giovannoni, S.J. (1996) Bias caused by template annealing in the amplification of mixtures of 16S rRNA genes by PCR. *Appl Environ Microbiol* **62**: 625-630.

- Suzuki, Y., Inagaki, F., Takai, K., Nealson, K.H., and Horikoshi, K. (2004) Microbial diversity in inactive chimney structures from deep-sea hydrothermal systems. *Microb Ecol* **47**: 186-196.
- Takai, K., and Horikoshi, K. (1999) Genetic diversity of archaea in deep-sea hydrothermal vent environments. *Genetics* **152**: 1285-1297.
- Takai, K., and Horikoshi, K. (2000a) Rapid detection and quantification of members of the archaeal community by quantitative PCR using fluorogenic probes. *Appl Environ Microbiol* **66**: 5066-5072.
- Takai, K., and Horikoshi, K. (2000b) *Thermosipho japonicus* sp. nov., an extremely thermophilic bacterium isolated from a deep-sea hydrothermal vent in Japan. *Extremophiles* **4**: 9-17.
- Takai, K., and Nakamura, K. (2010) Compositional, physiological and metabolic variability in microbial communities associated with geochemically diverse, deep-sea hydrothermal vent fluids. *Geomicrobiology: Molecular and Environmental Perspective*: 251-283.
- Takai, K., Inoue, A., and Horikoshi, K. (2002) *Methanothermococcus okinawensis* sp. nov., a thermophilic, methane-producing archaeon isolated from a Western Pacific deep-sea hydrothermal vent system. *Int J Syst Evol Microbiol* **52**: 1089-1095.
- Takai, K., Sugai, A., Itoh, T., and Horikoshi, K. (2000) *Palaeococcus ferrophilus* gen. nov., sp. nov., a barophilic, hyperthermophilic archaeon from a deep-sea hydrothermal vent chimney. *Int J Syst Evol Microbiol* **50**: 489-500.

- Takai, K., Komatsu, T., Inagaki, F., and Horikoshi, K. (2001) Distribution of Archaea in a black smoker chimney structure. *Appl Environ Microbiol* **67**: 3618-3629.
- Takai, K., Nakagawa, T., Reysenbach, A.L., and Hoek, J. (2006a) Microbial ecology of Mid-Ocean Ridges and Back-Arc Basins. In *Back-Arc Spreading Systems: geological, biological, chemical, and physical interactions*. Christie, D.M., Fisher, C.R., Sang-Mook, L., and Givens, S. (eds). Washington, DC: American Geophysical Union, pp. 185-213.
- Takai, K., Hirayama, H., Nakagawa, T., Suzuki, Y., Nealson, K.H., and Horikoshi, K. (2004a) *Thiomicrospira thermophila* sp. nov., a novel microaerobic, thermotolerant, sulfur-oxidizing chemolithomixotroph isolated from a deep-sea hydrothermal fumarole in the TOTO caldera, Mariana Arc, Western Pacific. *Int J Syst Evol Microbiol* **54**: 2325-2333.
- Takai, K., Hirayama, H., Nakagawa, T., Suzuki, Y., Nealson, K.H., and Horikoshi, K. (2005) *Lebetimonas acidiphila* gen. nov., sp. nov., a novel thermophilic, acidophilic, hydrogen-oxidizing chemolithoautotroph within the 'Epsilonproteobacteria', isolated from a deep-sea hydrothermal fumarole in the Mariana Arc. *Int J Syst Evol Microbiol* **55**: 183-189.
- Takai, K., Nakamura, K., Suzuki, K., Inagaki, F., Nealson, K., and Kumagai, H. (2006b) Ultramafics-Hydrothermalism-Hydrogenesis-HyperSLiME (UltraH3) linkage: a key insight into early microbial ecosystem in the Archean deep-sea hydrothermal systems. *Paleontological Research* **10**: 269-282.

- Takai, K., Gamo, T., Tsunogai, U., Nakayama, N., Hirayama, H., Nealson, K.H., and Horikoshi, K. (2004b) Geochemical and microbiological evidence for a hydrogen-based, hyperthermophilic subsurface lithoautotrophic microbial ecosystem (HyperSLiME) beneath an active deep-sea hydrothermal field. *Extremophiles* **8**: 269-282.
- Takai, K., Inagaki, F., Nakagawa, S., Hirayama, H., Nunoura, T., Sako, Y. *et al.* (2003) Isolation and phylogenetic diversity of members of previously uncultivated *epsilon-Proteobacteria* in deep-sea hydrothermal fields. *FEMS Microbiol Lett* **218**: 167-174.
- Takai, K., Nunoura, T., Ishibashi, J., Lupton, J., Suzuki, R., Hamasaki, H. *et al.* (2008) Variability in the microbial communities and hydrothermal fluid chemistry at the newly discovered Mariner hydrothermal field, southern Lau Basin. *Journal of Geophysical Research* **113**: G02031.
- Tamura, K., Dudley, J., Nei, M., and Kumar, S. (2007) MEGA4: Molecular Evolutionary Genetics Analysis (MEGA) software version 4.0. *Mol Biol Evol* **24**: 1596-1599.
- Tazumi, A., Kakinuma, Y., Misawa, N., Moore, J.E., Millar, B.C., and Matsuda, M. (2009) Identification and characterization of intervening sequences within 23S rRNA genes from more than 200 *Campylobacter* isolates from seven species including atypical campylobacters. *BMC Microbiol* **9**: 256.
- Tazumi, A., Nakanishi, S., Meguro, S., Kakinuma, Y., Moore, J.E., Millar, B.C., and Matsuda, M. (2010) Occurrence and characterisation of intervening sequences

- (IVSs) within 16S rRNA genes from two atypical *Campylobacter* species, *C. sputorum* and *C. curvus*. *Br J Biomed Sci* **67**: 77-81.
- Teyssier, C., Marchandin, H., Simeon De Buochberg, M., Ramuz, M., and Jumas-Bilak, E. (2003) Atypical 16S rRNA gene copies in *Ochrobactrum intermedium* strains reveal a large genomic rearrangement by recombination between *rrn* copies. *J Bacteriol* **185**: 2901-2909.
- Tivey, M., Craddock, P., Seewald, J., Ferrini, V., Kim, S., Mottl, M. *et al.* (2005) Characterization of six vent fields within the Lau Basin. In *American Geophysical Union, Fall meeting*: American Geophysical Union, pp. T31A-0477.
- Tivey, M.K. (2004) Environmental conditions within active seafloor vent structures: sensitivity to vent fluid composition and fluid flow. In *Subseafloor Biosphere at Mid-Ocean Ridges*. Wilcock, W., Cary, C., DeLong, E., Kelley, D., and Baross, J. (eds). Washington, DC: American Geophysical Union, pp. 137-152.
- Tivey, M.K. (2007) Generation of seafloor hydrothermal vent fluids and associated mineral deposits. *Oceanography* **20**: 50-65.
- Tor, J.M., Kashefi, K., and Lovley, D.R. (2001) Acetate oxidation coupled to Fe (III) reduction in hyperthermophilic microorganisms. *Applied and Environmental Microbiology* **67**: 1363-1365.
- Van Dover, C.L. (2000) *The Ecology of Dee-Sea Hydrothermal Vents*. Princeton, New Jersey: Princeton University Press.

- Van Dover, C.L., Reynolds, G.T., Chave, A.D., and Tyson, J.A. (1996) Light at deep-sea hydrothermal vents. *Geophysical research letters* **23**: 2049-2052.
- Vannier, P., Marteinsson, V.T., Fridjonsson, O.H., Oger, P., and Jebbar, M. (2011) Complete genome sequence of the hyperthermophilic piezophilic, heterotrophic and carboxydophilic archaeon *Thermococcus barophilus* MP. *Journal of bacteriology*: JB. 01490-01410v01491.
- Villemur, R., Constant, P., Gauthier, A., Shareck, M., and Beaudet, R. (2007) Heterogeneity between 16S ribosomal RNA gene copies borne by one *Desulfotobacterium* strain is caused by different 100-200 bp insertions in the 5' region. *Can J Microbiol* **53**: 116-128.
- Von Damm, K., Bray, A., Buttermore, L., and Oosting, S. (1998) The geochemical controls on vent fluids from the Lucky Strike vent field, Mid-Atlantic Ridge. *Earth and Planetary Science Letters* **160**: 521-536.
- Von Damm, K.L. (1995) Controls on the chemistry and temporal variability of seafloor hydrothermal fluids. In *Seafloor Hydrothermal Systems: Physical, Chemical, Biological, and Geological Interactions*. Humphris, S.E., Zierenberg, R. A., Mullineaux, L. S., Thomson, R. E. (ed). Washington, DC: American Geophysical Union, pp. 222-247.
- Voordeckers, J.W., Starovoytov, V., and Vetriani, C. (2005) *Caminibacter mediatlanticus* sp. nov., a thermophilic, chemolithoautotrophic, nitrate-ammonifying bacterium isolated from a deep-sea hydrothermal vent on the Mid-Atlantic Ridge. *Int J Syst Evol Microbiol* **55**: 773-779.

- Voordeckers, J.W., Do, M.H., Hugler, M., Ko, V., Sievert, S.M., and Vetriani, C. (2008) Culture dependent and independent analyses of 16S rRNA and ATP citrate lyase genes: a comparison of microbial communities from different black smoker chimneys on the Mid-Atlantic Ridge. *Extremophiles* **12**: 627-640.
- Wang, Q., Garrity, G.M., Tiedje, J.M., and Cole, J.R. (2007) Naive Bayesian classifier for rapid assignment of rRNA sequences into the new bacterial taxonomy. *Appl Environ Microbiol* **73**: 5261-5267.
- Whitaker, R.J., Grogan, D.W., and Taylor, J.W. (2003) Geographic barriers isolate endemic populations of hyperthermophilic archaea. *Science* **301**: 976-978.
- White, J.R., Navlakha, S., Nagarajan, N., Ghodsi, M.R., Kingsford, C., and Pop, M. (2010) Alignment and clustering of phylogenetic markers--implications for microbial diversity studies. *BMC Bioinformatics* **11**: 152.
- Wilson, T., Amirbahman, A., Norton, S., and Voytek, M. (2010) A record of phosphorus dynamics in oligotrophic lake sediment. *Journal of Paleolimnology* **44**: 279-294.
- Winn, C.D., Cowen, J.P., and Karl, D.M. (1995) Microbes in deep-sea hydrothermal plumes. In *The Microbiology of Deep-Sea Hydrothermal Vents*. Karl, D.M. (ed). New York, NY: CRC Press, pp. 255-273.
- Yurkov, V., and Beatty, J.T. (1998) Isolation of aerobic anoxygenic photosynthetic bacteria from black smoker plume waters of the Juan de Fuca ridge in the Pacific ocean. *Appl Environ Microbiol* **64**: 337-341.

Zhou, H., Li, J., Peng, X., Meng, J., Wang, F., and Ai, Y. (2009) Microbial diversity of a sulfide black smoker in main endeavour hydrothermal vent field, Juan de Fuca Ridge. *The Journal of Microbiology* **47**: 235-247.

Zivanovic, Y., Armengaud, J., Lagorce, A., Leplat, C., Guérin, P., Dutertre, M. *et al.* (2009) Genome analysis and genome-wide proteomics of *Thermococcus gammatolerans*, the most radioresistant organism known amongst the Archaea. *Genome Biol* **10**: R70.

Appendix A: *Sulfurihydrogenibium kristjanssonii* sp. nov., a hydrogen and sulfur-oxidizing thermophile isolated from a terrestrial Icelandic hot spring.

Flores, GE, Liu, Y, Ferrera, I, Beveridge, TJ and Reysenbach, A-L (2008) *International Journal of Systematic and Evolutionary Microbiology* **58**: 1153-1158.

Summary

Three thermophilic, aerobic, hydrogen- and sulfur-oxidizing bacteria were isolated from an Icelandic hot spring near the town of Hveragerdi and were determined to share >99% 16S rRNA gene sequence similarity. One of these isolates, designated strain I6628^T, was selected for further characterization. Strain I6628^T is a motile rod, 1.5–2.5 µm long and about 0.5 µm wide. Growth occurred between 40 and 73°C (optimally at 68°C), at pH 5.3–7.8 (optimally at pH 6.6) and at NaCl concentrations between 0 and 0.5% (w/v). Strain I6628^T grew with H₂, S⁰ or S₂O₃²⁻ as an electron donor with O₂ (up to 25%, v/v; optimally at 4–9%) as the sole electron acceptor. CO₂ and succinate were utilized as carbon sources but no organic compounds, including succinate, could be used as an energy source. The G+C content of the genomic DNA was determined to be 28.1 mol%. Phylogenetic analysis of the 16S rRNA gene sequence indicated that strain I6628^T is a member of the genus *Sulfurihydrogenibium*, the closest cultivated relative being the recently described strain *Sulfurihydrogenibium rodmanii* UZ3-5^T (98.2% sequence similarity). On the basis of the physiology and

phylogeny of this organism, strain I6628^T represents a novel species of the genus *Sulfurihydrogenibium*, for which the name *Sulfurihydrogenibium kristjanssonii* sp. nov. is proposed. The type strain is I6628T (=DSM 19534^T =OCM 901^T =ATCC BAA-1535^T).

**Appendix B: Electron microscopy encounters with unusual thermophiles helps
direct genomic analysis of *Aciduliprofundum boonei*.**

Reysenbach, A-L and Flores, GE (2008) *Geobiology* **6**: 331-336.

Abstract

Terry Beveridge's enthusiasm about the ingenuity of microorganisms has stimulated many new avenues of microbial research. One example where Terry's observations helped direct the scientific process was in the analysis of the draft genome of the thermoacidophilic archaeum, *Aciduliprofundum boonei*. This deep-sea vent heterotroph ferments peptides as its primary metabolic pathway, using numerous enzymes encoding for proteolytic or peptidolytic activities. An almost complete modified Embden–Meyerhof–Parnas pathway operates in the gluconeogenic direction. Terry was particularly intrigued by the S-layer and flagellum of *A. boonei*. Although only putative genes for the S-layer protein could be identified, several genes encoding for glycosyl transferases were located in the draft genome that could glycosylate the S-layer proteins and protect the proteins from the acidic environment. Furthermore, *A. boonei* possesses a unique organization to its flagellum genes and may represent a third organizational type within the Archaea.

Appendix C: Summary of MAR 16S rRNA gene clones

All archaeal and bacterial sequences have been deposited to GenBank under accession numbers HQ893885-HQ894378. Files are archived in the share_alrlab\MAR08 Clones on the PSU research server.

Table 1: Summary of archaeal clones detected in deposits from the Mid-Atlantic Ridge. Classifications were made using the RDP-classifier.

Taxa affiliation	Archaeal Clone Frequency (%)									
	Rb-2		Rb-5		Rb-6		LS-7		TAG-13	
<i>Euryarchaeota</i>										
Unclassified	4	(5.80)					7	(28.00)		
<i>Archaeoglobi</i>										
<i>Archaeoglobales</i>										
Unclassified			1	(1.85)	1	(1.47)				
<i>Archaeoglobaceae</i>										
<i>Archaeoglobus</i>	40	(57.97)	29	(53.70)	38	(55.88)	12	(48.00)	49	(94.23)
<i>Geoglobus</i>	2	(2.90)							3	(5.77)
<i>Methanococci</i>										
<i>Methanococcales</i>										
<i>Methanocaldococcaceae</i>										
<i>Methanocaldococcus</i>	14	(20.29)	3	(5.56)	4	(5.88)				
<i>Methanococcaceae</i>										
<i>Methanothermococcus</i>	2	(2.90)	5	(9.26)	1	(1.47)				
<i>Thermococci</i>										
<i>Thermococcales</i>										
<i>Thermococcaceae</i>										
Unclassified	1	(1.45)								
<i>Thermococcus</i>	4	(5.80)	14	(25.93)	24	(35.29)	1	(4.00)		
'Aciduliprofundales'							3	(12.00)		
<i>Chrenarchaeota</i>										
<i>Thermoprotei</i>										
Unclassified							1	(4.00)		
<i>Desulfurococcales</i>										
Unclassified	1	(1.45)								
<i>Desulfurococcaceae</i>										
<i>Aeropyrum</i>	1	(1.45)					1	(4.00)		
<i>Staphylothermus</i>			2	(3.70)						
Total	69		54		68		25		52	

Table 2. Summary of bacterial clones detected in deposits from the Mid-Atlantic Ridge. Classifications were made using the RDP-classifier.

Taxa affiliation	Bacterial Clone Frequency (%)				
	Rb-2	Rb-5	Rb-6	LS-7	TAG-13
<i>Aquificae</i>					
<i>Aquificales</i>					
<i>Caldithrix</i>	1 (1.96)				
<i>Thermovibrio</i>					1 (1.75)
<i>Bacteroidetes</i>					
Unclassified	1 (1.96)	1 (2.50)		4 (6.67)	1 (1.75)
<i>Flavobacteria</i>					
<i>Flavobacteriales</i>					
<i>Flavobacteriaceae</i>		1 (2.50)			
<i>Sphingobacteria</i>					
<i>Sphingobacteriales</i>					
<i>Flexibacteraceae</i>	2 (3.92)	1 (2.50)			
<i>Deinococcus-Thermus</i>					
<i>Deinococci</i>					
<i>Thermales</i>					
<i>Thermaceae</i>					
<i>Oceanithermus</i>				4 (6.67)	
<i>Proteobacteria</i>					
Unclassified	1 (1.96)	2 (5.00)			1 (1.75)
<i>Alphaproteobacteria</i>					
<i>Rhodobacterales</i>					
<i>Rhodobacteraceae</i>	3 (5.88)		1 (2.63)		
<i>Deltaproteobacteria</i>					
<i>Desulfobacteriales</i>					
<i>Desulfobulbaceae</i>					
Unclassified				1 (1.67)	
<i>Desulfobulbus</i>				1 (1.67)	
<i>Desulfocapsa</i>		1 (2.50)			
<i>Desulfotalea</i>					1 (1.75)
<i>Epsilonproteobacteria</i>					
Unclassified	2 (3.92)			18 (30.00)	15 (26.32)
<i>Campylobacteriales</i>					
Unclassified	1 (1.96)	1 (2.50)	2 (5.26)	7 (11.67)	7 (12.28)
<i>Campylobacteriaceae</i>					
<i>Sulfurospirillum</i>		3 (7.50)	3 (7.89)	2 (3.33)	
<i>Helicobacteriaceae</i>					
Unclassified		1 (2.50)	1 (2.63)	2 (3.33)	2 (3.51)
<i>Sulfurovum</i>	13 (25.49)	18 (45.00)	23 (60.53)	8 (13.33)	18 (31.58)
<i>Sulfurimonas</i>		8 (20.00)	7 (18.42)	1 (1.67)	
<i>Hydrogenimonaceae</i>					
<i>Hydrogenimonas</i>	10 (19.61)			4 (6.67)	1 (1.75)
<i>Nautiliales</i>					
Unclassified				1 (1.67)	
<i>Nautiliaceae</i>					
<i>Caminibacter</i>				2 (3.33)	4 (7.02)
<i>Nautilia</i>					1 (1.75)
<i>Nitratiruptor</i>				1 (1.67)	
<i>Nitratifractor</i>	2 (3.92)			2 (3.33)	4 (7.02)

<i>Gammaproteobacteria</i>					
Unclassified	12 (23.53)	1 (2.50)	1 (2.63)		1 (1.75)
<i>Methylococcales</i>					
<i>Methylococcaceae</i>	2 (3.92)			1 (1.67)	
<i>Thiotrichales</i>					
<i>Piscirickettsiaceae</i>					
<i>Thiomicrospira</i>	1 (1.96)				
<i>Thiotrichaceae</i>					
<i>Leucothrix</i>		2 (5.00)			
<i>Thermodesulfobacteria</i>					
<i>Thermodesulfobacteriales</i>					
<i>Thermodesulfobacteriaceae</i>				1 (1.67)	
Total	51	40	38	60	57